A PARAMETRIC STUDY OF THE FACTORS AFFECTING THE OPEN AND FILLED HOLE PERFORMANCE OF FIBER REINFORCED COMPOSITE MATERIALS

Dissertation

Submitted to

The School of Engineering of the

UNIVERSITY OF DAYTON

In Partial Fulfillment of the Requirements for

The Degree

Doctor of Philosophy in Materials Engineering

by

Margaret Frances Pinnell

UNIVERSITY OF DAYTON

Dayton, Ohio

August1995

A PARAMETRIC STUDY OF THE FACTORS AFFECTING THE OPEN AND FILLED HOLE PERFORMANCE OF FIBER REINFORCED COMPOSITE MATERIALS

Approved by:

James M. Whitney, Ph. D.
Professor of
Engineering Mechanics
Committee Chairman

James A. Snide, Ph. D.
Director of Graduate
Materials Engineering
Committee Member

Fred K. Bogner, Ph. D.
Chairman of Civil Engineering &
Engineering Mechanics
Committee Member

Peter O. Sjöblom, Ph. D.
Structures Lab
Research Institute
Committee Member

John E. Kauflin, Ph. D.
Professor of
Mathematics
Committee Member

Donald L. Moon, Ph. D.
Associate Dean/Director
Graduate Engineering & Research
School of Engineering

Joseph Lestingi, D. Eng., P.E.
Dean
School of Engineering

ABSTRACT

A PARAMETRIC STUDY OF THE FACTORS AFFECTING THE OPEN AND FILLED HOLE PERFORMANCE OF COMPOSITE MATERIALS

Pinnell, Margaret Frances
The University of Dayton, 1995

Advisor: Dr. James M. Whitney

The overall objective of this research was to experimentally determine the failure processes which occur in open and filled hole composite specimens subjected to tensile and compressive loading and in composite bearing specimens. An emphasis was placed on determining the effect of fiber stiffness, matrix properties, fiber orientation and laminate stacking sequence on these processes and the associated failure strengths. In an effort to obtain these objectives, bearing and open and filled hole tension and compression tests were conducted on four material systems having a variety of lay-ups and stacking sequences. Failure characteristics of tested specimens were studied using fractographic techniques. Failure progression was tracked through incremental loading. Results of the fractographic analysis showed a majority of the failures to initiate by matrix cracking and delamination. The initial failure modes were found to have little effect on the final failure modes or strengths. Experimental results showed fiber type, matrix type and lay-up to be the parameters which most significantly affect the open and filled hole tensile strength. Open and filled hole compression strength was found to be dependent upon lay-up and matrix type. Filled hole specimens were found to provide much greater compression strength than the open hole specimens. Hole size and matrix type were the only parameters found to affect the bearing strength. Experimental data suggests that stacking sequence, hence the occurrence of interlaminar stresses had little effect on the failure modes or strengths.

ACKNOWLEDGMENTS

I would like to express my sincerest gratitude to Mr. Ron Cornwell, Mr. Jim Lute and Mr. Ron Esterline of the University of Dayton Research Institute for their help with specimen fabrication, machining and testing, to Mr. William Ragland and Mr. Bradley Pinnell also of the University of Dayton Research Institute for their assistance in the area of fractography, to Mr. Daniel Laufersweiler and Mr. Edward J. Porter of Universal Technology Corporation for their help in nondestructive evaluation, to Dr. Endle Iarve of AdTech Systems Research for the information his model provided and to Lt. Jeff Schaff of the Materials Laboratory (WRDC/MLBM) for his assistance and guidance in this research. The help provided by these individuals is greatly appreciated and was instrumental to the success of this research.

I would also like to acknowledge and thank my advisor, Dr. James Whitney, and the other members of my committee for their guidance and for the time they took to participate on this committee. My sincere appreciation is also extended to Dr. James Snide, Director of Graduate Materials Engineering, for his support and encouragement and for providing the flexibility which enabled me to maintain a healthy balance of work and family.

DEDICATION

This work is dedicated to my children Ronnie, Erin and Marie who helped me to keep a proper perspective on what really matters in life, to my husband, Brad, and my mother, Patricia Riddick, for their endless patience, support and encouragement, to my Grandmother, Marie Maloney, for making me believe that anything is possible and finally, to my father, Ronald Hudock, who is with me always in heart, mind and spirit.

TABLE OF CONTENTS

ABSTRACT iii

ACKNOWLEDGMENTS iv

DEDICATION v

LIST OF FIGURES viii

LIST OF TABLES xii

NOMENCLATURE xiii

CHAPTER

I. INTRODUCTION 1

Problem Description
Objective
Results

II. LITERATURE REVIEW 8

Bolted Composite Joints and Fasteners
Composite Joint Design and Modeling
Fractography of Composite Materials

III. EXPERIMENTAL PROCEDURES 26

Materials, Fiber Orientations and Stacking Sequences
Quality Control and Physical Properties
Mechanical Testing
Fractographic Analysis
Statistical Analysis
Two Dimensional Analysis of Stress Concentrations

IV. PARAMETRIC STUDY 47

Quality Control and Mechanical Testing Results
Analysis of Parameters
Two Dimensional Analysis of Stress Concentrations

V. FRACTOGRAPHIC ANALYSIS 75

Post Failure Analysis
Incremental Loading Study

VI. SUMMARY AND CONCLUSIONS 111

VII. RECOMMENDATIONS 119

APPENDICES

Appendix A 122

Appendix B 126

Appendix C 131

Appendix D 133

REFERENCES 135

LIST OF FIGURES

1.	Photomicrograph showing drilling induced damage in the form of delamination and backface damage.	16
2.	Macroscopic failure modes of bolted composite joints.	21
3.	Microscopic fracture types for continuous fiber reinforced composite materials.	23
4.	Basic modes of loading for various fracture types.	23
5.	Longitudinal tension specimen	33
6.	Transverse tension specimen	33
7.	In-plane shear specimen.	33
8.	Unnotched, open and filled hole compression and tension test specimen.	35
9.	Modified edge stabilized compression fixture.	36
10.	Setup used for unnotched and notched tension and compression tests.	37
11.	Bearing test specimen configuration.	39
12.	Setup used for conducting the bearing tests.	40
13.	Longitudinal and transverse cross-sections of tested unnotched, open and filled hole compression and tension specimens.	42
14.	Far field normalized failure stress for the graphite/epoxy materials.	52
15.	Far field normalized failure stress for the graphite/PEEK materials.	52
16.	Unnotched, open and filled hole tensile moduli for the various material, lay-up combinations.	53
17.	Open and filled hole compressive moduli for the various material, lay-up combinations.	53
18.	Unnotched, open and filled hole tensile failure strain for the various material, lay-up combinations.	54
19.	Open and filled hole compressive failure strain for the various material, lay-up combinations.	54
20.	Normalized bearing strength for the graphite/epoxy materials.	61

21. Normalized bearing strength for the graphite/PEEK materials. 61

22. Normal plot of effects: Tensile data. 65

23. Normal plot of effects: Compressive data. 66

24. Normal plot of effects: matrix comparison. 67

25. Normal plot of effects: notched versus unnotched comparison. 68

26. Results of the extended isotropic analysis. 73

27. Ratio of the notched to unnotched strength for the open and filled hole tension specimens. 74

28. Macrophotograph of tested graphite/epoxy open and filled hole tension specimens showing that the presence of the fastener had little effect on the macroscopic failure modes for these materials. 76

29. Macrophotograph of tested graphite/PEEK open and filled hole tension specimens showing that the presence of the fastener had little effect on the macroscopic failure modes for these materials. 77

30. Macrophotograph of tested graphite/epoxy open and filled hole compression specimens showing that the presence of the fastener suppressed the majority of the damage to a region outside the washer area. 78

31. Macrophotograph of tested graphite/PEEK open and filled hole compression specimens showing that the presence of the fastener suppressed the majority of the damage to a region outside the washer area. 79

32. Photomicrographs of tested AS-4/3501-6 open and filled hole tension and compression specimens showing that the presence of the fastener had little effect on the microscopic failure mode for the tensile case, but was effective in suppressing the majority of the damage to a region outside the washer area for the compressive case. 80

33. Photomicrographs of tested AS-4/3501-6, open hole tension specimens showing that stacking sequence and lay-up did not have a significant effect on the microscopic failure modes. 83

34. Photomicrograph of tested AS-4/3501-6 open and filled hole compression specimens showing that stacking sequence and lay-up had little effect on the microscopic failure modes. 84

35. Photomicrographs of tested AS-4/3501-6 (material 1) and IM-8/3501-6 (material 2), open and filled hole tension specimens showing slightly more delamination in the material containing the IM-8 fiber than in the material containing the AS-4 fiber. 86

36. Photomicrographs of tested AS-4/3501-6 (material 1) and IM-8/3501-6 (material 2), open and filled hole compression specimens showing slightly more delamination in the material containing the IM-8 fiber than in the material containing the AS-4 fiber. 88

37. Photomicrographs of tested IM-8/3501-6 (material 2) and IM-8/APC-2 (material 4), open hole tension specimens showing that matrix material had little effect on the microscopic failure mode for the case of tensile loading. 90

38. Photomicrographs of tested AS-4/3501-6 (material 1) and AS-4/APC-2 (material 3), open and filled hole compression specimens showing that matrix material had little effect on the microscopic failure mode for the open hole case, but a rather significant effect on the microscopic failure modes for the filled hole case. 91

39. Macrophotographs of tested graphite/epoxy bearing specimens showing a bearing type failure mode and slightly more damage for the smaller hole diameter specimen (Ba) than for the larger hole diameter specimen (Bb). 93

40. Macrophotographs of tested graphite/PEEK bearing specimens showing a bearing type failure mode and slightly more damage for the smaller hole diameter specimen (Ba) than for the larger hole diameter specimen (Bb). 94

41. Identification of the coordinate axis used to locate damage around the circumference of the hole. 96

42. Radiographs and cross-sections obtained from tested graphite/epoxy, open hole tension specimens showing lay-up to have some effect on the location of damage initiation. Damage initiation occurred by transverse or angle ply cracks at approximately 40% of the failure stress. 97

43. Radiographs and cross-sections obtained from tested graphite/epoxy, open hole tension specimens showing damage initiation to be essentially independent of fiber type and to occur at 35% to 45% of the failure load. 99

44. Radiographs and cross-sections obtained from tested open hole tension specimens showing damage initiation in the graphite/epoxy (material 1) specimen to 100

occur by intralaminar fracture of the angle plies while damage initiation in the graphite/PEEK (material 3) specimen to occur by translaminar fracture of the zero degree plies.

45. Radiographs and cross-sections obtained from tested graphite/epoxy, open and filled hole compression specimens showing that the presence of the fastener had little effect on the mode of damage initiation for the filled hole compression specimens. 106

46. Radiographs and cross-sections obtained from tested graphite/PEEK, filled hole compression specimen (3-5-FHC) showing damage initiation to occur by fiber buckling of the zero degree plies at approximately 97% of the failure stress. 108

47. Approximate Interlaminar normal stress distribution vs. y. 122

48. Moments about the z axis for a 16 ply, symmetric laminate. 122

49. Definition of laminate and material coordinate systems 124

LIST OF TABLES

1.	Composite Constituent Properties.	26
2.	Two Level Factorial Design Used in This Investigation.	44
3.	Physical Property Data.	47
4.	Laminate Property Data.	48
5.	Unnotched Tension Data.	49
6.	Open Hole Tension Data.	49
7.	Filled Hole Tension Data.	50
8.	Unnotched Compression Data.	50
9.	Open Hole Compression Data.	51
10.	Filled Hole Compression Data.	51
11.	Results of the Acoustic Emissions Output.	59
12.	Correlation of Acoustic Emissions Output with a Change in Modulus for the Graphite/Epoxy Material.	59
13.	Bearing Data.	60
14.	Main and Interaction Effects for the Graphite/Epoxy Material.	63
15.	Main and Interaction Effects for the Graphite/PEEK material.	63
16.	Main and Interaction Effects: Matrix Comparison	64
17.	Main and Interaction Effects: Notched versus Unnotched Comparison.	64
18.	Values of K_T as determined from the extended isotropic analysis.	72
19.	Comparison of Observed and Predicted Failure Initiation Modes and Locations.	109
20.	Approximation of Interlaminar Normal Stresses at Midply.	125

NOMENCLATURE

A_{ij}	components of laminate stiffness [psi]
d	hole diameter [in]
e_+, e_-	average effects at high and low level
E_{11}, E_{22}, G_{12}	longitudinal, transverse and shear moduli [psi]
h	laminate thickness [in]
K_T	stress concentration factor
m, n	direction cosines
M_Z	moments about the z axis
n_i	number of observations for trial
N	total number of observations
N_x, N_y, N_{xy}	components of stress resultant [lb/in]
P	probability of effect
$P_{bearing}$	bearing failure load [lbs]
P_f	failure load [lbs]
Q_{ij}	components of reduced stiffness (material coordinates) [psi]
Q_{ij}^k	components of reduced stiffness (laminate coordinates) [psi]
r	hole radius
s_i^2	variance for each trial
s^2	pooled estimate of run variance
$S_{kl}^{t\,(c)}$	components of the tensile (compressive) strength
SE	standard error
t	specimen thickness [in]
v_i	degrees of freedom for each trial

V_f	fiber volume [%]
V	variance
x	distance from hole center [in]
X_c, X_t	compressive and tensile strength [psi]
yi	trial mean
y_j	individual repeated measure
w	specimen width [in]
ε_1, ε_2	components of strain [in/in]
$X_{kl}^{t\,(c)}$	coefficient for tension (compression)
ρ_c, ρ_f, ρ_r	composite, fiber and resin densities [lb/in^3]
$\sigma_{bearing}$	ultimate bearing strength [psi]
$\sigma_{kl}^{t\,(c)}$	components of tensile (compressive) normal and shear stress [psi]
σ_l	local failure stress [psi]
σ_f	far field failure stress [psi]
$\underline{\sigma_0}$	reference stress [psi]
σ_0	remote applied stress [psi]
σ_y	local stress [psi]
σ_y^k	component of stress acting on the kth ply [psi]
σ_{zmax}	maximum interlaminar normal stress [psi]
ν_{12}	Poisson's Ratio

CHAPTER 1

INTRODUCTION

Although considered to be a relatively new class of materials, continuous fiber, polymer matrix composite materials are finding increasing applications in the aerospace industry. Some aerospace applications of composite materials include the B-1 and F-16 horizontal and vertical stabilizers, the L-1011 aileron, the C-141 leading edge, the 767 inboard aileron and rudder and the DC-10 aileron actuator access panel, landing gear door and upper vertical stabilizer [1]. Although composite materials are being widely used in the aerospace industry, they are by no means trouble free. One problem associated with composite materials arises from the nearly inevitable need to join composite parts in the assembly of an aerospace structure. The most common method of joining composite parts is through the use of single- or multiple- bolted mechanical fasteners. The main problem with the use of mechanical fasteners is that they require that a hole be drilled in the composite part. Drilled holes significantly disturb the internal structure of the composite since the material in the hole region is cut out, breaking the continuity of the fibers. Material discontinuities produce areas of high stress concentrations which have been found to reduce the load carrying capability of the composite structure as much as 70 % [1-7]. Another problem associated with the use of mechanical fasteners in composite joints is the general lack of understanding of the effect of parameters such as constituent material properties, fiber orientation and stacking sequence, number and spacing of bolts, end distance, bolt clearance and load distribution on the overall performance of these joints [4, 8, 9]. Additionally, the composite design community lacks a model which adequately takes into consideration the effect of the aforementioned parameters on the failure modes when predicting the overall performance of bolted composite joints. Although many two- and three- dimensional models exist, none are consistently used or widely agreed upon.

In an effort to avoid the problems associated with drilled-hole bolted composite joints several joining alternatives have been suggested and/or attempted. Perhaps the most prevalent of these alternatives is the use of adhesively bonded joints. Although this alternative is becoming more viable with improvements in adhesives technology, several problems arise with the use of bonded joints. One such problem is that only relatively low rates of load transfer can be attained with bonded joints due to the low shear strengths of the adhesive and composite laminate. Other problems with bonded joints include existence of high thermal strains in the bonded region due to the relatively high cure temperatures of the adhesives and the environmental degradation of adhesive properties. Additionally, bonded joints prohibit easy disassembly of composite structures, thus making maintenance and repair difficult [5, 10]. Another proposed alternative to bolted composite joints is the use of a multi-shim joint consisting of thin metal shims interleaved with composite layers. This method is not attractive since the multi-shim joint is difficult to fabricate and therefore cost prohibitive [10]. Molded hole composites is another method which has been proposed to replace drilled holes for use in bolted composite joints. This method generates bolt holes by routing the fibers around a circular mold during fabrication of the composite structure. Although molded hole composites have been shown to provide significant strength increases as compared to drilled hole composites, fabrication of molded hole structures is tedious and time consuming and would be expensive to manufacture into parts for aerospace structures. Therefore, fabrication of molded hole composites must be simplified or automated before this concept can be incorporated into the aerospace industry [2, 3, 11, 12]. Modification of hole shape to minimize stress concentrations, reinforcing the region near the hole, stitching or tufting the hole edge and embedding the hole in a soft high strain material are some other alternatives suggested for reducing the problems associated with drilled hole bolted composite joints [13-17].

It is apparent that none of the aforementioned joining alternatives provides sufficient solutions to the problems associated with drilled hole bolted composite joints. Perhaps the only way in which some of these problems can be resolved is through optimization by design. To aid

in this design optimization process an adequate model is needed. Before an adequate model can be developed, the parameters which affect the strength and failure of bolted composite joints subjected to a variety of loading conditions must be determined.

Problem Description

Material discontinuities associated with drilled hole, bolted, composite joints produce areas of high stress concentrations which reduce the load carrying capability of the composite structure. In order to minimize this strength reduction, the composite joint must be designed to provide optimum performance. Before optimum designs can be achieved, engineers must be able to identify those parameters which most significantly affect composite joint performance and have a thorough understanding of the associated failure process. Although many studies have been conducted in the area of bearing, open hole tension and compression performance of composite materials, none of these studies systematically considered the potential key parameters associated with bolted composite performance. Furthermore, little effort has been exerted to identify damage initiation and propagation in bolted composite joints and to understand the effect of various parameters on the failure process. Of particular concern is the role of the matrix material in the failure process. Matrix dominated failures such as matrix cracking and delamination require an understanding of the three-dimensional state of stress, while fiber dominated failures can be sufficiently modeled with a two-dimensional stress analysis. Therefore, an understanding of the mode of damage initiation and propagation in bolted composite joints may have important ramifications concerning the level of stress analysis required in the design of bolted composite joints. Another deficiency which exists in the area of bolted composite joints is an understanding of the filled hole performance of composite materials. Although filled holes are encountered much more frequently than open holes in joint applications, the current literature reveals numerous studies in the area of open hole performance of composite materials with little reference to any work being done in the area of filled hole performance of composite materials. This observation is exemplified by the fact that current composite materials evaluation procedures utilize open hole data rather than filled hole data to characterize stress concentration effects. It is

for these reasons that a systematic study needs to be conducted in the area of bearing and open and filled hole tension and compression performance of composite materials with an emphasis on identifying key parameters and failure processes.

Objectives

The overall objective of this research was to experimentally determine the failure processes which occur in open and filled hole composite specimens subjected to tensile and compressive loading and in composite bearing specimens. An emphasis was placed on determining the effect of fiber stiffness, matrix properties, fiber orientation and laminate stacking sequence on these processes and the associated failure strengths. Mechanical testing, incremental loading and fractographic analysis were used to obtain these objectives.

Results

The research described in this dissertation provided the composite community with an in-depth, systematically obtained understanding of the parameters which affect bolted, composite joint performance and the effect that these variables have on the material failure characteristics. Results of the fractographic analysis supplied invaluable information concerning the initiation and propagation of failure in bolted composite joints. Additionally, experimental procedures were developed which will be useful to researchers in the future. Finally, the results obtained from this research will be useful in the development of failure criteria and models capable of predicting the strength of a bolted composite joint.

Fiber type was found to have a statistically significant effect on the open and filled hole tensile strength of the graphite/epoxy (AS-4/3501-6, IM-8/3501-6) and graphite/PEEK (AS-4/APC-2, IM-8/APC-2) composite material systems studied. Some interaction between fiber type and stacking sequence was found to exist for the PEEK matrix specimens. No significant differences were observed in the mode of failure initiation or propagation in the open and filled hole tensile specimens for the two different fibers studied. Fiber type was found to have essentially no effect on the open and filled hole compression strength for both the epoxy and PEEK matrix material

systems. Fiber type did not appear to have a notable effect on the mode of failure initiation or propagation for the open and filled hole compression specimens. For the graphite/epoxy open and filled hole compression specimens, failure was found to initiate by intralaminar cracking and delamination at the hole edge. Final failure of the open hole compression specimens occurred in a shear or compressive type mode through the hole while, final failure of the filled hole compression specimens occurred in a compressive or shear type failure mode occurring around the washer edge. Bearing strength was found to be essentially independent of fiber type. No effect of fiber type on the final failure modes was observed for either of the matrix materials. All of the specimens failed in a bearing type failure mode.

The graphite/PEEK specimens were found to provide consistently higher open and filled hole tensile strengths than the graphite/epoxy specimens. The matrix material was found to have some effect on the mode and stress level at which failure initiated for the open and filled hole tensile specimens. For the epoxy matrix materials, failure was found to initiate by intralaminar fracture of the off-axis plies whereas failure initiation in the graphite/PEEK materials occurred by translaminar fracture of the 0 degree plies. The graphite/epoxy specimens were found to provide consistently higher open and filled hole compression strengths than the graphite/PEEK specimens. Failure initiation of the graphite/PEEK open and filled hole compression specimens was found to occur by buckling of the zero degree plies. Failure initiation of the graphite/epoxy specimens occurred by intralaminar fracture of the off-axis plies. Final failure of the graphite/epoxy specimens was characterized by kink bands consisting of multiple plies whereas final failure of the graphite/epoxy specimens occurred by kinking of the individual plies. The graphite/PEEK specimens were found to provide consistently higher bearing strengths than the graphite/epoxy specimens. A significant amount of local yielding was observed in the graphite/PEEK bearing specimens whereas virtually no local yielding was observed for the graphite/epoxy bearing specimens.

The bearing, open and filled hole tensile and compressive strengths were found to be independent of stacking sequence for all the materials studied. Similarly no difference in mode of failure initiation was observed for a given material and loading condition.

Lay-up was found to have a statistically significant effect on the open and filled hole tensile and compressive strength for all materials studied. In general, lay-ups consisting of 0 and 60 degree layers were found to provide slightly higher tensile and compressive strengths than those containing 0, 45 and 90 degree plies. The only effect that lay-up appeared to have on the failure mode was the ply in which failure initiated and the direction in which this damage propagated. Lay-up did not have a significant effect on the bearing strengths or failure modes for any of the materials studied.

The presence of the fastener in the filled hole specimens was found to have little effect on the tensile strength of the materials studied. The only effect that the presence of the fasteners was found to have on the ultimate failure mode of the graphite/epoxy and graphite/PEEK tensile specimens was to suppress the delaminations to a region outside of the washer area and to encourage a greater degree of intralaminar fractures of the angle plies. The presence of the fastener was found to have a significant effect on both the strength and failure mode of the specimens loaded in compression. The stress levels at which damage initiation and ultimate failure occurred were significantly higher for the filled hole compression specimens than the open hole compression specimens. The lateral constraint provided by the torqued fastener appeared to be effective in suppressing a majority of the damage to a region outside the washer area. Hole size was found to have a significant effect on the bearing strengths. For all the materials studied, the damage appeared to be slightly more significant for the smaller hole size specimens than the larger hole sized specimens.

Data obtained from a currently existing three-dimensional stress analysis and failure criteria provided useful information concerning the location and mode of initial damage. However, the applicability of a technique such as this is questioned, since there appears to be little correlation between the damage initiation mode and strengths with the ultimate failure mode and

strengths. Additionally, the experimental data suggests that stacking sequence, hence the occurrence of interlaminar stresses has little effect on the ultimate failure modes or strengths.

The technique used for the incremental loading study which consisted of loading the specimen to a percentage of failure stress then subjecting it to radiography was found to be very useful in identifying the failure initiation stress and location for the open hole test specimens. Material cross-sectioning of tested specimens provided useful information concerning the mode and location of initial and ultimate failure.

CHAPTER 2

LITERATURE REVIEW

Bolted Composite Joints and Fasteners

As indicated previously, in aerospace structures the joining of composite parts via mechanical fasteners is nearly unavoidable. During service the composite joint will transfer loads from one structural member to another. In most cases a structure will require a multiple bolt configuration to transfer the loads adequately [5]. Load transfer occurs via shear forces in the bolt and by frictional forces which are generated at the interface between the joined members. The magnitude of the load transfer occurring by frictional forces is dependent upon the interface conditions and the amount of torque used to tighten the bolt [14]. Although necessary, the use of mechanical fasteners significantly reduces the strength of the structure. Reductions in strength as great as 35 - 70% have been reported [6, 7, 18]. This reduction in strength is attributed to stress concentrations which occur in the area of the drilled hole.

Composite constituent properties are believed to have a significant effect on the notched strength performance of composite materials. Notch sensitivity in composite materials is governed largely by the matrix material. A notch sensitive material fails when the stress concentration at the hole edge equals the failure stress of the material. A notch insensitive material is one which allows some forms of strain relief (such as local yielding) to occur at the hole edge, resulting in minimal strength degradation. The failure strains for notch insensitive materials are directly proportional to the reduction in the specimen cross-section due to the presence of the hole [19-21]. Generally, brittle matrix composite materials such as graphite/epoxy are considered to be more notch sensitive than ductile matrix composite materials such as graphite/PEEK. Naik and Sai Ram showed that as the modulus of elasticity of the matrix material increases, the stress concentration factor decreases. Conversely, as the modulus of the

matrix material decreases, the stress gradient becomes much greater at the peak stress point in a direction perpendicular to the loading axis [22]. Guynn and Bradley showed that for composite materials having a ductile matrix, damage propagates away from the hole edge prior to catastrophic failure, thus allowing final failure to precipitate to a distance away from the hole, thereby making the material less notch sensitive [23]. Although most epoxy matrix composite materials are considered to be relatively brittle, Soutis, et. al. found that epoxy matrix composites are not ideally brittle and that some stress relief occurs in the vicinity of the hole [18]. Although brittle matrix composite materials have been shown to be more notch sensitive than ductile matrix composite materials, the overall performance of brittle versus ductile matrix composite in bolted joint applications is debated. Shalev and Reifsnider conducted a study to determine the effect of the matrix material on the open hole tensile and compressive performance of composite materials. They found that the onset of failure was not controlled by the relative toughness of the matrix, as the composite material having the tougher matrix consistently failed first [17]. Conversely, in two separate studies, Naik and Sai Ram and Walsh, et. al., found that composite materials having tougher matrices exhibited superior notched strength performance over composites having less tough matrices [22, 24]. In addition to the matrix properties, the fiber properties have also been shown to affect the bolted joint performance of composite materials. Naik and Sai Ram conducted an investigation to determine the effect of fiber stiffness on the notched strength performance of composite materials. The results from this investigation indicate that higher modulus fibers result in lower stress concentration factors occurring at the hole edge, thereby enhancing the notched strength performance of the composite material [22]. There has also been some speculation that the remaining constituent of a composite material, the fiber matrix interface, may have some effect on the notched strength performance of composite materials. Beaumont indicates that a reduction in the fiber matrix bond strength may increase fracture toughness but will result in poor transverse properties, including delamination resistance [25]. The overall effect of fiber matrix interface strength on bolted composite joint performance is

ambiguous. Therefore, studies need to be conducted to determine the nature or existence of this effect.

Two other factors which are believed to affect the strength of a bolted composite joint are the fiber orientation and stacking sequence. The fiber orientation refers to the direction in which the individual, unidirectional plies are oriented, while the stacking sequence refers to the order in which these plies are placed with respect to one another [9, 26-32]. The effect of fiber orientation and stacking sequence on the notched strength performance of composite materials is related to the presence of interlaminar stresses occurring at the hole edge. Interlaminar normal and shear stresses are generated during mechanical or thermal loading of angle ply laminates as a result of stiffness discontinuities resulting from a mismatch of the individual ply deformations. These stresses occur in a boundary layer region which is generally believed to be approximately equal to one laminate thickness and are not accounted for in two-dimensional analyses such as classical lamination theory. These high interlaminar normal and shear stresses occurring at boundary regions can initiate and propagate delaminations and transverse cracks resulting in a substantial degradation of mechanical properties and a non-linear material response [33]. The magnitude and sign of interlaminar stresses depends primarily on the stacking sequence of the laminate. For a curved boundary, such as a hole edge, both the magnitude and sign of the interlaminar stresses fluctuate along the hole edge. Regions of high interlaminar normal tensile stresses in this region may cause delamination to occur at the hole edge [9, 26-28, 30-50].

Since the magnitude and sign of interlaminar stresses in the vicinity of a hole is largely dependent upon the stacking sequence of a composite laminate it is logical to conclude that stacking sequence affects both the strength and mode of failure of a bolted composite joint. Although many studies have been conducted to assess the overall effect of stacking sequence on the notched strength performance of composite materials, much of the literature presents conflicting results. Some authors report that stacking sequence has little effect on the notched strength performance of composite materials while others found that stacking sequence affects both the strength and failure mode [26-28, 30-32, 51, 52]. Whitney and Kim found that unnotched

tensile strength was affected by stacking sequence, while the notched tensile strength appeared to be essentially independent of stacking sequence. Additionally, tensile failure of the notched specimens occurred prior to delamination at the free edge. Therefore, delamination due to interlaminar stresses did not have any significant influence on the notched strength for graphite/epoxy laminates having a quasi-isotropic fiber orientation [27]. Similarly, Aronsson, concluded that the influence of stacking sequence on the strength of composite materials is dependent on whether the laminate is notched or unnotched and the type of notch [28]. Ditcher and Webber found the stacking sequence and thickness of cross-ply laminates to affect the unnotched compression performance of composite materials [38]. Smith and Pascoe found there to be no obvious stacking sequence effect on the pin-bearing strengths of carbon fiber reinforced composite materials. They did, however, find some influence of stacking sequence on the failure mode for these specimens. Stacking sequences with zero degree plies on the surface failed by a splitting and delamination of the surface plies, while stacking sequences having the zero degree plies near the center of the laminate exhibited more interior delaminations [26]. Conversely, Quinn and Matthews found there to be definite dependence of bearing strength on stacking sequence for glass/epoxy composite materials [52]. In a study conducted by Boeman, the interlaminar deformations were measured on a ply-by-ply basis at both the straight free edge and at the hole boundary of composite panels using Moiré Interferometry. Boeman concluded from this study that the magnitude of the transverse and tangential interlaminar strains at the hole edge are directly dependent upon both fiber orientation and stacking sequence [35, 53]. Rybicki and Schmueser conducted a three-dimensional analysis which concurred with these results. They found that stacking sequence controlled the magnitude and sign of the interlaminar stress distribution around a hole [46]. Experimentally, Legace found that stacking sequence had a significant effect on both the strength and failure mode of composite materials having a fiber orientation of $[+\theta / -\theta / 0]_S$. He concluded that stacking sequences of the form $[+\theta / 0 / -\theta]_S$ provide the best notched strength performance, since very little delamination occurs in this case. He also found the lamination angle, θ, to have an effect of the notched strength performance of

composite materials [39]. In an experimental and analytical investigation conducted by Jen, Kau and Hsu on open hole tensile performance of quasi-isotropic composite laminates, it was found that stacking sequence affects the initiation and growth of damage in composite laminates [30]. Ratwani and Kan conducted fatigue tests on various stacking sequence of open hole, graphite/epoxy, quasi-isotropic laminates. From this investigation it was found that for the loading conditions considered, damage growth, failure mode and strength depended greatly on stacking sequence. It was also found that the location of delaminations and matrix cracking for the different stacking sequences studied corresponded with the positions of interlaminar shear or normal stresses as predicted by a finite element analysis [47].

Many studies have also been conducted to determine the effect of fiber orientation on the notched strength performance of composite materials. It is generally agreed upon that fiber orientation does have an effect on the notched strength performance of composite materials. Chang, et. al., conducted several studies to determine the effect of fiber orientation on damage growth and strength of bolted composite joints subjected to tensile and compressive loading. From these studies it was found that ply orientation affected both the mode of failure and strength of these joints. They concluded further that grouping plies of the same orientation together is very deleterious to the strength of a notched composite and can significantly affect the failure mechanisms of composites containing holes [29, 33, 50, 51, 54]. Similarly, in two separate investigations, Rybicki and Schmueser, and Collings found the notched tensile performance of graphite/epoxy composite materials to be dependent upon fiber orientation as well as hole size and specimen width. From this study, Collings also found the failure initiation site to be dependent upon the fiber orientation [10, 46]. Hart-Smith arrived at the same conclusions in a comprehensive experimental investigation conducted on quasi-isotropic, graphite/epoxy and graphite-glass/epoxy bolted joints [6]. In a study conducted by Xue, et. al., it was concluded that fiber orientation does affect the bearing strength of composite laminates with the optimum configuration being an orientation with 60 - 70 % of the fibers in the zero degree direction [8].

The amount of "clamp-up" or torque used to tighten a fastener is another factor which is believed to influence the performance of a bolted composite joint. The recommended production torque level for a 0.25 inch diameter fastener is between 55 and 70 inch-pounds [16]. Many studies have been conducted to determine how either under torquing or over torquing a bolt affects the tensile, compressive and bearing performance of composite joints. Results of these studies indicate four ranges of torque for which different trends have been noted [7, 9, 10, 14,16, 55-57]. The case in which a pin is present without any washer or bolt represents the range of zero torque. For this case the material surrounding the hole edge has no lateral constraint [14]. The second range of torque, commonly referred to as "finger tight" occurs between the values of 0 to 10 inch-pounds. In two separate studies conducted by Collings and Eriksson, the bearing strength was found to be greater for this range of torque versus the range of zero torque [10, 14]. Similarly, Matthews, et. al., and Eriksson found the presence of the finger tight bolts to increase the tensile and compressive strength of bolted composite joints [14, 56]. Although an increase in bearing, tensile and compressive strength was noted for the specimens having lateral constraint provided by finger tight bolts versus the unconstrained specimens, no difference in failure modes was noted [10]. The third range of torque is from 10 to 40 inch-pounds. In this range of torque a significant increase in bearing, tensile and compressive strength has been observed with increasing bolt torque. The increase in strength is attributed to the lateral constraint provided by the torqued fastener. The lateral constraint provided by the fastener helps to inhibit and constrain ply delaminations and transverse cracking due to interlaminar stresses occurring at the hole edge thereby allowing the composite joint to sustain higher loads. Additionally, friction generated between the washer and the laminate helps to redistribute the stresses to a region away from the hole edge [7, 9, 14, 16, 55-58]. It is in this torque range that a change in failure mode can first be noted. In the case of bearing loading, this change in failure mode is from longitudinal splitting or brooming to a mode in which both fiber and matrix failure occur [58]. For tensile and compressive loading failure is found to occur at the washer edge instead of at the hole edge [56]. The last range of torque is between 40 to 75 inch-pounds. For this range of torque no discernible increase

in joint strength is noted with increasing bolt torque [7]. Very high levels of bolt torque (greater than 200 inch-pounds) have been found to cause initial failure in the composite material in the form of delaminations [16].

Another factor which strongly influences the performance of a bolted composite joint is the type of fastener used. The three type of fasteners used in the aerospace industry include screws, rivets and bolts. Of these three types, bolts have been found to provide the strongest joints where there is not a requirement for a smooth aerodynamic surface [9]. The size of the fastener in relation to the hole defines the fit of the fastener. The fastener fit is classified as either clearance or interference fit. Clearance fit fasteners are those in which the fastener clearance ranges from -0.000 inches to 0.0004 inches and interference fasteners are those in which the clearance is less than -0.000 inches. Although interference fit fasteners have been found to provide strength and durability improvements, increased fatigue life and increased load sharing in joints with multiple rows of fasteners, to help retard fuel leakage in tank areas and to provide the reaction torque needed for the installation of one sided fasteners, the use of these fasteners in composite structures is generally avoided. This is due to the fact that installation of interference fit fasteners in composite materials can produce unacceptable delamination type damage in the structure as a result of the inherently low interlaminar strength of these materials [59]. Fasteners may be installed as either countersunk or protruding head. Countersunk fasteners are more commonly used in the aerospace industry since they can provide the smooth aerodynamic surface needed in many of these applications [9, 59]. In a study conducted by Packman, et. al., it was found that protruding head fasteners significantly outperformed countersunk fasteners for the numerous conditions studied. The countersunk fasteners were found to precipitate tension failures at larger edge distances due to the effectively larger hole. Additionally, the eccentric loading nature of the countersunk fasteners sometimes resulted in the fastener head transversely digging into the laminate [7]. Fastener material type has also been shown to influence the performance of a bolted composite joint. Although commonly used, metallic fasteners can corrode galvanically in the presence of graphite/epoxy composite materials. Titanium appears to

be somewhat resistant to this form of corrosion and therefore is commonly used as a fastener material for bolted graphite fiber composite joints [59].

Mechanically fastened composite joints require that a hole be drilled in the structure. Due to the inherent low interlaminar strength of composite materials, hole defects can be generated during the drilling process [16, 60-62]. This drilling induced damage is characterized by small, multi-level delaminations occurring in a localized region surrounding the hole and localized, backface damage in the form of fiber breakage and matrix cracks, Figure 1. Drilling induced damage can result in a loss of stiffness and strength in the structure, particularly when that structure is loaded in compression or subjected to fatigue loading [16, 60, 61]. Experience has shown that drilling induced damage in composite structures can be minimized by using only sharp bits at high rpm with slow feed rates and by applying some type of backing pressure during the drilling process [60, 61]. Several studies have been conducted to assess the affect of drilling induced damage on the bolted joint performance of composite materials. Andrews, et. al., conducted an investigation to determine the effect of four common hole defects. These defects included chip-out, delamination, oversized holes and overheated epoxy matrix. Andrews, et. al. concluded from this investigation that both the pin bearing and fatigue response were adversely affected by the presence of the various hole defects. Additionally, Andrews, et. al. found that the presence of hole defects had an effect on the failure mode of composite materials subjected to the aforementioned loading conditions [60]. In another study, Fracchia and Bohlman studied the effect of assembly induced delaminations on the bolted joint performance of composite materials. From this investigation, it was found that graphite/epoxy and graphite/PEEK specimens retained approximately 93-99% of their undamaged strength during static compression tests. They also found that most of the specimens tested did not exhibit delamination growth during compression-compression fatigue loading. Additionally, failure of the fatigue specimens occurred at loads comparable in magnitude to the failure loads measured during static loading [16]. Similarly, in a study conducted by Hart-Smith no discernible difference could be detected in the performance of undamaged versus damaged bolt holes [6].

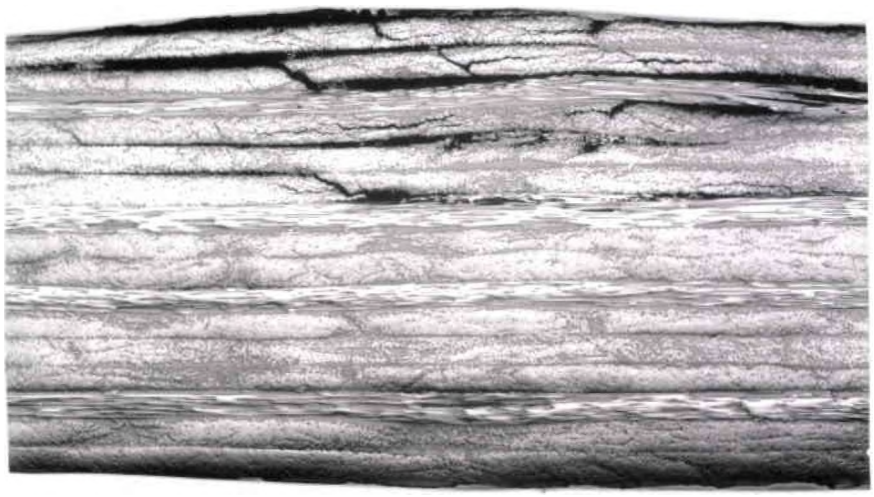

Figure 1. Photomicrograph showing drilling induced damage in the form of delamination and backface damage.

Design parameters such as size and shape of the hole and bolt spacing have also been shown to have an effect on the performance of a bolted composite joint [4, 6, 9, 10, 21, 50, 55, 62]. Lin and Ko and Chang, et. al., found the stress concentration factor to increase with increasing hole size. The magnitude of this hole size effect on the notched strength performance of composite materials is dependent on the structure width and the material thickness [2l, 29]. Similarly, Collings showed the bearing strength of graphite/epoxy composite materials to decrease with increasing hole size. However, this hole size effect was found to virtually disappear when the hole was laterally constrained by the presence of a torque tightened fastener [10]. Lin and Ko also showed that the shape of the hole can affect the notched strength performance of composite materials. They found the strength may be reduced, raised or unchanged as the hole becomes more elliptical. The overall effect of hole shape appears to be dependent upon lamina properties, fiber orientation, stacking sequence and loading conditions [63]. Although the majority of the design parameters are determined from single-hole data, the overall strength of a bolted joint depends on such parameters as the number and spacing of bolts, bolt clearance, load distribution among the bolts and material properties. Furthermore, the

validity of extracting single-hole data to multiple-hole applications is questioned [4-6, 62]. Godwin, et. al. showed that the assumption that a multiple-bolt joint may be represented by a number of single-bolt joints loaded in parallel is unrealistic. This is due to the fact that stress interactions occur in the case of multiple-bolt joints which can reduce the strength of the joint. These stress interactions cannot be accurately modeled by single-bolt test pieces [62]. Chamis adds that multiple-bolt composite joints are generally designed by assuming that all the bolts in the joint share equal load where in reality the first row of bolts will usually transfer more load [55]. There is little reference in the open literature as to any work being done to assess the effect of these parameters associated with multiple- versus single-bolt holes. Hart-Smith found the strengths of two-row bolted joints to be only slightly higher than the strengths of single-row joints in graphite/epoxy specimens but found the multiple-bolt hole to be significantly stronger than the single bolt hole for hybrid, glass/graphite/epoxy specimens. From this, it is apparent that some interaction exists between material properties and the stress interactions which exist in multiple-bolt specimens [6].

Other factors which affect bolted joint performance of composite materials include temperature and moisture. These factors can influence both the strengths and failure modes of bolted composite joints and appear to be somewhat material dependent [55, 64, 65]. From the literature it is apparent that little work has been done to determine the overall effects of temperature and moisture on the bolted joint performance of composite materials.

Composite Joint Design and Modeling

Design of a bolted composite joint is a rather complex process involving many steps. These steps include significant mechanical testing as well as both simple and advanced analysis methodology [4, 55, 64]. Preliminary mechanical testing involves static and fatigue coupon tests to assess a material's compression, tension, shear, bending and bearing performance [64]. Since the integrity of a mechanically fastened composite joint depends mainly on the material's local bearing strength, bearing and filled-hole testing are of particular importance in this preliminary phase [55, 67]]. Also during coupon level testing, the compression and interlaminar shear

strength reduction factors associated with high temperature exposure and moisture saturation are evaluated. The strength reduction factors are used in the development of design allowables. Sub-component and full-scale aircraft structural tests are later performed to verify structural integrity and load paths within the test article [64].

Analytical techniques consist of both simple and advanced methods. The simple methods are generally used during the preliminary design and optimization phase [66]. During this phase, the bolted joints are designed to resist certain failure modes which most commonly occur in practical applications. These failure modes include local bearing, net tension , wedge-type splitting, shear out and tension with shear out and are discussed in greater detail in the Fractography of Composite Materials section [55]. A load distribution analysis is conducted to determine the load distribution between the fasteners and around material cut-outs. Generally, this analysis is performed on rather large structures by means of a two-dimensional, coarse mesh, finite element model. In this analysis, contact between the members in the joint is generally ignored, the hole is reduced to a point and the group of fasteners is represented by a spring or beam element [4, 66]. After the load distribution analysis, the local stress distribution around the fastener is determined by a detailed finite element analysis or by some other appropriate technique. It is during this phase of the design process where a three-dimensional analysis technique capable of determining interlaminar stresses may be important. A bolted joint's dependence on laminate stacking sequence will determine the necessity for such an analysis [29, 66]. The final step in the design of a bolted composite joint involves determination of the joint strength via application of an appropriate failure criteria. Some problems associated with composite failure criteria include the fact that they require a large amount of experimentally determined parameters and are somewhat inaccurate in determining the strength of a joint [66].

Many two- and three-dimensional models and analyses exist which are applicable to the design of bolted composite joints. The majority of these analyses focus on determining the local stress distribution around a hole or fastener or on predicting the notched strength of a composite material. Composite failure criteria, including the Maximum Stress, Maximum Strain, Point Stress

and the Average Stress Theories are discussed in detail in references [41, 44, 45, 49, 68]. The majority of the analyses and models described in the literature incorporate one or more of these failure criteria. The Maximum Stress and Maximum Strain theories are similar in that they predict failure to occur in a ply of a laminate when either the longitudinal, transverse or shear stress or strain reaches a limiting value as determined from simple one-dimensional stress experiments [45, 49, 68, 69]. The Tsai-Hill criteria is also a ply level failure criteria which uses basic laminate property data. However, this criteria is capable of accounting for stress interactions. The Point Stress and Average Stress criteria proposed by Whitney and Nuismer predicts the static strength of laminates with holes and cracks. The Point Stress criteria assumes that failure occurs when the stress over an experimentally determined characteristic distance away from the notch is equal to or greater than the strength of the notched laminate. Similarly, the Average Stress criteria assumes failure to occur when the average stress over an experimentally determined characteristic distance equals the unnotched laminate strength [44]. In a similar analysis, El-Zein and Reifsnider use an elasticity solution along with the average stress criterion to predict the strength of a notched composite plate on a ply-by-ply basis [70]. Garbo and Ogonowski used a closed form analytical approach based on the anisotropic theory of elasticity, laminated plate theory and the Tsai-Hill theory to predict the open hole static strength of a composite laminate. This analysis predicts not only strength but location of failure initiation and critical plies [71]. Using a similar approach, Lin and Ko developed a model for predicting strength of composite materials containing elliptical holes [2]. Konish and Whitney propose the extended isotropic analysis for determining the in-plane stress distribution in the vicinity of a hole of an orthotropic material [72].

Determination of interlaminar stresses in the vicinity of a hole necessitates the use of a three-dimensional analysis. Many models are presented in the literature which incorporate such an analysis. One such model proposed by Zhang and Ueng attempts to simplify the problem by utilizing a three-dimensional approach only in the immediate vicinity of the hole and treating the remaining region as an orthotropic plate. This analysis provides useful information concerning

the interlaminar stresses at the edge of a hole in a composite plate subjected to uniaxial stress [48]. In another elastic, three-dimensional analysis, Ko and Lin determine the interlaminar stress distributions around a circular hole in balanced, symmetric laminates subjected to in-plane loading [36]. Ko, Lin and Chin extend this analysis by incorporating a failure criteria in conjunction with the aforementioned interlaminar stress determination to predict the delamination initiation load and location [37]. Chang and Chang utilize a nonlinear finite element analysis to determine damage growth in bolted composite joints subjected to tensile loading and to predict the residual strength of the joints containing initial damage. This analysis takes into consideration material and geometrical nonlinearities and accounts for the redistribution of stresses and strains within and near the damaged area in a laminate [50]. Matthews, et. al. applied a new element derived from a standard, 20 noded, isoparametric brick element to determine the interlaminar stress distribution in the vicinity of the hole. This technique was capable of analyzing the bolted joint performance of composite materials having some form lateral constraint such as a torqued fastener [56]. Iarve, et. al. utilized a spline variational method for conducting a three-dimensional stress analysis of drilled and molded open hole composite laminates. Results of this analysis were used in conjunction with a Maximum Stress type failure criteria to predict the onset of failure on a ply-by-ply basis [73, 74].

Fractography of Composite Materials

Fractography of composite materials is a relatively new science. This, along with the fact that the failure mode of a bolted composite joint depends on numerous parameters, makes characterizing these failures very difficult. Nonetheless, some generalizations concerning macroscopic and microscopic features of bolted composite joint failure have been made. Before discussing some of the generalities associated with bolted composite joint failure, it is important to understand the basic mechanism of load transfer which occurs in composite materials. In continuous fiber composite materials the stress is transmitted from fiber to fiber by matrix shear. This shear stress results from the relative displacement which occurs between matrix and fiber. The matrix shear stress will result in a traction at the fiber matrix interface. Failure of the matrix

will occur when the shear stress in the matrix equals the shear strength of that material. Failure of the matrix can be followed by subsequent matrix failures, by failure of the fiber matrix interface or by failure of the fibers themselves. Generally it is assumed that the fiber matrix interface remains intact upon initial fiber fracture. In this case a portion of the load is redistributed over the length of the fractured fiber as the fiber elastically contracts [25].

Macroscopic failures of bolted composite joints can occur by bearing, shear-out, cleavage or net tension, or by a combination of these failure modes, Figure 2. With the exception of the bearing mode, all of these modes occur catastrophically at relatively low levels of stress. Therefore, joints are generally designed such that they fail in a bearing type mode [8]. The mode of failure for bolted composite joints is dependent upon many design and material parameters including fastener material and configuration, bolt spacing, end distance, bolt torque, temperature and moisture effects, material lay-up and material constituent properties [7, 8, 55, 62, 75].

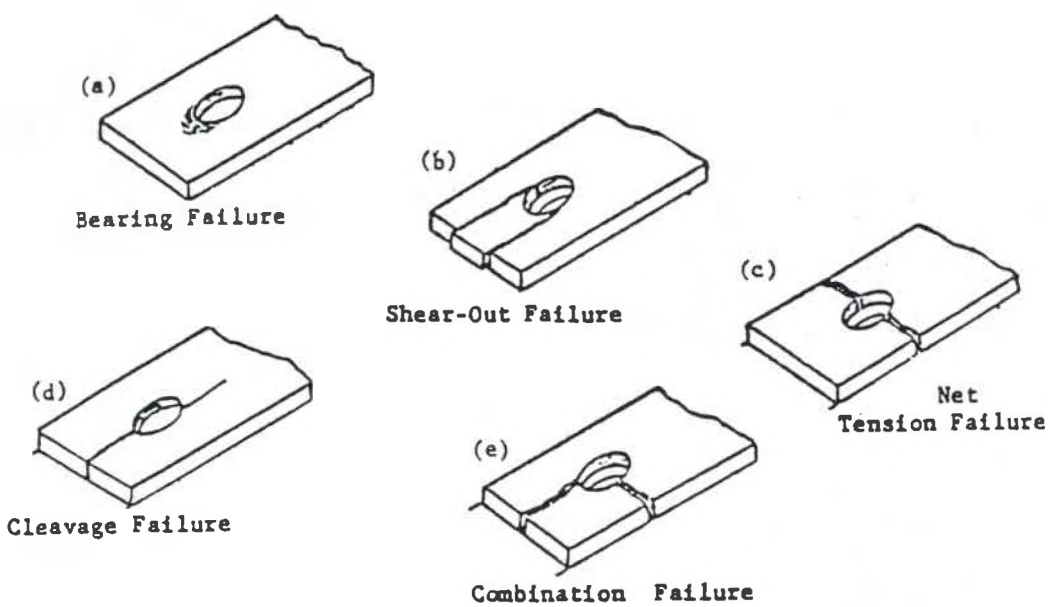

Figure 2. Macroscopic failure modes of bolted composite joints [75].

Bearing failures initiate at approximately 45 degrees with respect to the loading direction and generally involve some hole elongation [7, 64]. Shear-out failures generally initiate at the local bearing point parallel to the loading direction, and are characterized by a "shearing out" of the laminate ahead of the bolt. To design against this mode of failure, laminate thickness, edge distance and laminate shear strength must be considered [7, 55, 64]. Similarly, cleavage failure or wedge type splitting initiates at the local bearing point and propagates to the free edge. Since this type of failure is caused by the lateral pressure of the bolt against the laminate, parameters such as bolt diameter, laminate thickness, edge distance and laminate transverse tensile strength are very important for this mode of failure [7, 55, 75]. Net tension failures initiate perpendicular to the loading direction and propagate to the free edge. This mode of failure depends greatly upon the net-section width, laminate thickness and the laminate tensile strength [55, 75].

Basically, three types of microscopic fractures occur in continuous fiber reinforced composite materials. These include interlaminar, intralaminar and translaminar fractures, Figure 3. All three fracture types can occur under Mode I tension, Mode II in-plane shear or Mode III antiplane shear, Figure 4. Intralaminar fractures occur internally within a ply whereas interlaminar fractures or delaminations occur between plies. Both of these fracture types occur within the laminate plane and are dominated by matrix fracture and fiber/matrix separation with little or no fiber fracture. Continuous fiber reinforced composite materials are particularly susceptible to interlaminar and intralaminar fractures due to their inherent low in-plane fracture resistance. Although all three modes of loading are considered to be critical for joint failures, the majority of interlaminar and intralaminar fractures occur under a combination of Modes I and II type loading. Mode I tension delaminations represent the weakest fracture type. For this case the maximum principal tensile stresses lie perpendicular to the plane of failure, resulting in brittle cleavage type failure of the matrix material. Failures of this type are characterized by river markings and resin microflow. The relative smoothness of the fracture surface is indicative of the crack velocity. In general, smooth surfaces are associated with low crack velocities. The fracture surface of a composite failing by Mode II interlaminar shear is characterized by a rough

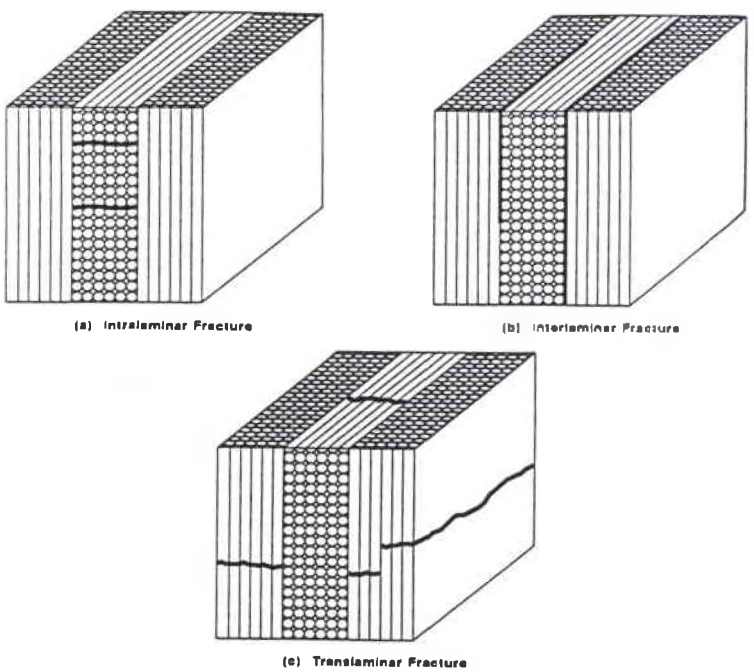

Figure 3. Microscopic fracture types for continuous fiber reinforced composite materials [61].

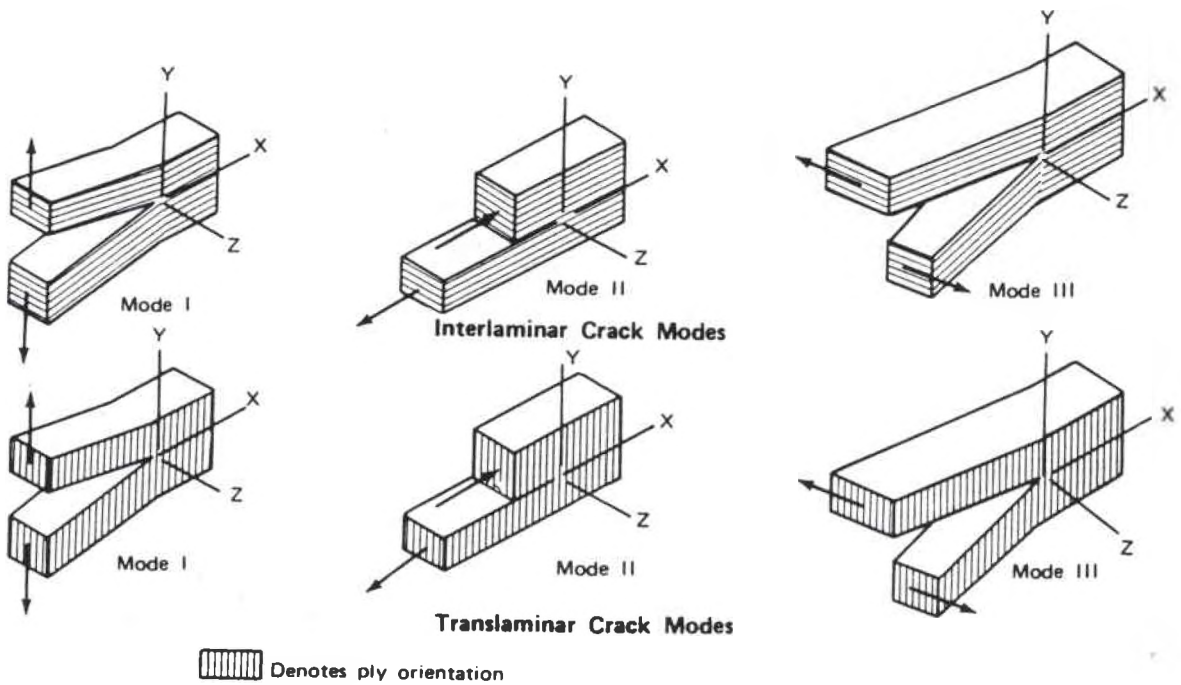

Figure 4. Basic modes of loading for various fracture types [61].

topography and a somewhat dull appearance. These fracture surfaces contain translucent, vertical and parallel resin platelets aligned perpendicular to the direction of crack propagation in relatively narrow fracture zones. Failures due to complex loading such as compression buckling or flexure generally involve interlaminar mixed mode delaminations. Mixed mode delaminations are characterized by a fracture surface containing characteristics of both Mode I tension and Mode II interlaminar shear fractures. In contrast to interlaminar and intralaminar fractures, translaminar fractures occur transverse to the laminated plane and involve significant fiber fracture. Translaminar fractures may occur either in tension or compression. Translaminar tension fractures are characterized by rough topographies containing fiber end fracture, fiber pullout and matrix fracture with little to no delamination. Composites having a strong fiber matrix interface fail in groups or bundles giving the fracture surface a more planar appearance. In this case, the pulled out fibers will generally contain some residual traces of resin on their surface. Conversely, composites having a relatively weak fiber matrix interface will exhibit more complex fracture surfaces. Pulled out fibers in this case will have a smooth surface [16, 25]. Translaminar compression fractures are dominated by fiber buckling, fiber end fracture, resin shear fracture and post-fracture damage. A laminate's lateral through the thickness stability or fiber matrix interfacial strength will determine the amount of fiber buckling which occurs for translaminar compression fractures. For laminates with little lateral stability or poor fiber matrix interfacial strength, compression microbuckling dominates. Microbuckling involves the localized buckling of the individual fibers accompanied by localized delaminations. The kinking of the fiber causes fracture in at least two locations separated by a distance which is approximately equal to five to ten fiber diameters. Laminates exhibiting superior lateral constraint of fiber matrix interfacial strength fail in a shear type mode with the individual fiber ends exhibiting a slant type fracture [16].

Most studies conducted in the area of bolted composite joints involve some fractographic analysis. Compression failure mechanisms at holes have been studied by numerous authors. In most cases, these authors report failure which initiates at the hole and grows in an unstable fashion across the width of the coupon. Initial failure involves the development of a damage zone

which is dominated by local fiber buckling and/ or shear crippling at the hole edge. The fiber buckling and shear crippling is accompanied by local matrix deformation or delamination depending on the ductility of the resin [19-21, 33, 51, 57, 76-80]. Whether delamination precedes fiber microbuckling or not was not evident from the information presented in the literature. Fractographic studies in the area of open hole tension reveal that failure generally occurs through the hole transverse to the direction of loading in a tensile type mode [11, 27, 30]. For off-axis unidirectional coupons, failure was found to initiate at the hole boundary and propagate in a direction parallel to the fibers [70]. The majority of bearing studies conducted reported bearing type failures for their specimens [24, 52, 60, 81, 82].

CHAPTER 3

EXPERIMENTAL PROCEDURES

Materials, Fiber Orientations and Stacking Sequences

The experimental portion of this investigation was designed to provide information concerning the effect of fiber stiffness, matrix properties, stacking sequence and fiber orientation on the open and filled, drilled hole tension and compression performance and drilled hole bearing performance of continuous fiber, polymer matrix composites. In order to determine the effect of fiber stiffness on the aforementioned properties and failure modes, two graphite fibers having significantly different elastic moduli were studied. These fibers included the AS-4 and IM-8 fibers both from Hercules, Inc. Properties of these fibers are listed in Table 1.

TABLE 1

CONSTITUENT MATERIAL PROPERTIES

Constituent	Density [LB/in^3]	Tensile Strength [ksi]	Tensile Modulus [msi]	Tensile Strain [%]
AS-4	0.065	580	32	1.60
IM-8	0.065	770	44	1.61
3501-6	0.046	10	0.643	1.70
APC-2	0.048	13	0.520	5.00

The AS-4 fiber was chosen because it represents a baseline composite constituent for which a large database and much experience exists. This fiber is also commercially available in a variety of matrices and is relatively inexpensive. The IM-8 fiber was chosen because it has significantly higher stiffness and strength than the AS-4 fiber thus allowing for a determination of the effect of fiber stiffness on notched strength performance of composite materials. As indicated from the literature, the notch sensitivity of a composite material is governed largely by the relative toughness of the matrix material. Composites having brittle matrices are regarded as notch

sensitive whereas composites having ductile matrices are regarded as relatively notch insensitive [19-22]. Additionally, the matrix material has been shown to provide lateral support to fibers when a composite structure is subjected to a compressive load. High stiffness matrix materials are capable of providing strong lateral support to the fibers in which case the compressive failure mode is dominated by fiber shearing. Conversely, low stiffness matrix materials do not provide strong lateral support to the fibers in which case the compressive failure mode is dominated by fiber buckling [23, 80]. In order to evaluate the effect of matrix properties on the notched strength performance of composite materials, both a relatively tough thermoplastic matrix material and a relatively brittle thermoset matrix material were used in this investigation. The matrices chosen included Hercules thermoset epoxy, 3501-6 and ICI's thermoplastic matrix material, APC-2. Mechanical properties of these materials are given in Table 1, [83, 84]. The 3501-6 and APC-2 materials were chosen for this investigation because they represent baseline epoxy and thermoplastic matrices, respectively. These materials are well characterized, relatively inexpensive, commercially available and can be processed with relative ease. The four resulting material systems studied in this investigation include:

(1) AS-4/3501-6;
(2) IM-8/3501-6;
(3) AS-4/APC-2;
(4) IM-8/APC-2.

Stiffness discontinuities between plies result in the generation of interlaminar stresses near free edge regions during in-plane loading of composite laminates. It has been shown in previous investigations that interlaminar stresses can have a notable affect on the damage initiation and growth mechanisms in laminated composites [40-43]. Additionally, the strength of the laminate may be significantly reduced by the occurrence of premature delamination and matrix cracking resulting from interlaminar stresses This situation is further complicated in areas of material discontinuities, such as a notch or bolt hole, where the sign and magnitude of the interlaminar stresses fluctuate around the circumference of the hole. It is well known that the nature of the interlaminar stresses occurring at free edges is largely determined by the laminates stacking sequence and fiber orientation [9, 26, 27, 30-40, 44-50, 85]. As defined in Chapter II of

this dissertation, the fiber orientation refers to the direction in which the individual, unidirectional plies are oriented, while the stacking sequence refers to the order in which these plies are placed with respect to one another. If laminate stacking sequence is shown to have an effect on the overall performance of a bolted composite joint, then this indicates that the interlaminar stresses may have a significant effect on the damage initiation mechanisms. In this case, the use of a three-dimensional stress analysis for these joints is required. In order to determine the effect of stacking sequence and interlaminar stresses on the notched strength performance and failure modes of composite materials, several different stacking sequences and fiber orientations were used in this investigation. Originally, the same set of stacking sequences and fiber orientations were to be used for all four material systems. However, some of the graphite/thermoplastic laminates were machined 90 degrees to the desired orientation, resulting in three additional lay-ups. Furthermore, due to the high cost of the IM-8/APC-2 material, only one stacking sequence of the two fiber orientations was examined for that material. The fiber orientations originally chosen for this investigation included a quasi-isotropic orientation consisting of +45, -45, 0 and 90 degree layers and a +60, -60, 0 combination. The quasi-isotropic fiber orientation was chosen as a baseline because it represents a fiber orientation which is commonly used in bolted composite joint applications. The +60, -60, 0 fiber orientation was chosen based on the results of a quick approximation of the relative magnitude of the interlaminar stresses occurring at the free edge. This approximation technique, proposed by Pagano and Pipes, incorporates moment equilibrium at the free edge of the laminate [40-43]. Details of this technique are included in Appendix A. The interlaminar stresses occurring at the straight free edge were considered when choosing this fiber orientation such that undesirable delamination failures initiating at this location would not serve as the initiating or dominant failure mode. Additionally, it was desirable to choose a fiber orientation which would generate significantly different interlaminar stresses than the baseline quasi-isotropic fiber orientation. For both fiber orientations, outer 0 degree layers were avoided under the advice of R. F. Zabora to help prevent premature failure associated with

the testing of untabbed tensile specimens. The resulting fiber orientations and stacking sequences used in this investigation include:

	AS-4/3501-6 & IM-8/3501-6	AS-4/APC-2	IM-8/APC-2
(1)	$[45/90/-45/0]_{2S}$	$[-45/0/45/90]_{2S}$	$[-45/0/45/90]_{2S}$
(2)	$[45/-45/0/90]_{2S}$	$[-45/45/90/0]_{2S}$	
(3)	$[60/0_2/-60]_{2S}$	$[-30/90_2/30]_{2S}$	
(4)	$[60/-60/0_2]_{2S}$	$[60/-60/0_2]_{2S}$	$[30/-30/90_2]_{2S}$

The required composite panels were laid up by hand and processed in the autoclave in accordance with the manufacturers' recommended processing cycles.

A material, lay-up designation code was used to identify the specimens for a particular set of experimental parameters. This designation code consisted of a material number followed by the lay-up number followed by the test type followed by the specimen number, X-Y-T-#.

Where:

MATERIAL	X
AS-4/3501-6	1
IM-8/3501-6	2
AS-4/APC-2	3
IM-8/APC-2	4

LAY-UP	Y
$[45/90/-45/0]_{2S}$	1
$[45/-45/0/90]_{2S}$	2
$[60/0_2/-60]_{2S}$	3
$[60/-60/0_2]_{2S}$	4
$[-45/0/45/90]_{2S}$	5
$[-45/45/90/0]_{2S}$	6
$[-30/90_2/30]_{2S}$	7
$[30/-30/90_2]_{2S}$	8

TEST TYPE	T
Tension	T
Compression	C
Open Hole Tension	OHT
Filled Hole Tension	FHT
Open Hole Compression	OHC
Filled Hole Compression	FHC
Bearing (0.125 in. dia. hole)	Ba
Bearing (0.250 in. dia. hole)	Bb

Therefore, a specimen of the AS-4/3501-6 material having the $[45/-45/0/90]_{2S}$ lay-up tested under filled hole compression testing conditions would be coded as: 1-2-FHC-#.

Quality Control and Physical Properties

To ensure that the materials being tested were free of processing defects, numerous quality control and physical properties tests were conducted. All fabricated and processed panels were subjected to immersion ultrasonic scanning to check for defects such as cracks, voids, matrix rich pockets or changes in thickness. An SRL Model 1750 Mini C ultrasonic inspection system equipped with a reflector plate was used to conduct the through transmission ultrasonic inspections. The inspections were conducted at a sound frequency of five MHz using a three inch focused transducer. A minimum of three material cross-sections were taken from various locations of each panel. These cross-sections were mounted in a room temperature cure epoxy, polished and examined under the microscope for defects such as voids and matrix rich areas. Initially the fiber and void content for each fabricated panel was determined in accordance with the ASTM D 3171-76: Standard Test Method for Fiber Content of Resin-Matrix Composites by Matrix Digestion [86]. However, since this method requires the use of hot sulfuric acid, is very time consuming, produces a large quantity of toxic waste and yields data of questionable accuracy it was later decided to estimate the fiber content, V_f, from the known fiber and resin densities, ρ_f and ρ_r, respectively and the experimentally determined composite density, ρ_c, using the following formula [45]:

$$V_f = ((\rho_c - \rho_r)/(\rho_f - \rho_r)) * 100\% \qquad (1)$$

Fiber volume values generated from the matrix digestion technique and from the approximation technique were compared and agreement to within 7 % was found for the two techniques. Density and specific gravity values were determined for each panel by weighing a small sample in both air and water and using the following formulae:

$$\text{Specific Gravity} = \text{wt (air)}/(\text{wt (air)} - \text{wt (water)}) \qquad (2)$$

$$\rho_c = \text{Specific Gravity} * 0.9975 \qquad (3)$$

A minimum of three samples were taken from each panel for density and specific gravity measurements.

Mechanical Testing

Mechanical testing subjects specifically designed test coupons to controlled loading conditions from which numerical data and fractographic information can be extracted. In the design of bolted, composite, aerospace structures, engineers are interested in strength values and failure characteristics associated with filled hole and notched tensile and compression tests and from bearing tests [67]. Basic material properties are also useful in the design of composite structures and are obtainable from basic laminate properties tests. It is for this reason that numerous mechanical tests were conducted for each of the material, lay-up combinations under investigation.

Prior to testing, specimens were machined from composite panels using a water cooled, diamond impregnated cut-off wheel. The straight sides of the specimens were lightly sanded to the final dimensions. For the open and filled hole compression and tension and bearing specimens, holes were drilled using a carbide drill bit at a speed of 815 RPM. A plywood jig was used to help position the hole correctly and glass/epoxy tab material was placed on both the top and bottom surfaces of the specimen being drilled to help minimize drilling induced damage. The notched specimens were visually inspected and subjected to both reflector plate and pulse echo ultrasonic inspection to check for drilling induced damage. Width and thickness measurements were made at a minimum of three locations along the length of the specimen and the data recorded. Hole diameter measurements were also made. Beveled glass/epoxy tabs were bonded to the bearing and laminate property specimens using a room temperature cure adhesive.

Laminate Property Tests

Laminate property tests were conducted for all four material systems using ASTM standardized test methods to provide basic lamina property data. The tests conducted include longitudinal 0 ^{o} tension (ASTM D3039-76), transverse 90 ^{o} tension (ASTM D3039-76) and in-plane shear, +-45 ^{o} tension (ASTM D3518-76), [86]. Although laminate property data exists for

both the AS-4/3501-6 and AS-4/APC-2 materials, this data was not used in this investigation since material and processing improvements have evolved and the previously generated data may no longer be accurate. Also, available manufacturer's data was not used for these materials because of the reliability concerns which exist with data obtained from this source. Specimen configurations for the laminate property tests are standard and are shown in Figures 5 through 7. A minimum of three specimens were tested for each test setup. Strain measurements were made for a minimum of two specimens for each test setup using rosette type strain gages from Micro Measurements. Tests were conducted on a Instron load frame at a loading rate of 0.05 inches per minute. Load versus strain data was recorded during testing. The resulting load versus strain curves were analyzed and laminate properties calculated in accordance with the formulae provided in reference [86]. Data used in calculating the moduli was obtained from the initial linear region of the load versus strain curves.

Notched Compression and Tension Tests

Unnotched and notched compression and tension tests were conducted for all the material, lay-up combinations under investigation. These tests included: (1) tension; (2) compression; (3) open hole compression; (4) filled hole compression; (5) open hole tension and (6) filled hole tension. A minimum of three and generally five specimens were tested to failure for each test setup. Strain measurements were made for a minimum of two specimens per test setup using both single and rosette type strain gages from Micro Measurements. Longitudinal strain in the compression specimens was measured using back to back strain gages to check for the occurrence of global buckling. Transverse strain was measured on only one side of the compression specimens and longitudinal and transverse strain was measured on only one side of the tension specimens. Strain gages for the unnotched specimens were located at the center of the test specimen whereas strain gages for the notched specimens were placed a distance of 2r or 0.250 inches from the hole edge. A distance of 2r was chosen because strain gages placed at this location measure the local strain but are outside of the strain gradient region associated with the hole [23]. Local strain was measured for the open and filled hole specimens such that

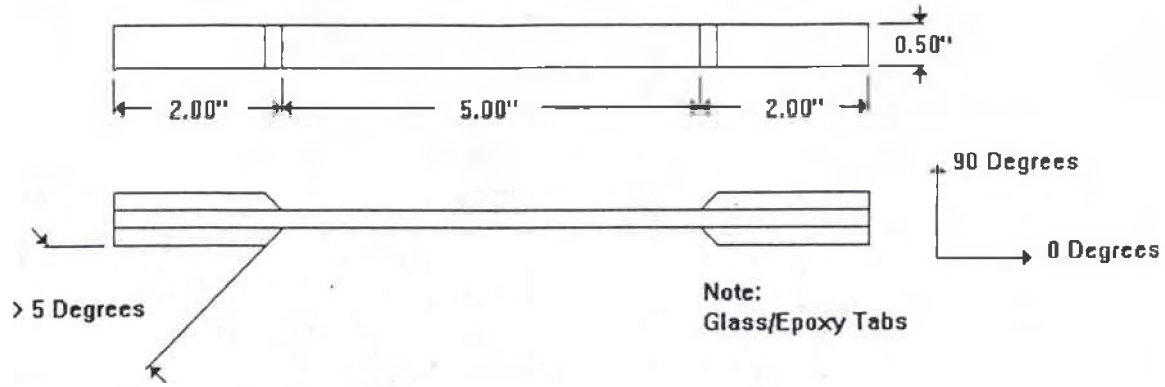

Figure 5. Longitudinal tension specimen.

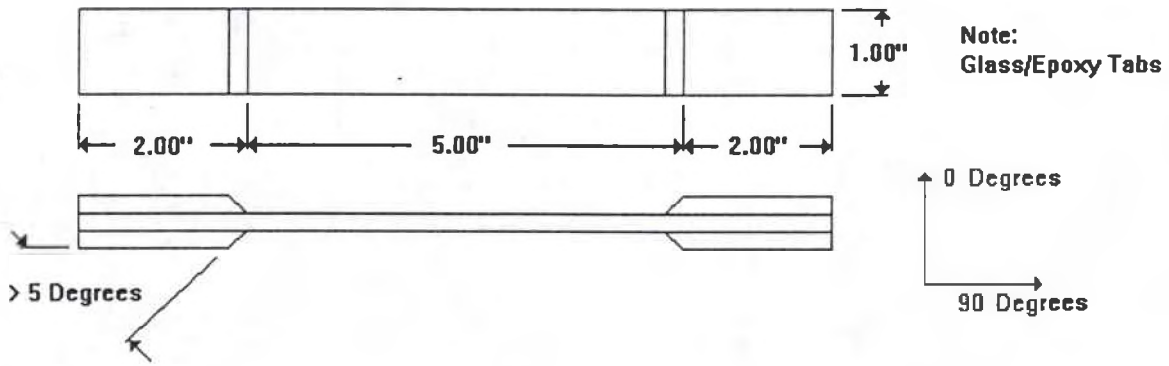

Figure 6. Transverse tension specimen.

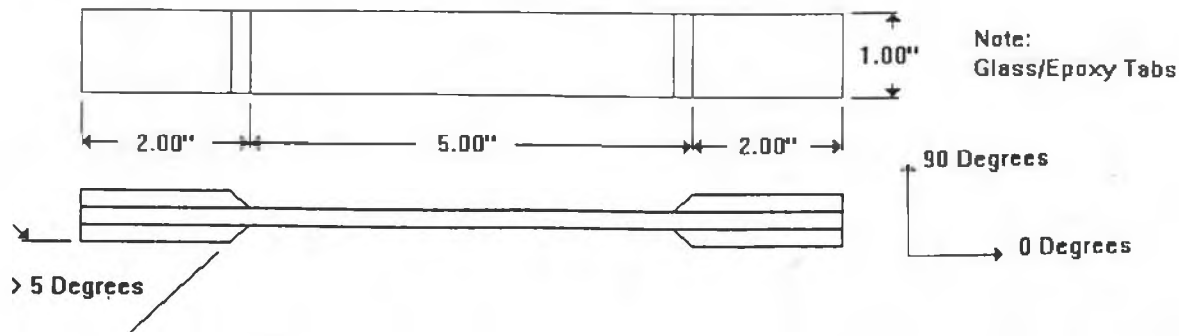

Figure 7. In-plane shear specimen.

information concerning the initiation of failure in the test specimen could be obtained. Acoustic emission was also utilized to monitor damage initiation in open and filled hole compression and tension specimens. The data was recorded in both hits and counts as a function of load. Unnotched, open and filled hole compression and tension tests were conducted on 55 kip MTS load frame using Model 647, 22 kip, side loading, wedge type grips. Tests were conducted at a loading rate of 0.05 inches per minute.

In order to eliminate specimen geometry as a variable in this investigation, consistent specimen configurations for all tension and compression tests were used. These specimen configurations were chosen in accordance with the information provided in the literature [87]. Specimen dimensions were chosen to minimize material usage without jeopardizing the validity of the data. A gage length of five inches was determined to be sufficient to provide uniform loading in the notched area of the specimen. A consistent width to diameter (W/D) ratio of six was used because it was determined to be sufficient to avoid free edge effects and effects due to specimen gripping. Tabless specimens were used to avoid problems associated with specimen tabs including tab failures and variability in the data generated from tab material, tab geometry and adhesive selection [87]. The specimen configuration used for the unnotched, open and filled hole compression and tension tests is shown in Figure 8.

A modified version of the Edge Stabilized Compression fixture designed by R. F. Zabora was used to prevent global buckling of all of the compression specimens. The fixture includes support plates and surfalloy coated grip inserts. The grip inserts were used for both compression and tension testing to avoid any influence of grip insert configuration on the test data. Although several anti-buckling fixtures were considered for this investigation the Zabora design was chosen based on the following merits: (1) The Zabora fixture allows for a variety of specimen sizes; (2) Many other anti-buckling devices such as the basic face plate have a gap between the specimen grip area and the face or edge support plates in which failure of the specimen has been found to occur. The Zabora fixture includes grip inserts containing a male notch. The notch in the grip area mates with a female notch in the edge support platesthus allowing for support over its entire

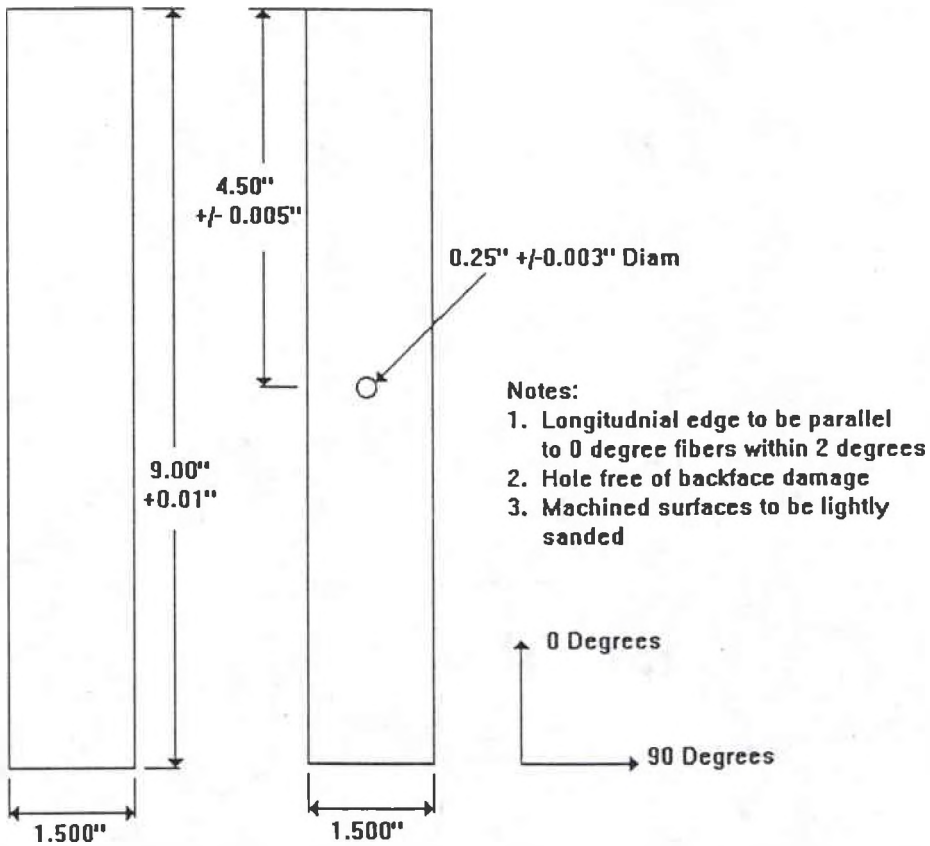

Figure 8. Unnotched, open and filled hole compression and tension test specimen.

length. Elimination of the gap between the grip and face plate helped to prevent unacceptable failures from occurring in the grip area; (3) The Zabora fixture has a large open area or cutout in the center of each support plate. Since compression tests were conducted on filled hole test specimens utilizing protruding head fasteners, an anti-buckling device containing a large open area was a necessary requirement of the fixture used for this investigation. This cutout also allowed for easy access to the specimen so that strain gages could be used during the testing. Additionally, the cutout reduced the amount of specimen surface area in contact with the support plate thereby minimizing the amount of friction generated between specimen and support plate. This helped to reduce the chance of generating misleadingly high test results; (4) The Zabora fixture allowed for shear loading of the test specimens as opposed to end loading. This is desirable because there are many problems associated with the use of end loaded compression specimens. One of the main problems associated with end loaded compression specimens is the need for highly, precision machined specimen ends. If the specimen ends are not parallel and

flat, non-uniform loading of the specimen can occur. Non-uniform loading can significantly affect the buckling and compression strength of the composite as well as the failure mode. Another problem with end loaded compression specimens is the occurrence of unacceptable failure modes such as end brooming.; (5) Surfalloy coating on the grip inserts allowed for the testing of a tabless coupon. The advantages of testing a tabless coupon were discussed earlier [31, 38, 45, 87, 88]. The support plates of the Zabora fixture were modified to accommodate the desired specimen dimensions and the grip inserts were modified to fit the available test machine. The modified fixture is shown in Figure 9. A photograph of the test setup is shown in Figure 10.

The initiation and propagation of damage occurring in bolted composite joints has been shown to be significantly affected by the presence of fasteners. In order to study the effects of fasteners on the compressive and tensile performance of composite materials, filled hole tests were conducted. Titanium (160 ksi UTS), 0.249 inch diameter bolts with accompanying washers and nuts donated by Lockheed Fort Worth Company were used for the testing of the filled hole

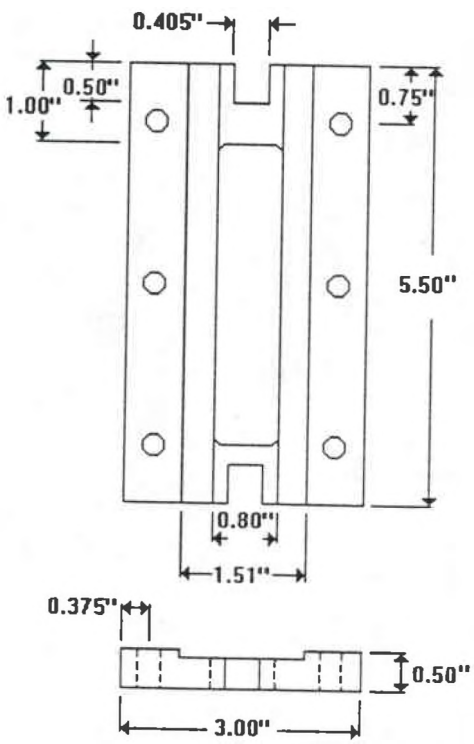

Figure 9. Schematic of support plates of the edge stabilized compression fixture.

flat, non-uniform loading of the specimen can occur. Non-uniform loading can significantly affect the buckling and compression strength of the composite as well as the failure mode. Another problem with end loaded compression specimens is the occurrence of unacceptable failure modes such as end brooming.; (5) Surfalloy coating on the grip inserts allowed for the testing of a tabless coupon. The advantages of testing a tabless coupon were discussed earlier [31, 38, 45, 87, 88]. The support plates of the Zabora fixture were modified to accommodate the desired specimen dimensions and the grip inserts were modified to fit the available test machine. The modified fixture is shown in Figure 9. A photograph of the test setup is shown in Figure 10.

The initiation and propagation of damage occurring in bolted composite joints has been shown to be significantly affected by the presence of fasteners. In order to study the effects of fasteners on the compressive and tensile performance of composite materials, filled hole tests were conducted. Titanium (160 ksi UTS), 0.249 inch diameter bolts with accompanying washers and nuts donated by Lockheed Fort Worth Company were used for the testing of the filled hole

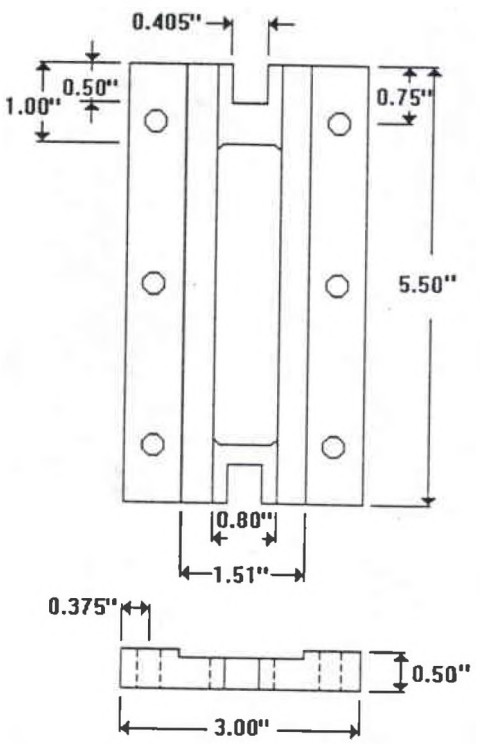

Figure 9. Schematic of support plates of the edge stabilized compression fixture.

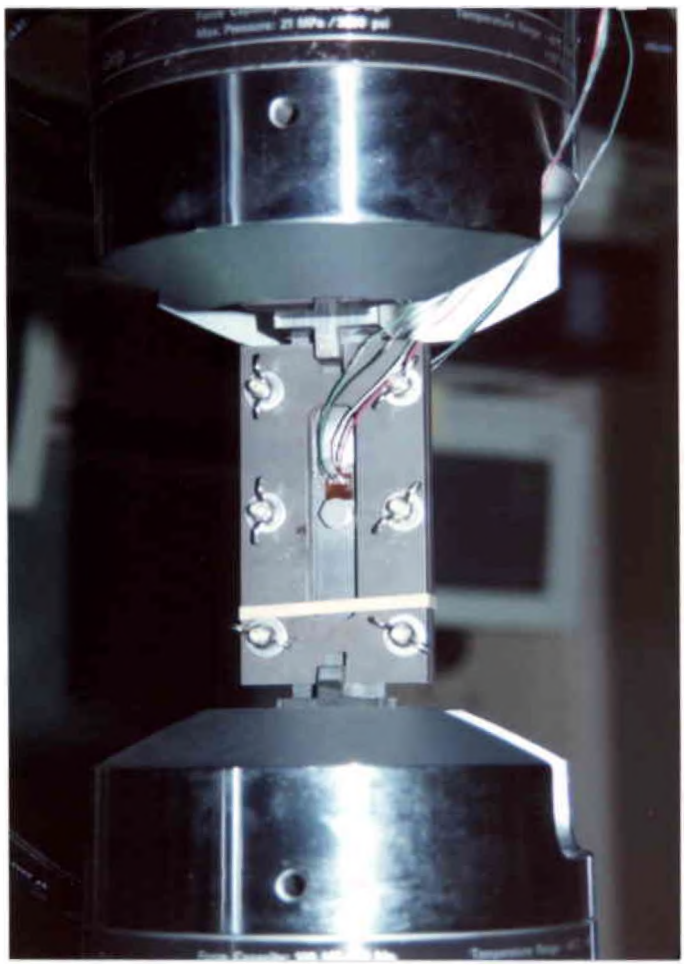

Figure 10. Setup used for unnotched and notched compression tests.

compression and tension specimens. The 0.001 inch difference between the hole and bolt diameter qualifies these bolts as clearance fit fasteners. Clearance fit fasteners were chosen for this investigation to avoid some of the problems associated with the installation of interference fit fasteners including unacceptable delamination type damage to the composite [59]. The fasteners were installed in accordance with the information obtained from the Hi-Shear Corporation [89]. The fasteners were used as protruding head fasteners instead of as countersunk fasteners to avoid the added machining associated with the installation of countersunk fasteners and to simplify bolt installation during testing. Additionally, protruding head fasteners have been found to significantly out perform countersunk fasteners [7]. It is believed that the increase in strength

associated with bolted composite test specimens is due to the lateral constraint provided by the fastener. Two mechanisms have been found to produce this effect. The first mechanism is associated with the washer which acts as a constraint, inhibiting and suppressing delamination and enabling the composite to sustain higher loads. The other mechanism is associated with the friction generated between the washer and the composite which results in a general redistribution of the stresses enabling increased loads to be sustained [9, 26]. The increase in strength has been found to be related to the amount of torque used to tighten the bolt. A torque in the range of 10-40 inch pounds has been found to provide strength increase and difference in failure modes over open hole test results [7, 23, 26, 55, 56, 62]. In order to provide useful information concerning the influence of fasteners on the composite compression and tension performance, bolts were tightened to a torque of 30 inch pounds using a torque wrench. Discussions with industry personnel indicated that a torque of 30 inch pounds is commonly used in the testing of filled hole composite specimens.

Load versus strain data was recorded for the unnotched, open and filled hole compression and tension tests. The resulting curves were analyzed. Both the local stress occurring at the hole and the far field stress were calculated for the notched tension and compression specimens using the following formulae.

$$\sigma_l = P_f / ((w-d)*t) \quad (4)$$

$$\sigma_{ff} = P_f / (w * t) \quad (5)$$

Where:

σ_l	=	local failure stress
σ_{ff}	=	far field failure stress
P_f	=	failure load
w	=	specimen width
t	=	specimen thickness
d	=	hole diameter

Calculated stress values were normalized to a fiber volume of 60%. The initial modulus was calculated for each specimen using the data obtained from the initial linear region of the load versus strain curve.

Bearing Tests

Bearing tests were conducted to provide useful information concerning the loaded hole performance and failure mode of composite materials and because bearing tests are commonly used in industry to characterize composite materials for bolted joint applications. Two bearing hole diameters: (a) 0.125 inch and (b) 0.250 inch were examined to provide information on the effect of hole diameter to composite performance. An end to diameter (E/D) ratio of four was maintained throughout the bearing tests, Figure 11.

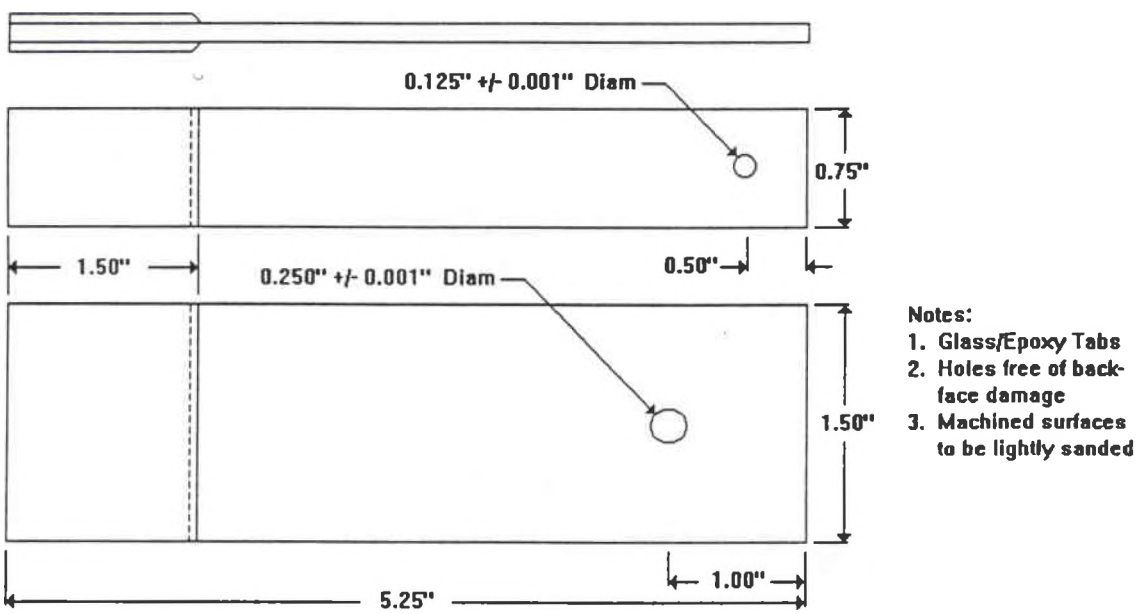

Figure 11. Bearing test specimen configuration.

With the exception of the specimen dimensions, the bearing tests were conducted in accordance with the SACMA recommended method [90]. A minimum of three specimens were tested for each setup. The bearing tests were conducted on an MTS load frame at a loading rate of 0.05 inches per minute. The tabbed end of the specimen was gripped by the load frame. A 0.124 inch and 0.240 inch hardened and ground steel pin was inserted into the 0.125 inch and 0.250 inch

holes, respectively to supply the bearing load. The bearing test set up is shown in Figure 12. The bearing tests were stopped when the first significant drop in load occurred. Bearing stress was calculated for each specimen using the formula given below. Values of bearing stress were normalized to a fiber volume of 60 %.

$$\sigma_{bearing} = P_{bearing} / (t * d) \quad (6)$$

Where:

$\sigma_{bearing}$	=	ultimate bearing strength
$P_{bearing}$	=	bearing failure load
t	=	specimen thickness
d	=	hole diameter

Figure 12. Setup used for conducting the bearing tests.

Fractographic Analysis

Failure of composite materials subjective to compressive stresses is complex in nature. The failure mechanism involves a combination of both local and global phenomenon. In order to fully understand the data generated from any mechanical test and in order to accurately model the stress and strain state generated when a composite material is subjected to a given loading

condition, one must have a full understanding of the nature of the failures occurring within the composite material. Additionally, information concerning failure initiation and propagation is needed in the development and application of any failure criteria. Post failure analysis of tested specimens provides insight into the nature of failure initiation and propagation, the effectiveness of the fiber matrix interface, the occurrence of interlaminar stresses, the occurrence of testing anomalies, the performance of material constituents and other information not attainable from test data alone. It is for the reasons mentioned above that a detailed post failure and incremental loading analysis was conducted on representative tension, compression and bearing test specimens [61].

Post Failure Analysis

Post failure analysis was conducted on tested bearing and open and filled hole compression and tension specimens. The fractographic analysis began with reflector plate and pulse echo ultrasonic inspection of the tested open and filled hole compression and tension specimens. Initially, the tested specimens were subsequently subjected to penetrant-enhanced radiography. However, it was later determined that this inspection technique did not provide any more information than the ultrasonic inspection for the specimens tested to failure. Macrophotographs were taken of each group of test specimens for a particular test setup to show failure uniformity within the group. The front and side surfaces of the damage area for representative test specimens from each group were then examined at low magnification. This information was recorded photographically. Longitudinal and transverse cross-sections were cut from representative test specimens using a low speed, diamond impregnated, water cooled, cut off wheel, Figure 13. Special care was taken to minimize the amount of additional damage generated within the specimen as a result of the cutting procedure. The cross-sections were mounted in a room temperature cure epoxy. The mounted cross-sections were sanded and polished then photomicrographed. The resulting photographs were closely examined and the failures were characterized to the greatest possible extent. Special care was taken to determine the effects of fiber stiffness, matrix stiffness, stacking sequence and the presence of filled and

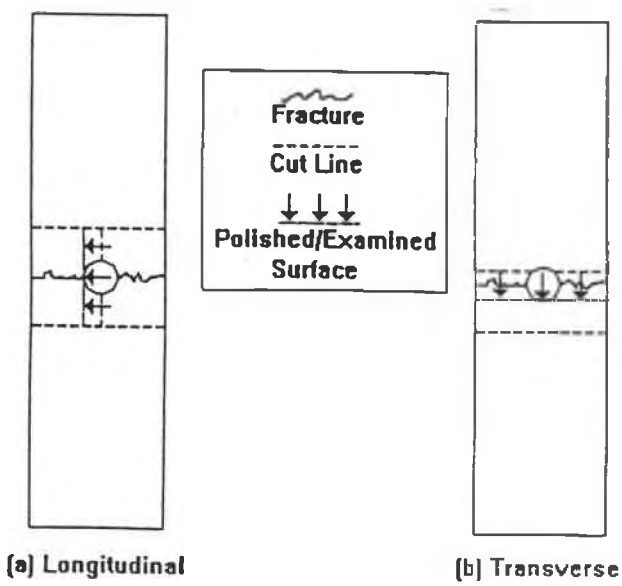

Figure 13. Longitudinal and transverse cross-sections of tested unnotched, open and filled hole tension and compression specimens.

unfilled bolt holes on the final failure mode. The area around the bolt hole in the filled and unfilled compression specimens was examined thoroughly to determine the location of interlaminar stresses and to determine if the fastener was effective in suppressing these stresses. Comparisons were made between filled and unfilled test specimens.

Incremental Loading Study

An incremental loading study was conducted on representative open and filled hole compression and tension specimens to determine the mode of damage initiation and propagation. In this study, the specimens were loaded to a percentage of failure load, removed from the load frame, then subjected to penetrant-enhanced radiography. The applied load was incrementally increased until final failure of the specimen occurred. Damage initiation and propagation was recorded photographically from the resulting radiographs. Originally, the initial loads used for this study were determined for each specimen from the results of the acoustic emissions and from the data generated from a three-dimensional spline variational technique for determining the stress distribution around an open hole [73]. These methods, however, predicted failure initiation to

occur at loads significantly less than what the radiographs showed. Since the majority of the radiographs showed damage initiation to occur at approximately 40 % of failure load, the incremental loading study for subsequent test specimens was initiated at 40 % failure load. Loading of the specimens for this study was accomplished in the manner described in section 3.3.2 of this dissertation. All specimens were subjected to radiography prior to any load being applied so that a baseline radiograph could be established. The specimen were exposed to the radio opaque fluid, zinc iodide, for a minimum of 30 minutes so that the penetrant could sufficiently saturate the specimen. A Phillips X-ray emitting unit equipped with a 25 Kilovolt, 5 milliamp generator tube was used for this study. Resulting radiographs were examined at a light table for areas indicating damage and later made into photographs.

A fractographic study using optical metallography was conducted for select specimens based on the results of the incremental loading study. Once the damage initiation load was determined for a given specimen type, a specimen of the same type was loaded to a similar stress level then subsequently subjected to penetrant enhanced radiography. The resulting radiographs were made into photographs and the photographs were examined for areas indicating damage. Longitudinal cross-sections were taken from the specimens in areas where damage was noted on the radiograph. These cross-sections were mounted, polished and photographed using the techniques described in section 3.4.1 of this dissertation. Resulting photographs were examined and the failure initiation mechanisms were identified to the greatest possible extent.

Statistical Analysis

The effect of a factor or variable is the change in response with transition from the low to the high level. The main effect of a variable measures the average effect of that variable over all conditions of the other variables. If factors do not act additively, then they are said to interact. The difference of means technique is commonly used to calculate and interpret main and interaction effects. In this technique the main effect of a variable is calculated simply by taking the difference of the means obtained at the high and low levels for a given factor. Similarly two

factor interaction effects are calculated by taking one-half of the difference in the average of a factor at the two levels of the interacting factor. Large values obtained for main or interaction effects represent those variables which have a significant effect on the resulting data [91].

In attempts to get an accurate assessment of the effect of the various parameters on the notched strength performance of composite materials, this investigation was designed in such a way that a statistical analysis capable of determining statistically significant effects could be applied. The investigation was set up as a two level, repeated measure factorial design. In this type of experimental design, the investigator selects a fixed number of levels for each of the variables (factors) and then conducts the investigation with all possible combinations. The advantages of the two level factorial design are that very few runs per factor need to be studied to get an indication of the major trends in data, the information generated from these designs is very useful in providing direction for future experimentation or setting up subsequent investigations and finally, the data generated from this type of design can be analyzed and interpreted using elementary arithmetic and common sense [91 - 96].

The variables of interest in this investigation included stacking sequence, lay-up, fiber type, matrix type and test type where test type refers to open versus filled hole. The investigation was originally designed so that the effect of matrix type could be analyzed directly. Experimental error, however, required that the statistical analysis of the data generated from this investigation be broken down into two parts resulting in an indirect analysis of the effect of matrix type. The statistical analysis was conducted independently for the tensile and compressive case. The resulting experimental design is shown in Table 2:

TABLE 2

TWO LEVEL FACTORIAL DESIGN USED IN THIS INVESTIGATION

	THERMOSET MATRIX:		
Variables	Level 1	Level 2	Total Levels
Stacking Seq.	Low	High	2
Lay-up	Low	High	2
Fiber	IM-8	AS-4	2
Test	Open Hole	Filled Hole	2

THERMOPLASTIC MATRIX:

Variables	Level 1	Level 2	Total Levels
Fiber	IM-8	AS-4	2
Test	Open Hole	Filled Hole	2

MATRIX COMPARISON:

Variables	Level 1	Level 2	Total Levels
Matrix	3501-6	APC-2	2
Test	Open Hole	Filled Hole	2

The low level of stacking sequence represents the $[+-45/0/90]_{2s}$ and $[+-60/0_2]_{2s}$ stacking sequences whereas the high level of stacking sequence represents the remaining two stacking sequences. The low level of lay-up corresponds to those lay-ups having 45 ^{o}, 90 ^{o} and 0 ^{o} layers while the high level of lay-up represents those having 0 ^{o} and 60 ^{o} layers. Table 2 describes a 2^4 factorial design for the thermoset matrix materials and a 2^2 factorial design for both the thermoplastic matrix materials and for a comparison of matrix types. Every attempt was made in the design of this investigation to ensure genuine replicate runs where the variation between runs made at some experimental condition is a reflection of the total variability afflicting runs made at different experimental conditions.

The difference of means technique was used to analyze the data generated in this investigation. The degrees of freedom, v, and the pooled estimate of the run variance, s^2, was calculated for each trial. The variance, V, was determined for each effect. An EXCEL spreadsheet was used to carry out the necessary calculations. Details of these calculations are included in Appendix B. Main and interaction effects were plotted on normal probability paper. Those effects which did not lie on a straight line when plotted on normal probability paper corresponded to those effects which could not be explained as having occurred simply as the result of random variation about a fixed mean. From this it was concluded that the changes in the levels of these variables had a statistically significant effect on the outcome of the data. The residuals of the variables not believed to have a significant effect on the data were also plotted on

normal probability paper. This was done as a check to the previous analysis. If all the points from the residual plot were found to lie close to the line, the conjecture that the eliminated effects had a significant effect on the experimental data was confirmed [91, 95, 96].

Two Dimensional Analysis of Stress Concentrations

It is well understood that the stress concentration factor for isotropic materials is the ratio of the maximum tensile hoop stress on the perimeter of the hole and the remote tensile stress applied on the plate. For orthotropic materials, however, this definition of stress concentration factor does not apply. This is apparent in composite materials in the form of a hole size effect for notched tensile specimens. Several techniques for determining the stress concentration factor in orthotropic materials exist. One such method which has shown good agreement with the exact orthotropic solution is the extended isotropic solution proposed by Konish and Whitney [72]. This analysis was applied to the open hole tensile data to determine the effect of fiber type, lay-up and matrix type on the materials ability to dissipate stress concentrations. The information obtained from this two dimensional analysis was compared with the experimental data. Details of this analysis are included in Appendix C.

CHAPTER 4

PARAMETRIC STUDY

Quality Control and Mechanical Testing Results

Quality Control and Physical Property Data

Data obtained from the quality control and physical property tests including ultrasonic inspection, material cross-sections, density, specific gravity and fiber content showed all of the processed panels to be of good quality. Average values obtained from the physical property tests are given in Table 3. The standard deviations are given in parentheses next to the average values. Visual and ultrasonic inspection of the drilled compression, tension and bearing specimens showed some drilling induced damage in a small region surrounding the hole for the graphite/epoxy specimens. Little to no drilling induced damage was noted for the thermoplastic matrix specimens.

TABLE 3

PHYSICAL PROPERTY DATA

Material	Sp. Gravity	Density [LB/in^3]	Fiber Volume [%]
AS-4/3501-6	1.59(7.5E-3)	0.057	60.78 (1.41)
IM-8/3501-6	1.59(2.4E-3)	0.057	61.14 (0.48)
AS-4/APC-2	1.60(1.5E-2)	0.058	59.01 (1.47)
IM-8/APC-2	1.59 (6.1E-3)	0.057	56.30 (1.28)

Laminate Property Data

Results of the laminate property tests including longitudinal 0 ^{o} tension (ASTM D3039-76), transverse 90 ^{o} tension (ASTM D3039-76) and in-plane shear, +-45 ^{o} tension (ASTM D3518-76) are given in Table 4 [86]. The data listed in this table is the average of three to five values. The standard deviations for the data sets are given in parentheses next to the average values. As can be seen from Table 4, the materials containing the IM-8 fibers provided the

highest longitudinal strength and modulus values for a given matrix material. This trend was expected since longitudinal tension data is governed predominantly by the fiber properties and the IM-8 fibers are significantly stronger and stiffer than the AS-4 fibers. Transverse data gives an indication of matrix and interfacial properties. Examination of Table 4 indicates that the thermoplastic matrix material provided greater transverse strength than the epoxy matrix material. The transverse modulus of all four materials was comparable. These results were expected, since the thermoplastic matrix material is inherently stronger than the epoxy matrix material, but not much stiffer. The AS-4 fiber was found to provide the highest transverse strength for the epoxy matrix composites, while the IM-8 fiber provided the highest transverse strength for the thermoplastic matrix composites. This result may indicate that the fiber, matrix interface is stronger for the AS-4 fiber than the IM-8 fiber in the epoxy matrix, but weaker than the IM-8 fiber in the thermoplastic matrix. The shear strength and modulus were found to be greater for the thermoplastic matrix composite materials than for the epoxy matrix composite materials. The Poisson's ratio for all four materials was found to be in the range of 0.29-0.32.

TABLE 4

LAMINATE PROPERTY DATA

Material	E_L [msi]	E_T [msi]	G_{LT} [ksi]	S_L [ksi]	S_T [ksi]	S_{LT} [ksi]	ν_{LT}
AS4/3501-6	17.8(0.17)	1.4(0.02)	701(45)	237(21)	8.3(0.5)	11.7(0.5)	0.31(0.03)
IM8/3501-6	24.1(1.38)	1.5(0.04)	790(28)	268(5)	6.6(0.9)	12.8(0.3)	0.32(0.04)
AS4/APC-2	16.2(6.63)	1.6(0.07)	905(59)	294(11)	10.6(0.5)	27.5(2.7)	0.32(0.06)
IM8/APC-2	23.3(0.71)	1.7(0.02)	909(21)	316(14)	14.0(0.4)	27.5(2.6)	0.29

Compression and Tension Data

Averaged data obtained from the unnotched, open and filled hole tension and compression tests is given in Tables 5 through 10. It should be noted that the majority of the unnotched compression specimens failed in the grip area rather than the gage area. Therefore, the validity of the data obtained from that source is questionable. Normalized values of far field strength are shown graphically in Figures 14 and 15. Moduli data is plotted in Figures 16 and 17 and the tensile and compressive failure strains are shown in Figures 18 and 19.

TABLE 5

UNNOTCHED TENSION DATA

Material	Failure Stress [psi]	Stress Std. Dev. [psi]	Local Normalized Strength(60%) [psi]	Long. Strain [in/in]	Trans. Strain [in/in]	Initial Modulus [psi]
1-1	99475	*6737*	95618	1.38E-02	4.14E-03	7.60E+06
1-2	88412	*2491*	89576	1.32E-02	4.49E-03	7.20E+06
1-3	128503	*3204*	124639	1.22E-02	3.74E-03	1.01E+07
1-4	131137	*9542*	130550	1.29E-02	3.53E-03	1.00E+07
2-1	114726	*6721*	113142	1.25E-02	4.05E-03	9.47E+06
2-2	121394	*2938*	118088	1.22E-02	4.06E-03	9.85E+06
2-3	171702	*9941*	169415	1.16E-02	3.62E-03	1.40E+07
2-4	187317	*14130*	184246	1.22E-02	3.73E-03	1.37E+07
3-5	112879	*8571*	114734	1.57E-02	4.93E-03	7.22E+06
3-6	107239	*10960*	107382	1.49E-02	4.73E-03	7.56E+06
3-7	90846	*3500*	90529	1.27E-02	2.53E-03	5.83E+06
3-4	156052	*16793*	156653	1.02E-02	6.15E-03	1.03E+07
4-5	148108	*11002*	156783	1.51E-02	5.42E-03	9.37E+06
4-8	104925	*4323*	112199	1.29E-02	2.51E-03	7.84E+06

TABLE 6

Material	Local Failure Stress [psi]	Local Stress Std. Dev. [psi]	Local Normalized Strength [psi]	Far Field Failure Stress [psi]	Far Field Normalized Strength [psi]	Long. Strain [in/in]	Trans. Strain [in/in]	Initial Modulus [psi]
1-1	61674	*3184*	59283	51435	49441	4.91E-03	1.52E-03	1.17E+07
1-2	54409	*4948*	55126	45404	46002	4.73E-03	1.58E-03	1.04E+07
1-3	86181	*6969*	83590	72061	69894	5.03E-03	1.89E-03	1.60E+07
1-4	90753	*3029*	90346	75710	75371	5.59E-03	1.42E-03	1.49E+07
2-1	79610	*9073*	78511	66443	65526	5.14E-03	1.71E-03	1.41E+07
2-2	79134	*7584*	76979	66033	64234	5.44E-03	1.44E-03	1.37E+07
2-3	126563	*12117*	124877	105559	104153	4.80E-03	1.23E-03	2.15E+07
2-4	132744	*6802*	130568	110829	109012	4.98E-03	2.45E-03	2.21E+07
3-5	61031	*7987*	62034	50918	51755	5.14E-03	1.55E-03	1.11E+07
3-6	62923	*2012*	63007	52554	52624	4.46E-03	1.51E-03	1.14E+07
3-7	55097	*967*	54905	46030	45869	6.11E-03	1.14E-03	9.25E+06
3-4	92194	*4167*	92549	77052	77349	5.03E-03	1.88E-03	1.63E+07
4-5	80623	*4371*	85345	67288	71229	5.28E-03	1.61E-03	1.42E+07
4-8	75009	*2523*	80209	62655	66999	6.26E-03	1.07E-03	1.19E+07

TABLE 7

FILLED HOLE TENSION DATA

Material	Local Failure Stress [psi]	Local Stress Std. Dev. [psi]	Local Normalized Strength [psi]	Far Field Failure Stress [psi]	Far Field Normalized Strength [psi]	Long. Strain [in/in]	Trans. Strain [in/in]	Initial Modulus [psi]
1-1	62824	*4057*	60388	52488	50453	5.66E-03	1.51E-03	9.48E+06
1-2	56258	*1985*	56999	46977	47596	5.27E-03	1.49E-03	9.41E+06
1-3	83471	*6912*	80961	69727	67630	5.04E-03	1.84E-03	1.42E+07
1-4	88139	*2884*	87744	73601	73271	5.76E-03	1.43E-03	1.40E+07
2-1	85013	*7073*	83839	70944	69964	5.70E-03	1.80E-03	1.22E+07
2-2	82890	*3106*	80632	69116	67233	5.55E-03	1.65E-03	1.28E+07
2-3	128487	*4170*	126776	107115	105688	5.24E-03	1.35E-03	2.11E+07
2-4	124566	*6280*	122524	103813	102111	5.06E-03	2.05E-03	1.82E+07
3-5	63830	*3225*	64879	53274	54149	5.91E-03	1.80E-03	9.05E+06
3-6	67629	*4987*	67719	56509	56584	6.49E-03	1.70E-03	8.35E+06
3-7	59391	*2475*	59184	49696	49523	6.41E-03	1.05E-03	8.55E+06
3-4	90825	*1220*	91175	75959	76251	5.40E-03	1.77E-03	1.28E+07
4-5	90749	*3846*	96065	75811	80252	6.32E-03	1.88E-03	1.88E+07
4-8	80249	*2340*	85813	66998	71643	7.07E-03	1.02E-03	1.13E+07

TABLE 8

UNNOTCHED COMPRESSION DATA

Material	Failure Stress [psi]	Normalized Strength [psi]
1-1	83401	80168
1-2	94568	95814
1-3	97101	94181
1-4	113716	113207
2-1	92206	90933
2-2	96714	94080
2-3	92499	91267
2-4	111278	109454
3-5	86895	88323
3-6	92954	93078
3-7	77287	77017
3-4	84486	84811
4-5	84101	89027
4-8	69084	73873

TABLE 9

OPEN HOLE COMPRESSION DATA

Material	Local Failure Stress [psi]	Local Stress Std. Dev. [psi]	Local Normalized Stress [psi]	Far Field Failure Stress [psi]	Far Field Normalized Strength [psi]	Long. Strain [in/in]	Trans. Strain [in/in]	Initial Modulus [psi]
1-1	57486	*5199*	55257	48061	46198	4.84E-03	1.37E-03	1.10E+07
1-2	55213	*1916*	55940	46117	46724	4.89E-03	1.05E-03	1.12E+07
1-3	82167	*3740*	79696	68656	66592	5.03E-03	1.07E-03	1.63E+07
1-4	82458	*6111*	82089	68846	68538	5.40E-03	2.23E-03	1.63E+07
2-1	58179	*1507*	57376	48510	47840	4.16E-03	1.08E-03	1.39E+07
2-2	56968	*5844*	55416	47596	46300	3.45E-03	7.80E-04	1.42E+07
2-3	80102	*6514*	79035	66799	65909	3.68E-03	2.22E-03	2.03E+07
2-4	70865	*10277*	69703	59068	58100	2.78E-03	6.45E-03	2.13E+07
3-5	51721	*3732*	52571	43167	43876	4.27E-03	1.47E-03	1.17E+07
3-6	56722	*1551*	56798	47356	47419	4.95E-03	1.20E-03	1.13E+07
3-7	59343	*997*	59136	49537	49364	6.19E-03	1.05E-03	9.46E+06
3-4	72664	*6076*	72944	60766	61000	4.33E-03	1.36E-03	1.60E+07
4-5	51414	*2400*	54426	42939	45454	3.62E-03	1.01E-03	1.47E+07
4-8	55981	*1979*	59862	46735	49975	4.46E-03	3.00E-04	1.11E+07

TABLE 10

FILLED HOLE COMPRESSION DATA

Material	Local Failure Stress [psi]	Local Stress Std. Dev. [psi]	Local Normalized Strength [psi]	Far Field Failure Stress [psi]	Far Field Normalized Strength [psi]	Long. Strain [in/in]	Trans. Strain [in/in]	Initial Modulus [psi]
1-1	106151	*10324*	102036	88638	85202	9.38E-03	3.42E-03	9.36E+06
1-2	97364	*9333*	98646	81340	82411	9.87E-03	3.76E-03	9.76E+06
1-3	101824	*8447*	98762	85115	82556	7.62E-03	3.75E-03	1.39E+07
1-4	106060	*5718*	105585	88594	88197	7.64E-03	3.38E-03	1.32E+07
2-1	94710	*7433*	93402	79012	77921	8.29E-03	2.13E-03	1.21E+07
2-2	91500	*4839*	89008	76272	74195	7.67E-03	1.70E-03	1.32E+07
2-3	106398	*3972*	104981	88827	87644	5.81E-03	2.22E-03	1.90E+07
2-4	104573	*5220*	102859	87213	85783	6.26E-03	1.83E-03	1.79E+07
3-5	95705	*4115*	97278	79973	81287	9.15E-03	2.91E-03	8.90E+06
3-6	102553	*8122*	102690	85593	85707	9.30E-03	3.92E-03	9.40E+06
3-7	90237	*4009*	89922	75414	75151	1.13E-02	2.27E-03	7.23E+06
3-4	107967	*7458*	108382	90115	90462	7.65E-03	2.42E-03	1.19E+07
4-5	93627	*5524*	99111	78114	82689	7.80E-03	2.85E-03	1.23E+07
4-8	77584	*4088*	82963	64740	69228	8.06E-03	1.22E-03	2.01E+07

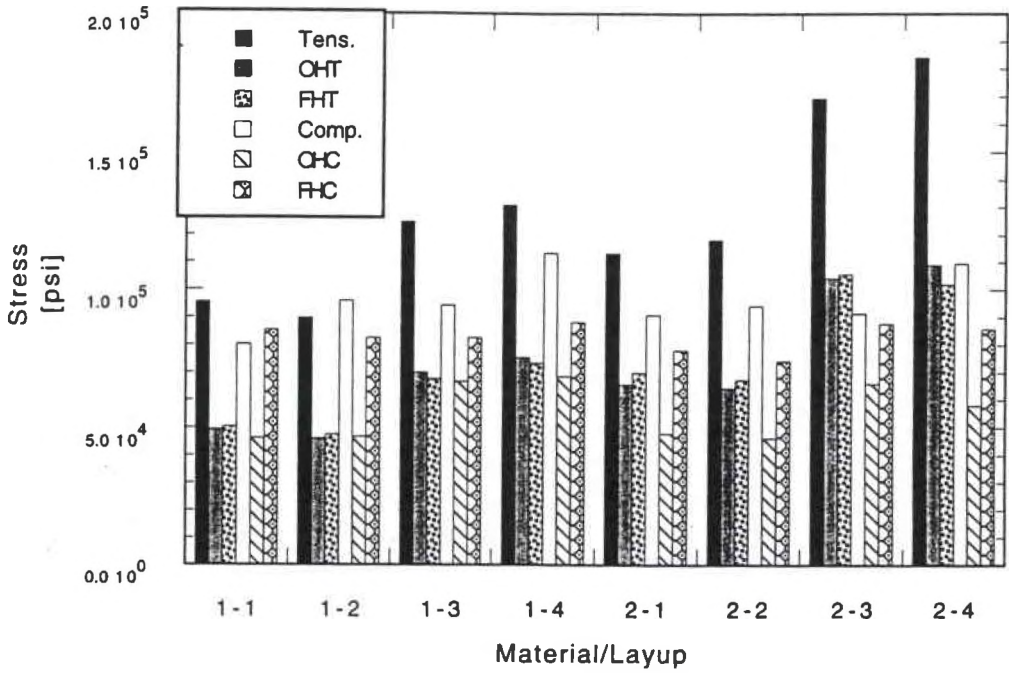

Figure 14. Far field normalized failure stress for the graphite/epoxy materials.

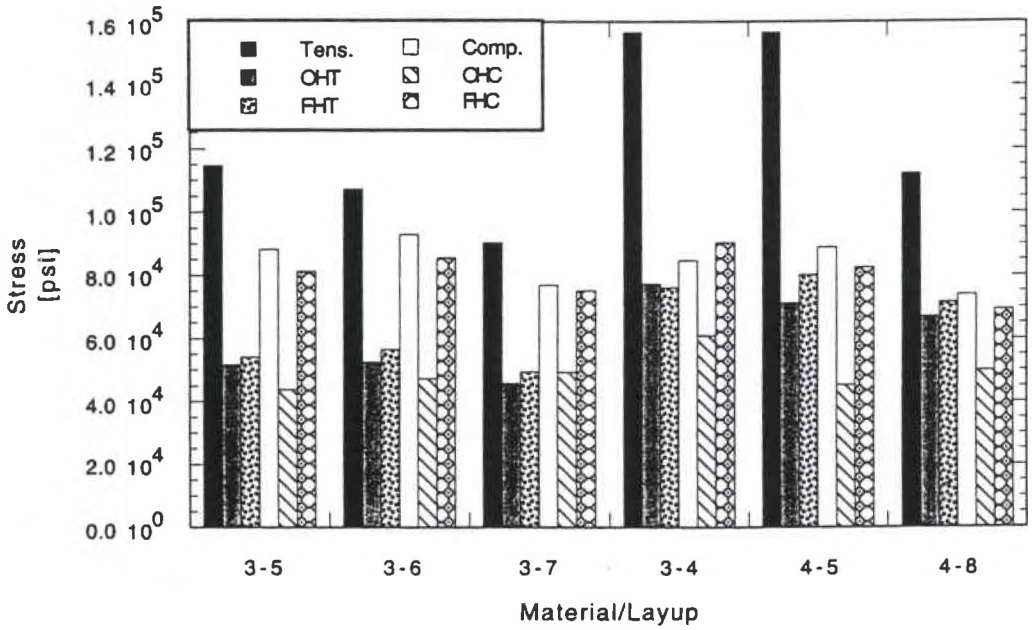

Figure 15. Far field normalized failure stress for the graphite/PEEK materials.

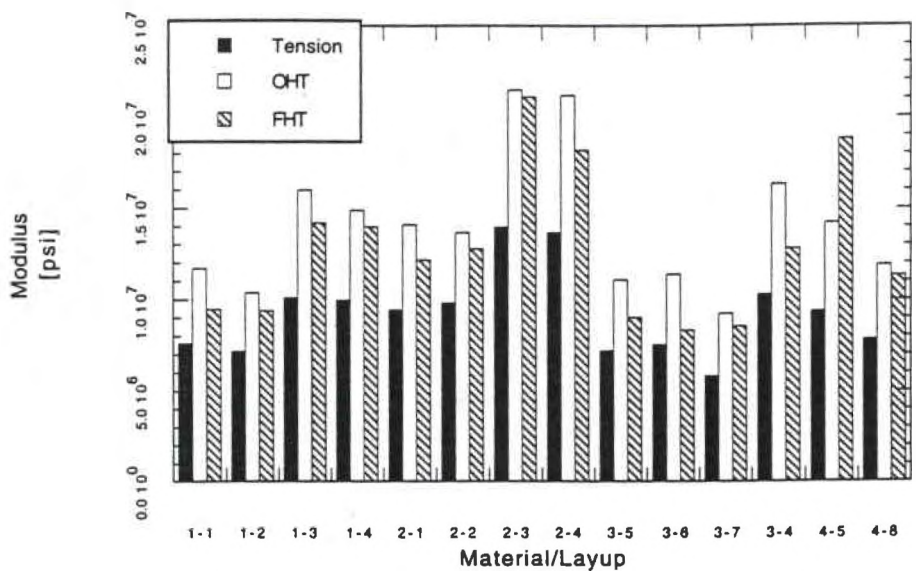

Figure 16. Unnotched, open and filled hole tensile moduli for the various material, lay-up combinations.

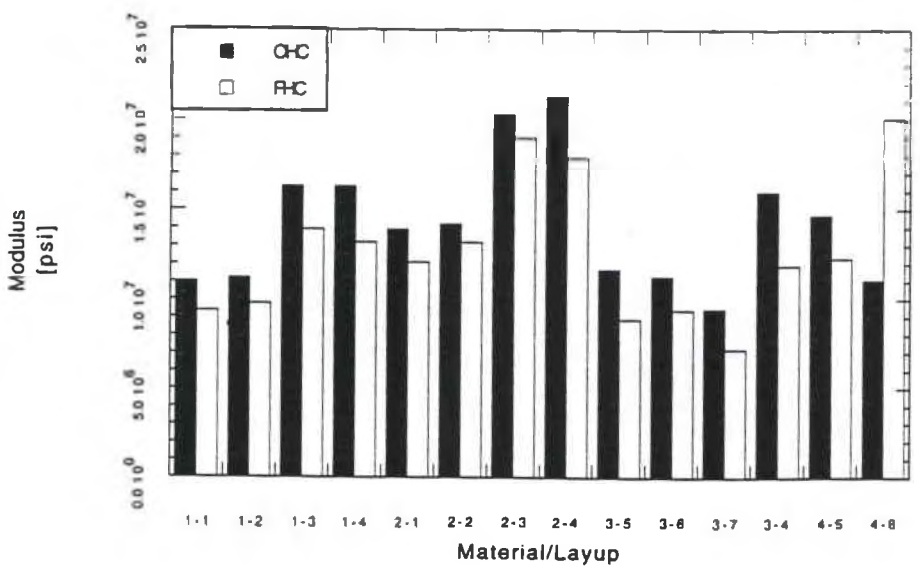

Figure 17. Open and filled hole compressive moduli for the various material, lay-up combinations.

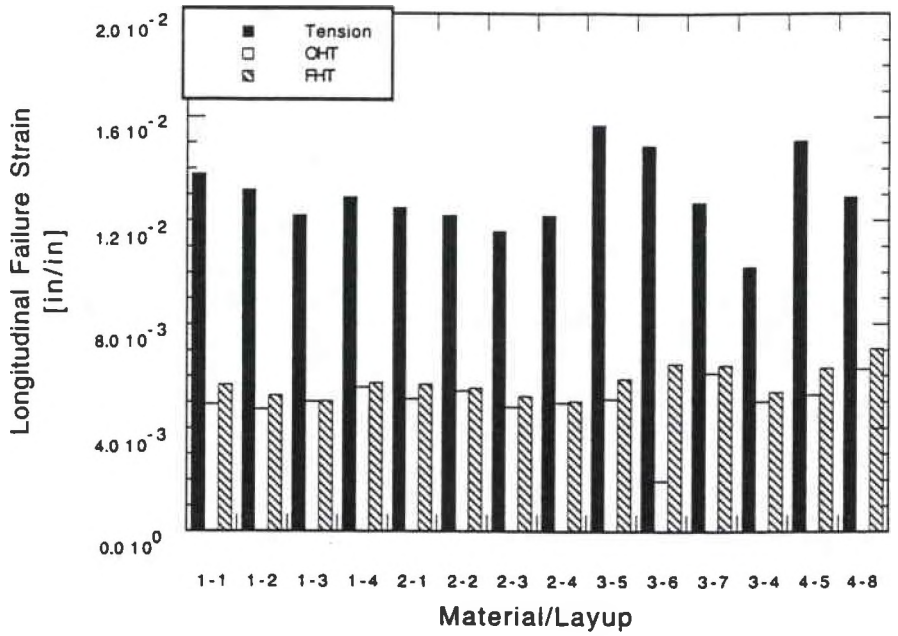

Figure 18. Unnotched, open and filled hole tensile failure strain for the various material, lay-up combinations.

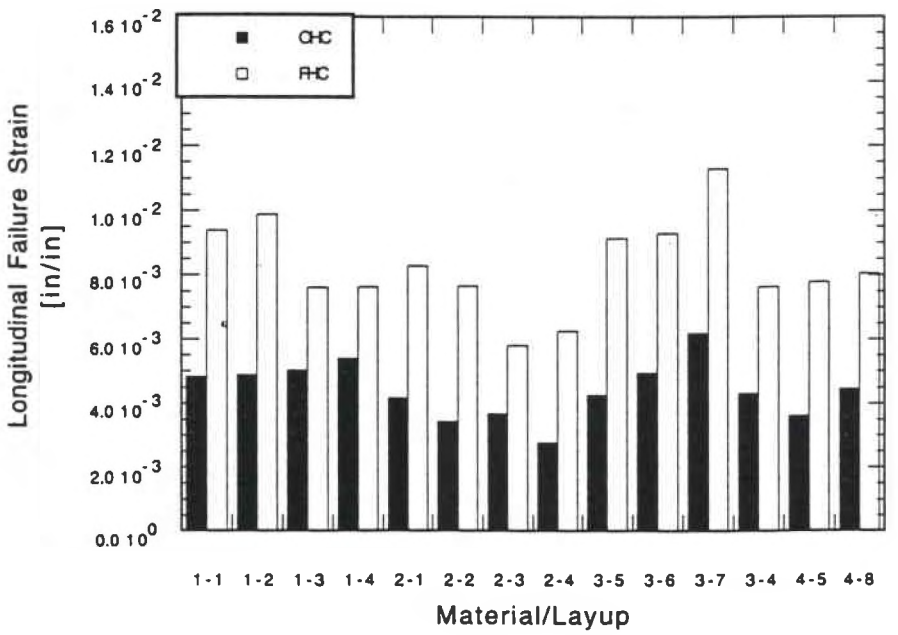

Figure 19. Open and filled hole compressive failure strain for the various material, lay-up combinations.

Data obtained for the open versus filled hole tension specimens indicated no significant difference in the tensile strength for any of the material, lay-up combinations studied. Conversely, the filled hole compression specimens were found to provide significantly higher strengths than the open hole compression specimens. The higher compression strengths obtained for the filled hole compression specimens may be attributed to the presence of the torqued fastener which provided lateral constraint to the notched test specimen. The lateral constraint provided by the fastener may have helped to inhibit and constrain ply delaminations and transverse cracking from occurring at the hole edge, thereby allowing the filled hole compression specimens to sustain higher loads then the open hole compression specimens. Additionally, it is believed that the friction generated between the washer and the laminate in the filled hole test specimens helped to redistribute the stresses to a region away from the hole edge [7, 9, 14, 16, 55, 56 58, 79]. The stress redistribution associated with the presence of the washer was apparent for the filled hole compression specimens as failure occurred predominantly at the washer edge instead of the hole edge. Since no discernible difference was detected for the open versus filled hole tensile specimens, interlaminar stresses and the failure modes associated with these stresses may not be a critical factor in the notched tensile performance of composite materials. The observation that the presence of the fastener had a significant effect on the strength of notched compression specimens but no effect on the strength of notched tensile specimens may be attributed to the difference in critical failure modes for the tensile versus compressive case. For compressively loaded specimens the critical failure mode generally is buckling. In this type of failure mode the occurrence of delaminations can result in a loss of lateral support to neighboring plies causing premature ply buckling. The critical failure mode for tensile specimens is a tensile type failure dominated by fiber fracture. The presence of delaminations has little effect on the initiation and propagation of tensile type failures.

Examination of plotted unnotched, open and filled hole tensile strength reveals that for a given lay-up of both matrix materials, the IM-8 fiber provided superior strength. This trend was expected since the majority of the tensile specimens failed macroscopically in a fiber dominated

mode where constituent fiber strength significantly affects the resulting composite strength. Therefore, composites containing the inherently stronger IM-8 fibers were able to outperform composites containing the AS-4 fibers. The effect of constituent fiber strength was found to be more apparent for the lay-ups containing a greater percentage of 0 degree plies where tensile strength becomes more dependent upon fiber strength. The superior notched tensile performance of composites containing the IM-8 fibers may also be attributed to the higher modulus of the IM-8 fibers. Naik and Sai Ram found that composites containing higher modulus fibers had lower stress concentrations factors resulting in superior notched strength performance for these materials [22]. It has been suggested that composites having a weaker fiber, matrix interface may have inferior compressive properties. This is due to the fact that premature fiber matrix failure can result in a loss of lateral support provided to the fibers by the matrix material, thereby allowing the fibers to buckle at low levels of stress [25]. Although the laminate property data indicated different interfacial strengths for the two fibers, values obtained for the open and filled hole compression strengths of the IM-8 and AS-4 fibers in both the epoxy and PEEK matrix composites were found to be very comparable. This result suggests that the fiber, matrix interfacial strength may not have a significant effect on the notched compression strength or failure mode for these materials. No consistent trend could be noted in regards to the effect of fiber type on the unnotched compression strength since the majority of these specimens did not fail in the gage area.

Comparison of the data obtained for lay-up four of the AS-4/3501-6 and AS-4/APC-2 materials revealed that the thermoplastic matrix provided superior unnotched, open and filled hole tensile strength. The superior performance of the graphite/PEEK material for tensile loading can be explained by two phenomena. The first of these is associated with the higher strength and toughness of the PEEK matrix over the epoxy matrix material which translates into superior composite tensile performance. The second phenomena is associated with the matrix material's ability to provide stress relief in the vicinity of the hole. Guynn and Bradley showed that composite materials having a more ductile matrix allow for a greater degree of stress relief to

occur. This results in lower stress concentration factors, thereby making these materials less notch sensitive [23]. For the case of compressive loading, however, the epoxy matrix composites were found to outperform the PEEK matrix composites. This apparent contradiction of Guynn and Bradley's conclusion regarding the effect of matrix properties on the notch sensitivity of composite materials can be explained by the fact that different mechanisms are responsible for determining the ultimate strength of notched composites loaded in tension and compression. Notched tensile specimens generally fail in a rather simple type tensile failure mode. In this case, the material's ability to dissipate stress concentrations at the hole is an important parameter in determining the ultimate strength of the composite material. For compressive loading however, failure of the composite is governed largely by the occurrence of fiber buckling and kink band formation. As indicated previously, the matrix material provides lateral support to the fibers which helps to constrain the fibers and make them more resistant to buckling and kinking. The degree of lateral support which a matrix material provides to it's fibers is dependent upon the stiffness properties of the matrix material. The higher stiffness of epoxy matrix material versus the PEEK matrix material may have allowed for a greater degree of lateral support provided to the fibers by the epoxy matrix material.

Unnotched, open and filled hole tensile and compressive values obtained for the different stacking sequences for all four of the materials studied were found to be fairly comparable. Some difference in strength was noted for the various lay-ups. For the graphite/epoxy material, lay-ups containing the 0 and 60 degree layers (lay-ups 3 & 4) were found to outperform those containing 0, 45 and 90 degree layers (lay-ups 1 & 2) for the case of unnotched, open and filled hole tensile and open hole compression loading. For the case of filled hole compression, no major difference in strength could be noted for the various lay-ups. The $[60/-60/0_2]_{2S}$ lay-up (lay-up 4) was found to outperform the $[-45/0/45/90]_{2S}$ and $[-45/45/90/0]_{2S}$ (lay-ups 5 & 6) for the case of unnotched, open and filled hole tensile and compressive performance of the AS-4/APC-2 material. The $[-45/0/45/90]_{2S}$ and $[-45/45/90/0]_{2S}$ lay-ups (lay-ups 5 & 6) were found to provide higher unnotched, open and filled hole tensile and filled hole compressive strength than the $[30/90_2/-30]$

$_{2S}$ lay-up (lay-up 7). This result can be attributed largely to the fact that the [30/90$_2$/-30] $_{2S}$ lay-up (lay-up 7) is made up only 90 and 30 degree plies making the data generated from the tests largely a reflection of the materials matrix properties instead of the fiber properties. For the IM-8/APC-2 material, the [-45/0/45/90]$_{2S}$ lay-up (lay-up 5) was found to outperform the [30/-30/90$_2$]$_{2S}$ (lay-up 8) for all but the open hole compression case. In this case, lay-ups five and eight were found to provide similar failure strengths.

As expected, the tensile and compressive moduli were greatest for the open hole case for a given material, lay-up combination. The composite tensile and compressive moduli were found to accurately reflect the composite's fiber constituent properties in that the IM-8/3501-6 and IM-8/APC-2 materials had higher moduli than that of the AS-4/3501-6 and AS-4/APC-2 materials, respectively. No significant difference was noted in the composite tensile and compressive moduli for the epoxy and PEEK matrix materials for a given fiber and lay-up.

For all material, lay-up combinations the longitudinal strain to failure was found to be lowest for the open hole tensile and compressive case and highest for the unnotched tensile and filled hole compressive case. The effect of matrix material on strain to failure was found to be dependent upon the material stacking sequence. Fiber type appeared to have little effect on the tensile failure strain, but some effect on the compressive failure strain. In general, the IM-8 fiber was found to have a lower strain to failure than the AS-4 fiber. This result cannot be accurately related to the constituent properties, since accurate compressive fiber properties do not exist. Lay-up and stacking sequence were found to have very little effect on the tensile failure strain. Some effect of lay-up and stacking sequence on compressive failure strain was noted, but no consistent trends could be determined.

Data obtained from acoustic emissions is given in Table 11. An attempt was made to correlate the first peak in the acoustic emissions output with the initial change in slope of the load strain curve for AS-4/3501-6 test specimens in Table 12. This was done in an effort to identify the load at which failure initiated in the test specimen. In some cases there was good correlation between these values and in other cases there was little correlation between these values.

TABLE 11

RESULTS OF THE ACOUSTIC EMISSIONS OUTPUT

MATERIAL	LAY-UP	INITIAL ACOUSTIC EVENT OHT [lbs]	FHT [lbs]	OHC [lbs]	FHC [lbs]
AS-4/3501-6	1	3200	4000	2200	4000
AS-4/3501-6	2	2800	3200	2000	3600
AS-4/3501-6	3	3900	5800	1800	1800
AS-4/3501-6	4	1800	4000	2200	1600
IM-8/3501-6	1	2600	4300	1800	700
IM-8/3501-6	2	1100	3900	1400	1800
IM-8/3501-6	3	3000	4750	2500	1500
IM-8/3501-6	4	1750	1500	1000	2000
AS-4/APC-2	5	2700	2900	1100	1100
AS-4/APC-2	6	900	700	900	600
AS-4/APC-2	7	1300	650	1300	1100
AS-4/APC-2	4	2100	9600	2200	1000
IM-8/APC-2	5	1600	1400	2100	3200
IM-8/APC-2	8	3500	400	900	1600

TABLE 12

CORRELATION OF THE ACOUSTIC EMISSIONS OUTPUT WITH CHANGE IN MODULUS

MATERIAL	LAY-UP	LOADING CONDITION	FAILURE LOAD [lbs]	Δ MODULUS LOAD [lbs]	AE LOAD [lbs]
AS-4/3501-6	1	TENSION	12960	6250	5600
AS-4/3501-6	1	OHT	6100	3800	3200
AS-4/3501-6	1	FHT	6545	1000	4000
AS-4/3501-6	1	OHC	5670	2925	2200
AS-4/3501-6	1	FHC	9750	1850	4000
AS-4/3501-6	2	TENSION	11800	5750	3400
AS-4/3501-6	2	OHT	5600	2900	2800
AS-4/3501-6	2	FHT	6170	1075	3200
AS-4/3501-6	2	OHC	6170	LTF	2000
AS-4/3501-6	2	FHC	10540	2700	3600
AS-4/3501-6	3	TENSION	16900	4950	6800
AS-4/3501-6	3	OHT	9660	4245	3900
AS-4/3501-6	3	FHT	9525	1985	5800
AS-4/3501-6	3	OHC	8665	5900	1800
AS-4/3501-6	3	FHC	10300	3700	1800
AS-4/3501-6	4	TENSION	17100	7650	6400
AS-4/3501-6	4	OHT	10065	4825	1800
AS-4/3501-6	4	FHT	9715	2200	4000
AS-4/3501-6	4	OHC	9475	8100	2200
AS-4/3501-6	4	FHC	11550	5900	1600

Noise associated with test fixturing may have produced false peaks in the acoustic emissions output which may explain the lack of correlation between acoustic emissions peaks and modulus data. Due to the lack of correlation between the acoustic emissions output and an initial change in modulus for the AS-4/3501-6 material, a similar analysis was not conducted for the remaining three materials.

Bearing Data

Data obtained from the bearing tests is given in Table 13 and shown graphically in Figures 20 and 21.

TABLE 13

BEARING DATA

Material	Bearing a Stress [psi]	Normalized Bearing a [psi]	Bearing b Stress [psi]	Normalized Bearing b [psi]
1-1	66490	63912		
1-2	70570	71499	58700	59473
1-3	68720	66654		
1-4	71450	71130	56350	56098
2-1	69930	68964	61700	60848
2-2	68860	66984	61260	59591
2-3	67600	66700	60720	59911
2-4				
3-5	74880	76110	70640	71801
3-6	73920	74019	73220	73318
3-7				
3-4	72500	72779	68710	68974
4-5	67980	71962	69450	73518

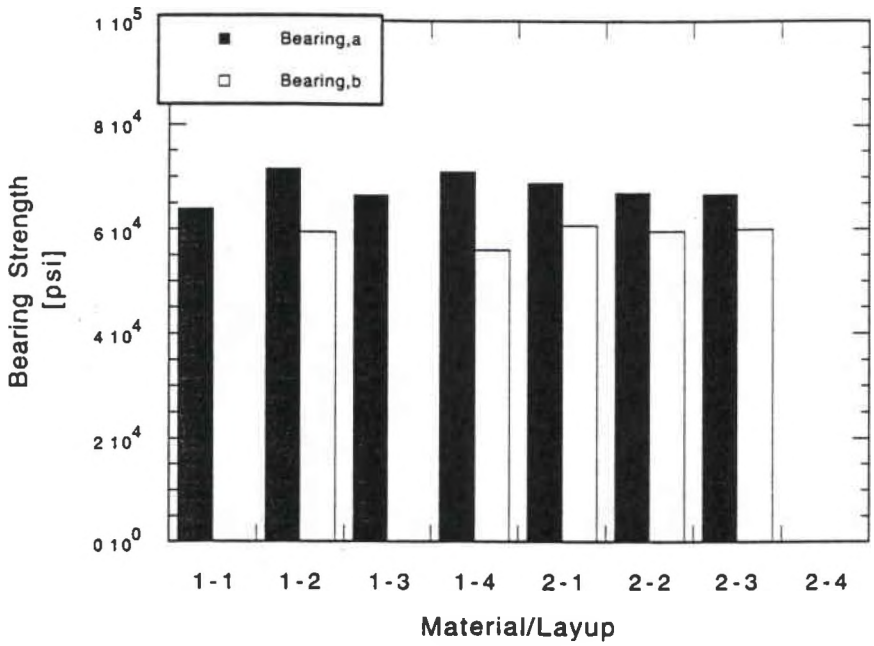

Figure 20. Normalized bearing strength for the graphite/epoxy materials.

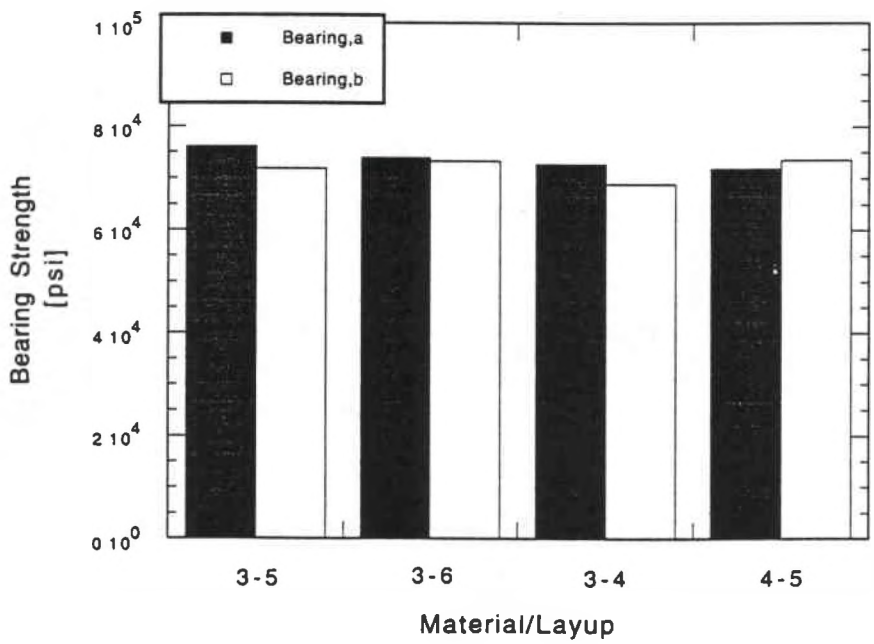

Figure 21. Normalized bearing strength for the graphite/PEEK materials.

Examination of this data revealed consistently higher bearing strengths for the 0.125 inch diameter hole versus the 0.250 inch diameter hole. The only exception to this trend was lay-up five of the IM-8/APC-2 material where the larger diameter hole provided slightly greater bearing strength. The dependence of the bearing strengths on hole size may be attributed to the normal stress distribution occurring ahead of the hole. Previous investigations have shown that although the stress concentration is the same for all hole sizes, the normal stress distribution is more concentrated for the case of the smaller hole [14, 26, 58]. Therefore, smaller hole size specimens generally result in higher strengths as was the case in the data obtained from the majority of the bearing tests. The difference in data obtained for the two hole diameters was found to be less for the PEEK matrix materials than for the epoxy matrix materials. Additionally, the graphite/PEEK material was found to provide higher bearing strengths than the graphite/epoxy material. This apparent dependence of bearing strength on matrix material and the interaction found to exist between matrix material and hole size may be attributed to the relative notch sensitivity of the matrix material studied. As indicated previously, composite materials having a more brittle matrix such as epoxy matrix composites are more notch sensitive than those composites having a more ductile matrix such as PEEK matrix composites. The greater notch sensitivity of the graphite/epoxy composites resulted in higher stress concentrations occurring at hole edge which translated into lower bearing strengths for the graphite/epoxy materials. Comparable bearing strengths were obtained for the IM-8 and AS-4 fibers in a given matrix material. This apparent lack of dependence on fiber constituent properties is most likely attributed to the fact that the majority of the bearing failures occurred in a matrix dominated mode. Stacking sequence appeared to have some effect on the bearing strength for the graphite/epoxy material, however no consistent trend in the data could be noted. Conversely, the bearing strength appeared to be independent of stacking sequence for the graphite/PEEK material. As indicated previously, the dependence of strength on stacking sequence is associated with the occurrence of interlaminar normal and shear stresses induced during loading. Therefore, these results suggest that interlaminar stresses may be important in bearing loading for the graphite/epoxy material. The

bearing strength of the graphite/PEEK material was found to be essentially independent of stacking sequence. This result may be attributed to the PEEK matrix material's ability to resist the delamination type failure mode associated with interlaminar stresses.

Analysis of Parameters

A summary of the results obtained from the statistical analysis are given in Tables 14 through 17. The main effects were plotted on normal probability paper and the resulting curves are shown in Figures 22 through 25.

TABLE 14

MAIN AND INTERACTION EFFECTS FOR THE GRAPHITE/EPOXY MATERIALS

	Tension		Compression		Bearing	
Variable	Effect	SE	Effect	SE	Effect	SE
MAIN						
Mean (I)	74.20	4.25	70.36	4.21	65.43	4.40
Test (1)	-0.04	8.50	-27.32	8.43	8.83	8.79
Fiber (2)	-26.56	8.50	2.40	8.43	0.85	8.79
Lay-up (3)	-31.20	8.50	-12.55	8.43	0.79	8.79
Stac. Seq. (4)	0.54	8.50	2.32	8.43	0.91	8.79
INTERACTION						
1X2	0.49	8.50	0.02	8.43	1.06	8.79
1X3	-2.51	8.50	-5.72	8.43	0.16	8.79
1X4	-1.16	8.50	0.28	8.43	-2.11	8.79
2X3	7.50	8.50	0.08	8.43	-0.08	8.79
2X4	0.47	8.50	-0.93	8.43	1.43	8.79
3X4	2.91	8.50	0.90	8.43	-0.37	8.79

TABLE 15

MAIN AND INTERACTION EFFECTS FOR THE GRAPHITE/PEEK MATERIALS

	Tension		Compression		Bearing	
Variable	Effect	SE	Effect	SE	Effect	SE
MAIN						
Mean (I)	59.39	3.55	62.90	4.73	71.68	2.48
Test (1)	-4.94	7.09	-36.35	9.46	1.16	4.97
Fiber (2)	-18.24	7.09	3.55	9.46	4.45	4.97
Stac. Seq. (3)	7.29	7.09	-5.54	9.46	-2.83	4.97
INTERACTION						
1X2	0.74	7.09	-13.20	9.46	2.14	4.97
1X3	-2.31	7.09	-11.34	9.46	0.69	4.97
2X3	-43.54	7.09	-44.06	9.46	-51.64	4.97

TABLE 16

MAIN AND INTERACTION EFFECTS: MATRIX COMPARISON

Variable	Tension Effect	Tension SE	Compression Effect	Compression SE	Bearing Effect	Bearing SE
MAIN						
Mean (I)	63.80	2.67	70.84	6.61	68.74	2.75
Test (1)	-0.05	5.34	-15.63	13.21	10.09	5.50
Matrix (2)	-0.99	5.34	2.34	13.21	-6.86	5.50
Stac. Seq. (3)	-23.55	5.34	-6.24	13.21	3.48	5.50
INTERACTION						
1X2	0.58	5.34	0.91	13.21	-12.47	5.50
1X3	-1.65	5.34	-3.36	13.21	-4.88	5.50
2X3	0.86	5.34	0.70	13.21	0.97	5.50

TABLE 17

MAIN AND INTERACTION EFFECTS: NOTCHED VS. UNNOTCHED

Variable	Tension Effect	Tension SE	Compression Effect	Compression SE
MAIN				
Mean (I)	94.83	7.93	80.59	6.48
Notched (1)	-57.51	15.86	-29.34	12.96
Filled (2)	-0.89	15.86	57.45	12.96
Fiber (3)	-28.37	15.86	2.09	12.96
Lay-up (4)	-37.82	15.86	-15.05	12.96
INTERACTION				
1X2	28.08	15.86	36.71	12.96
1X3	-4.56	15.86	4.21	12.96
1X4	-3.07	15.86	1.41	12.96
2X3	12.15	15.86	1.10	12.96
2X4	19.82	15.86	11.86	12.96
3X4	12.13	15.86	-2.44	12.96

For the graphite/epoxy material, fiber and lay-up were found to have the largest effect on the open and filled hole tension data. As discussed in the previous section, the effect of fiber type on the open and filled hole tensile performance of composite materials is attributed to the constituent fiber strength as well as to the fiber modulus which affects the materials ability to dissipate stress concentrations occurring at the hole edge.

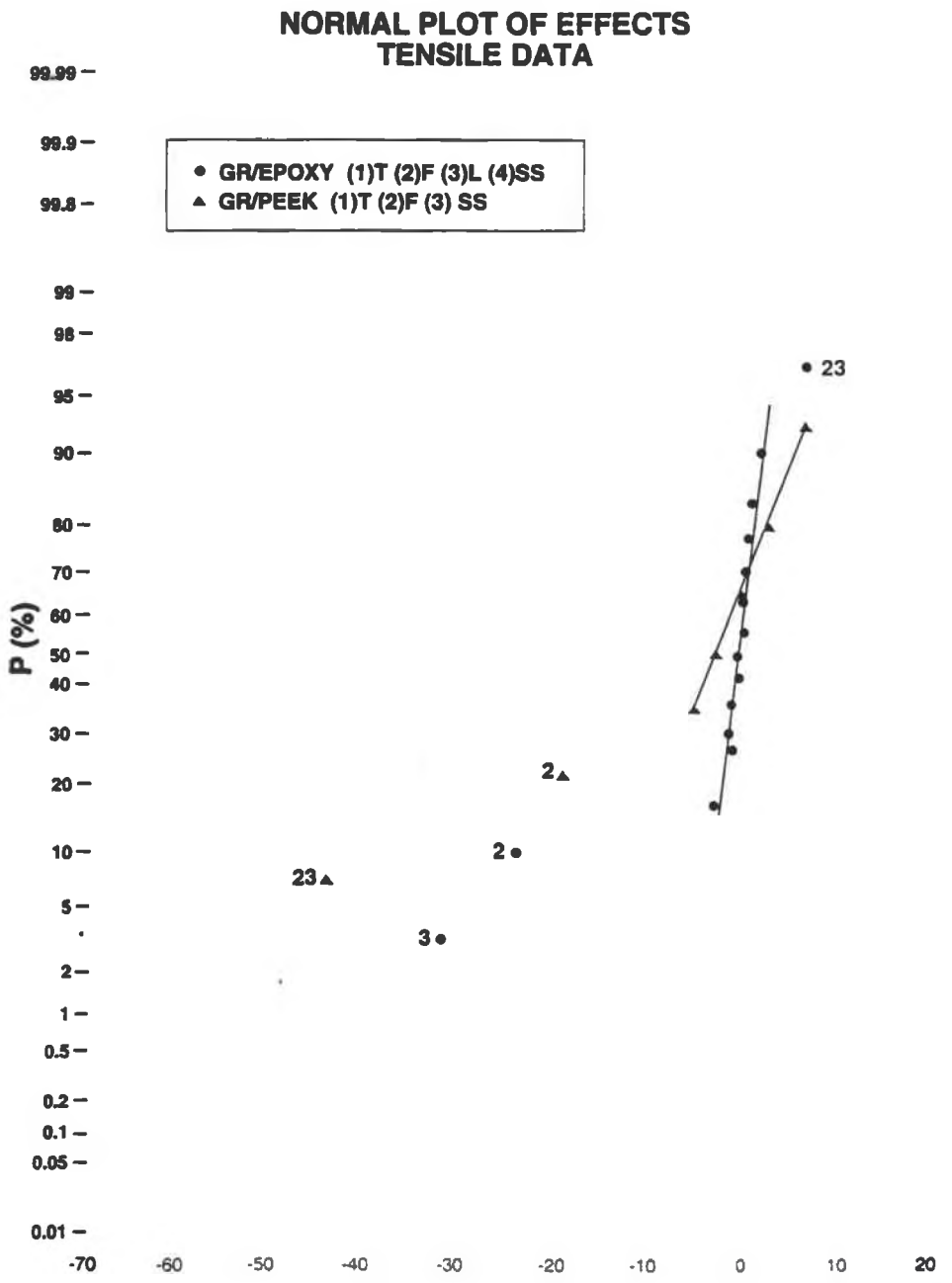

Figure 22. Normal plot of effects: Tensile data.

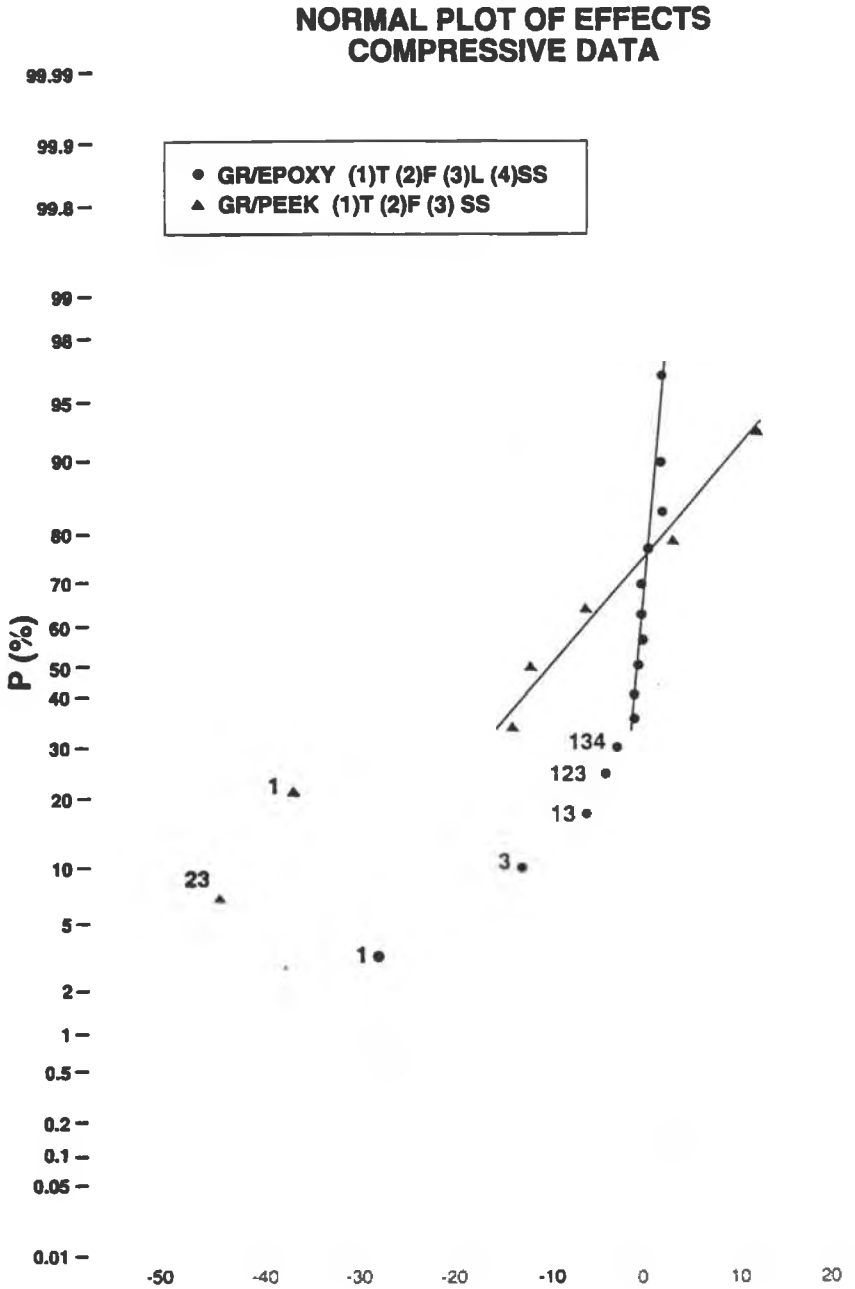

Figure 23. Normal plot of effects: Compressive data.

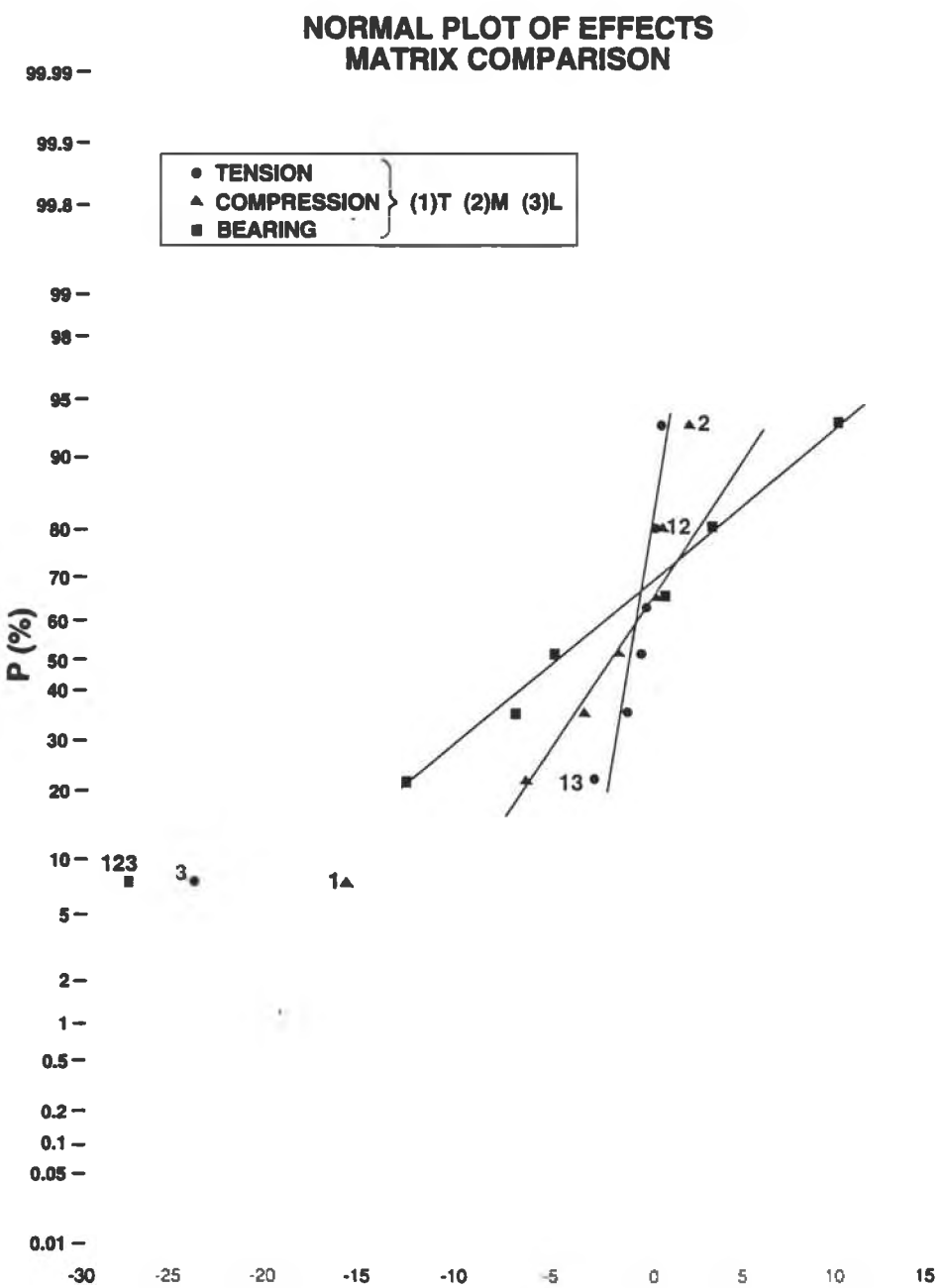

Figure 24. Normal plot of effects: Matrix comparison.

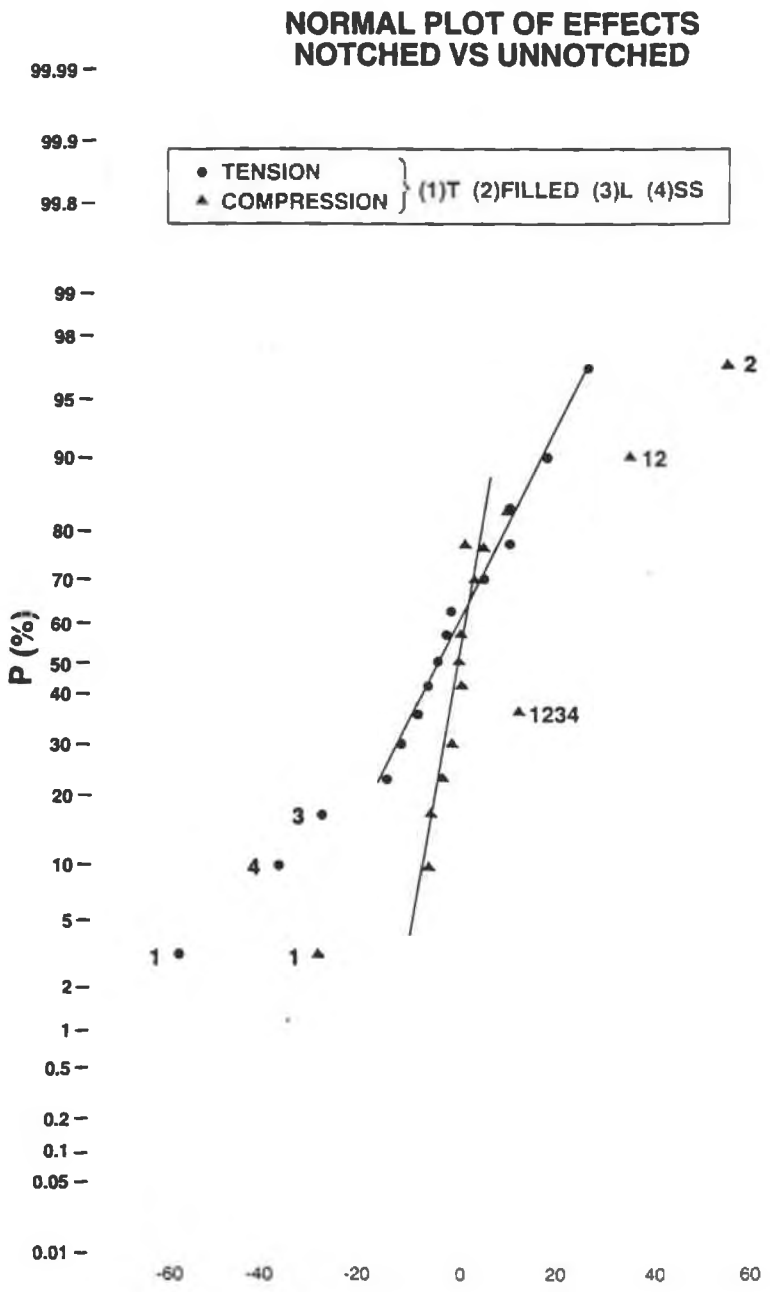

Figure 25. Normal plot of effects: Notched versus unnotched comparison.

Test type (open versus filled hole testing) and stacking sequence were found to have little effect on the open and filled hole tension data. Conversely, test type was found to be the factor which most significantly affected the open and filled hole compressive data. As discussed in previous sections of this dissertation, the dependence of test type on the notched compression strength of composite materials is due to the presence of the fastener for the filled hole specimens. The presence of the fastener provides lateral constraint to the specimen which helps inhibit interlaminar failures such as delamination which can be deleterious to the notched compression strength of composite materials. Lay-up was also found to have a some effect on the compressive data.

Although fiber type was found to have a significant effect on the tensile data, the compressive data appeared to be essentially independent of fiber type. This result is attributed to the difference in mechanisms which are believed to govern the initiation of failure for these types of loading. In the case of tensile loading, failure is initiated at the hole due to stress concentrations associated with the material discontinuity. Therefore, the materials ability to dissipate these stress concentrations has a large effect on the ultimate open and filled hole tensile strength. Fiber modulus and the matrix toughness are the constituent properties which determine this property. In the case of compressive loading, failure is dominated by fiber buckling and kinking. For this mode of failure, fiber, matrix interfacial strength and matrix stiffness are believed to be the governing constituent properties.

Stacking sequence appeared to have a greater effect on the compressive data than on the tensile data, but this effect does not appear to be significant. Similarly, stacking sequence did not appear to have a statistically significant effect on the bearing data. Therefore, the observations made in the previous section regarding the effect of stacking sequence on the graphite/epoxy bearing data may have been the result of random variation in the data instead of a true effect. The result that stacking sequence did not significantly affect the bearing, open and filled hole compression and tension data may imply that the occurrence of interlaminar stresses is

not an important consideration in the design of bolted graphite/epoxy joints. Therefore, the need for a three-dimensional stress analysis of bolted composite joints is debated.

Fiber and lay-up were found to be insignificant parameters with regards to bearing data. As expected, test type (0.125 versus 0.250 inch diameter hole size) was found to affect the bearing results. This is consistent with what was presented in Section 4.4.4 of this dissertation and is associated with the difference in the stress distribution occurring in the vicinity of the hole for the two hole sizes.

Although fiber type and stacking sequence were found to have a rather large effect on the tensile data obtained for the graphite/PEEK material a large interaction effect for these two parameters was also found to exist. In the difference of means technique the effect of a variable can only be interpreted individually if no evidence of interaction between that variable and another variable exists [91]. Therefore, no definite conclusions regarding the effects of individual parameters can be made based on the results obtained from this statistical analysis.

As with the graphite/epoxy materials, test type was found to be insignificant with regards to the open and filled hole tensile data for the graphite/PEEK material. Test type was found to have a rather large effect on the compressive data for the graphite/PEEK material. This result is consistent with what was found for the graphite/epoxy material. Fiber type and stacking sequence did not appear to have any effect on the open and filled hole compressive data for the PEEK matrix materials. No definite conclusions regarding the statistically significant effects on the open and filled hole compressive performance of the graphite/PEEK materials could be made since large interaction effects were noted among all three variables analyzed. None of the parameters studied were found to have a significant effect on the bearing data for the graphite/PEEK material. However, a large interaction between fiber type and stacking sequence was found to exist for the graphite/PEEK bearing case.

Results obtained from the difference of means technique indicated that matrix type did not have a significant effect on the strengths for any of the loading cases considered. These results are not consistent with those obtained from a cursory examination of the experimental

data as discussed in the previous section which suggested that matrix material did have some effect on the resulting strengths. One possible explanation for this inconsistency may be associated with the large scatter in the data obtained from the bearing, open and filled hole tension and compression tests. Although consistent, the difference in the data obtained from the two matrix materials was very subtle. Therefore, the statistical analysis may not have been able to differentiate this subtle difference from the scatter in the data. Additionally, a large interaction between test type and matrix type was noted for the bearing specimens which made it difficult to analyze these variable individually. As indicated previously, this interaction may be attributed to the relative notch sensitivity of the two matrix materials where the greater notch sensitivity of the graphite/epoxy material makes it more susceptible to the hole size effect discovered for the bearing specimens.

As expected, the data obtained from the statistical analysis comparing the notched versus unnotched data revealed that the presence of the notch does have a significant effect on the tensile and compressive data obtained for the graphite/epoxy materials. Additionally, this analysis verified the results obtained previously regarding the effect of the test type (open versus filled) on the tensile and compressive performance of the graphite/epoxy materials.

Two Dimensional Analysis of Stress Concentrations

For isotropic materials the stress concentration factor, K_T, is defined as the ratio of the maximum tensile hoop stress on the perimeter of the hole to the remote tensile stress on the plate. As indicated in previous sections of this dissertation, the notched strength of an orthotropic material depends on the hole size. This hole size effect is attributed to the fact that the strength of a notched composite is related to the in-plane elastic stresses occurring in a region adjacent to the hole boundary rather than those occurring at a point on the hole boundary as is the case with isotropic materials [72]. Because of the hole size effect, a direct application of the stress concentration factor to predict the notched strength of composite materials is not valid except in cases of very large holes (diameter greater than 1.0 inch). Instead, the point stress or average stress criterion is used to predict the notched strength of composite materials. In this analysis,

the ratio of the notched to unnotched tensile strength is a function of the orthotropic stress concentration factor, the hole radius and an experimentally determined characteristic distance [44, 45, 49].

Stress intensity curves obtained from the extended isotropic analysis are shown in Figure 26. The stress concentration factors obtained for the various material, lay-up combinations are given in Table 18.

TABLE 18

VALUES OF K_T AS DETERMINED FROM THE TWO DIMENSIONAL ANALYSIS

Material/Lay-up	K_T
1-1	3.00
1-2	3.00
1-3	3.48
1-4	3.48
2-1	3.00
2-2	3.00
2-3	3.54
2-4	3.54
3-5	3.00
4-5	3.00

The ratio of local to remote open and filled hole tensile strength as determined from the experimental data was found to be 1.20 for all materials and lay-ups considered. Ratios of notched to unnotched open and filled hole tensile strength are shown graphically in Figure 27. The orthotropic stress concentration factor, K_T, as determined from the extended isotropic analysis was found to be essentially independent of constituent material properties. Lay-ups consisting of 60 and 0 degree layers were found to have larger stress concentration factors than those containing the 0, 45 and 90 degree layers. No information concerning the effect of stacking sequence on stress concentrations could be determined since the extended isotropic analysis is a two-dimensional technique. For all cases studied the remote stress was regained a distance of 0.275 inches from the hole edge. Values of the experimentally determined ratios of local to remote stress were found to be significantly lower than the values provided by the extended isotropic analysis. As indicated in Table 18 and Figure 27, little correlation between the

experimentally determined ratio of notched to unnotched strength and the stress concentration factor as determined from the extended isotropic analysis exist. The experimentally determined ratio of notched to unnotched tensile strength appeared to be dependent upon material constituent properties as well as lay-up.

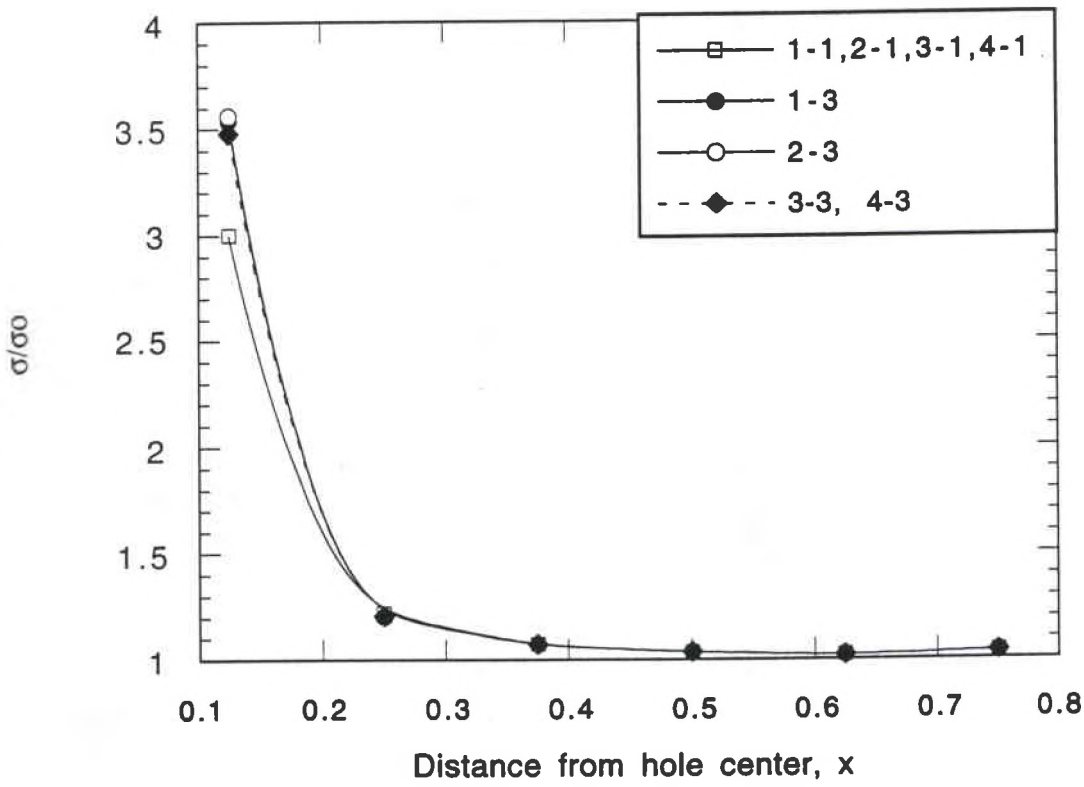

Figure 26. Results of the extended isotropic analysis.

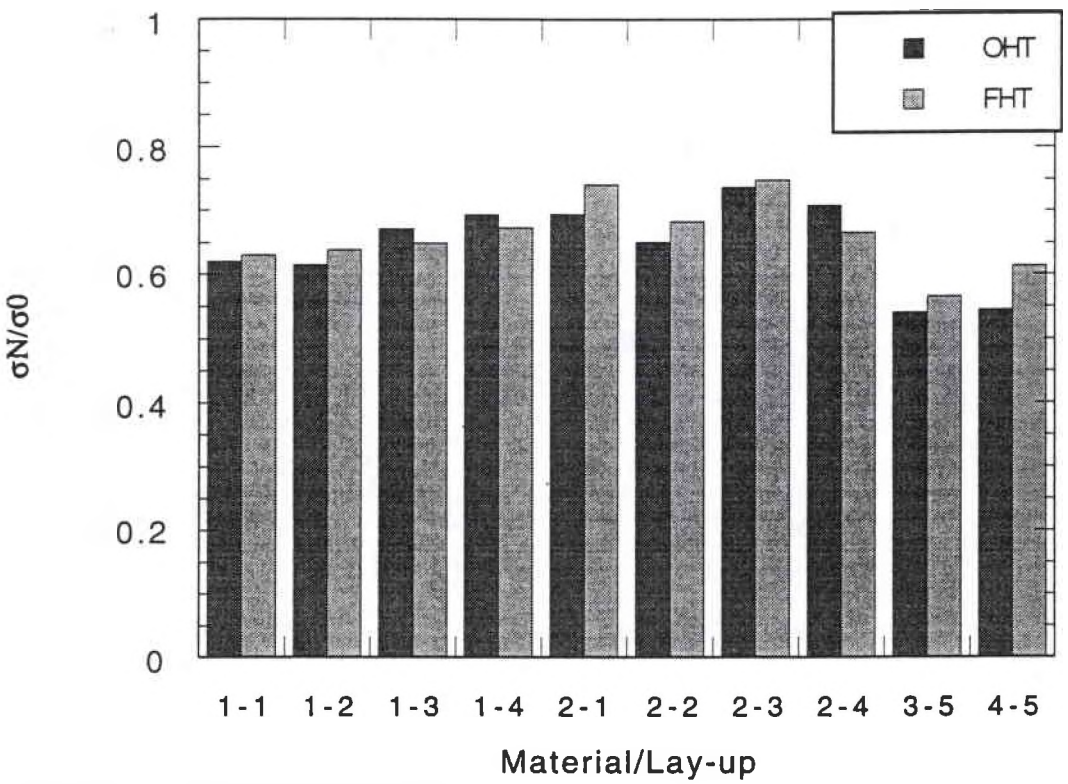

Figure 27. Ratio of the notched to unnotched strength for the open and filled hole tension specimens.

CHAPTER 5

FRACTOGRAPHIC ANALYSIS

Post Failure Analysis

Analysis of Compression and Tension Specimens

Macroscopic examination of tested unnotched, open and filled hole tension and compression specimens indicated that failures were fairly consistent within a given specimen group. With the exception of the unnotched compression specimens, the majority of the specimens failed within the gage area. For the unnotched compression specimens, failure generally took place at the grip edge. The majority of the notched tension and compression specimens failed through the hole. For the tension specimens the presence of the bolt and washer appeared to have little effect on the macroscopic failure mode, Figures 28 and 29. For the compression specimens however, the presence of the bolt/washer appeared to suppress the damage to a region outside of the bolt-washer area Figures 30 and 31. This is consistent with the results obtained in previous sections of this dissertation where it was found that the presence of the washer had little effect on the tensile data but a statistically significant effect on the compressive data. Microscopic examination of specimen cross-sections supported this result in that little difference was noted in the failure modes for the open versus filled hole tensile case and a more obvious difference was noted in the failure modes for the open versus filled hole compression case, Figure 32 Both the open and filled hole tensile specimens failed by a tensile failure mode occurring at the hole center. Longitudinal cross-sections of the graphite/epoxy and graphite/PEEK open and filled hole tensile specimens showed a failure mode characterized by multiple intralaminar and translaminar fractures of the angle and zero degree plies, respectively with some interior and face ply delaminations. For the filled hole tensile specimens, there appeared to be a slightly greater degree of intralaminar fracture occurring near the mid-ply than

(a) 1-1-OHT specimen

(b) 1-1-FHT specimen

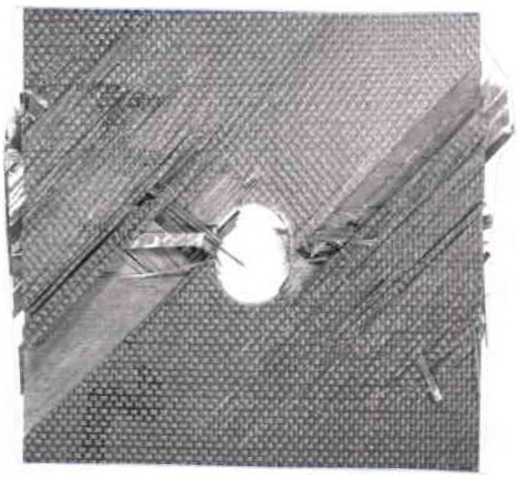

(c) 2-1-OHT specimen

(d) 2-1-FHT specimen

Figure 28. Macrophotographs of tested graphite/epoxy open and filled hole tension specimens showing that the presence of the fastener had little effect on the macroscopic failure modes for these materials.

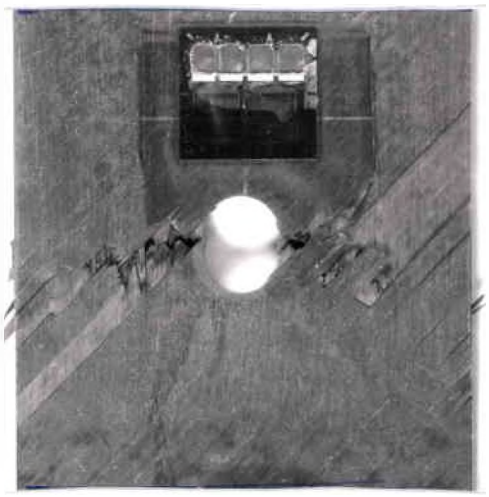

(a) 3-5-OHT specimen

(b) 3-5-FHT specimen

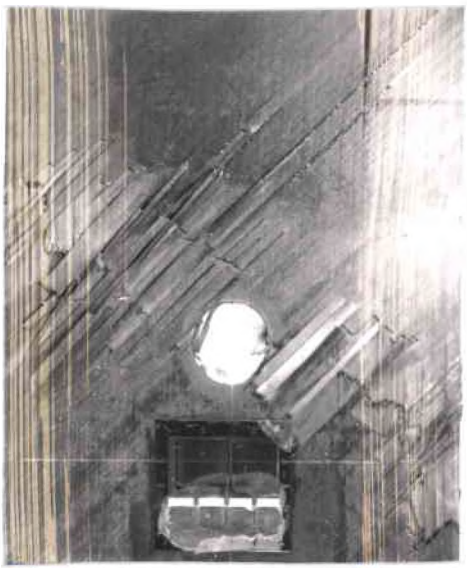

(c) 4-5-OHT specimen

(d) 4-5-FHT specimen

Figure 29. Macrophotographs of tested graphite/PEEK open and filled hole tension specimens showing that the presence of the fastener had little effect on the macroscopic failure modes for these materials.

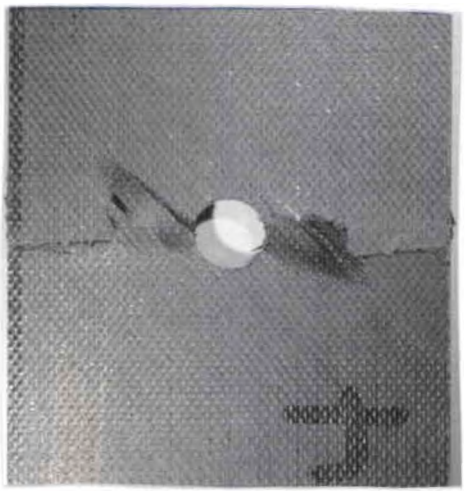

(a) 1-1-OHC specimen

(b) 1-1-FHC specimen

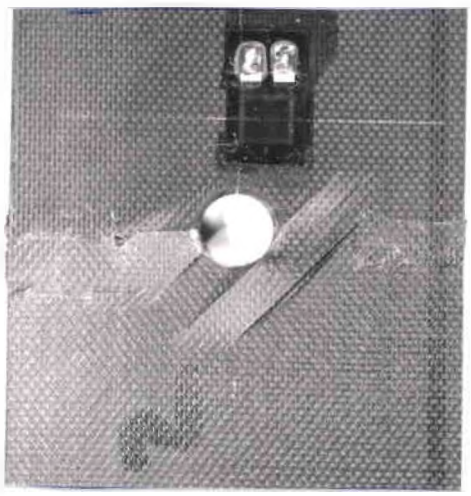

(c) 2-1-OHC specimen

(d) 2-1-FHC specimen

Figure 30. Macrophotographs of tested graphite/epoxy open and filled hole compression specimens showing that the presence of the fastener suppressed the majority of the damage to a region outside the washer area.

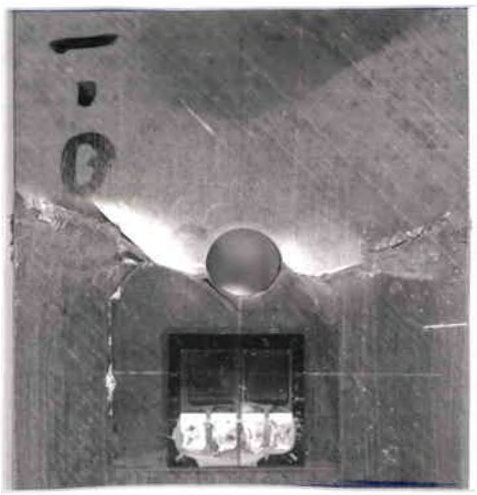

(a) 3-5-OHC specimen

(b) 3-5-FHC specimen

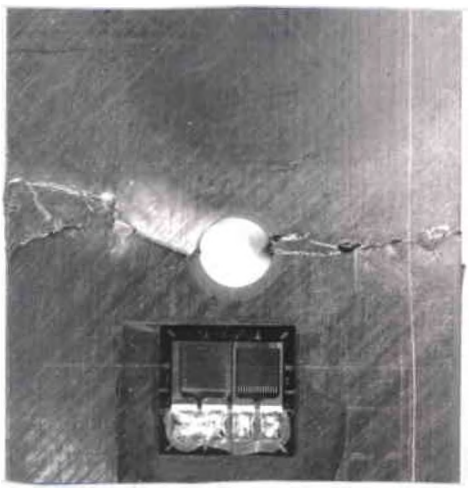

(c) 4-5-OHC specimen

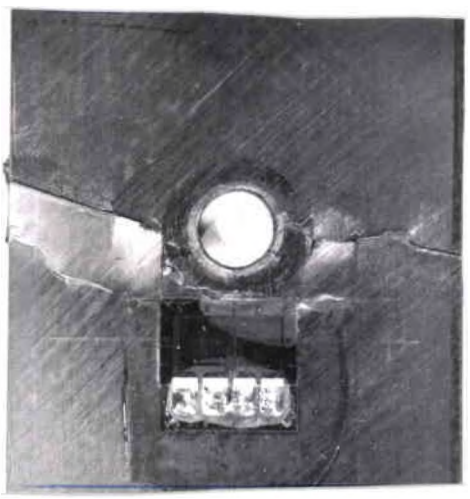

(d) 4-5-FHC specimen

Figure 31. Macrophotographs of tested graphite/PEEK open and filled hole compression specimens showing that the presence of the fastener suppressed the majority of the damage to a region outside the washer area.

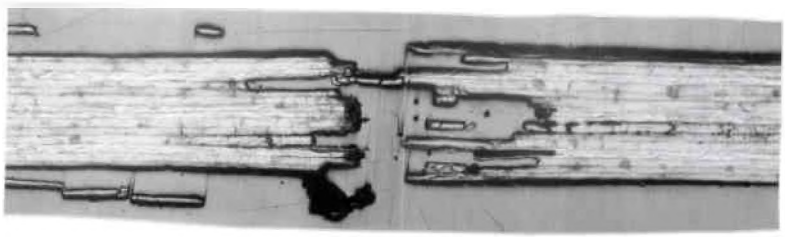

(a) 1-1-OHT specimen

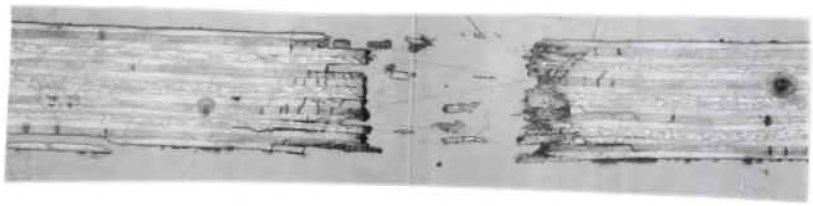

(b) 1-1-FHT specimen

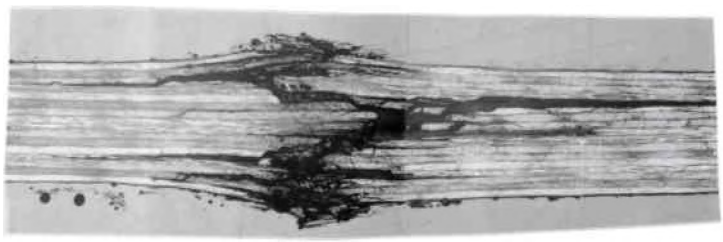

(c) 1-1-OHC specimen

(d) 1-1-FHC specimen

Figure 32. Photomicrographs of tested, AS-4/3501-6, open and filled hole tension and compression specimens showing that the presence of the fastener had little effect on the microscopic failure mode for the tensile case, but was effective in suppressing the majority of the damage to a region outside the washer area for the compressive case.

for the open hole specimens. Conversely, for the open hole tensile specimens, there appeared to be a slightly greater degree of face ply and interior delamination than for the filled hole case. Transverse cross-sections of the graphite/epoxy and graphite/PEEK open and filled hole tensile specimens indicated a failure mode dominated by intralaminar cracking and delamination. The majority of the intralaminar cracking was found to occur at or near the mid-ply and the majority of the delaminations were found to occur near the free edge of the specimen. Overall, the only effect that the presence of the bolt was found to have on the tensile failure of the graphite/epoxy and graphite/PEEK specimens was to suppress the delaminations to a region outside of the washer area and to encourage a greater degree of intralaminar fractures of the angle plies.

Two distinct regions of failure could be identified in most of the graphite/epoxy filled hole compression specimens. One such region corresponded to the washer edge and was dominated by buckling or kink band formation with interior delaminations. In this region, it appeared as if the specimen delaminated near the mid-ply, producing two sublaminates. One or both of these sublaminates failed by ply buckling, consisting of multiple intralaminar and translaminar fractures and displaced plies. The remaining sublaminate failed by shear in plies which were displaced from the mid-ply. The second region of failure was dominated by a shear type failure mode and occurred at the hole center. For some lay-ups this second region of failure was not observed. In most cases, the majority of the delaminations were found to occur in a region outside of the washer area. For the graphite/PEEK, open hole compression specimens, failure was found to be suppressed to a region outside of the washer area and dominated by ply kinking and fiber buckling. Failure of the open hole compression specimens occurred by a shear or compressive type failure mode at the hole edge. This mode of failure was accompanied by interior and face ply delaminations extending from the center damage region. Therefore, the lateral constraint provided by the fastener appeared to be effective in suppressing the majority of the damage to a region outside of the washer area for the filled hole compression specimens.

Overall failure characteristics of the open and filled hole tension specimens for the various stacking sequences and lay-ups were found to be quite similar for the materials studied.

This result is consistent with the experimental data which indicated the open and filled hole tensile strength to be essentially independent of stacking sequence, Figure 33. Lay-up was found to have an effect on the resulting open and filled hole tensile strength for the graphite/epoxy material. The lay-ups containing 0 and 60 degree laminae (lay-ups three and four) were found to provide higher open and filled hole tensile strengths than those containing 0, 45 and 90 degree laminae (lay-ups one and two). No obvious difference in open and filled hole tensile failure modes was noted for the various lay-ups. Therefore, the difference in strength obtained for the various lay-ups is most likely a reflection of the relative amount of fibers occurring in the direction of the applied load (zero degree direction) and not due to a difference in failure modes. Some interior and face ply delamination was found to occur for specimens of all lay-ups.

Failures of the open hole compression specimens appeared to be somewhat stacking sequence and lay-up dependent, Figure 34. For the graphite/epoxy materials, the overall failure mode was dominated by shear and compression accompanied by delamination. It appeared that the extent and location of these delaminations depended upon the stacking sequence for that material. For example, for the AS-4/3501-6 material, delaminations appeared to be more significant for the [45/90/-45/0]2s stacking sequence (lay-up 2) than for the $[45/-45/0/90]_{2s}$ stacking sequence (lay-up 1). Delaminations occurring for the two stacking sequence of the 0/60 degree lay-up were found to be somewhat more significant for the $[+60/-60/0_2]_{2s}$ stacking sequence (lay-up 4) than for the $[+60/0_2/-60]_{2s}$ stacking sequence (lay-up-3). Further examination of these failures revealed the delaminations to be continuous through major failure regions for the graphite/epoxy open hole compression specimens. This observation suggests that delamination caused by interlaminar stresses may have been an initial failure mode for these specimens. Since the presence of interlaminar stresses are largely dependent upon stacking sequence, then the observation regarding the effect of stacking sequence on the failure mode of open hole compression specimens contradicts the results obtained from the experimental data which indicated that stacking sequence did not have a significant effect on the open hole compression strength. This apparent contradiction in the results obtained from the fractographic

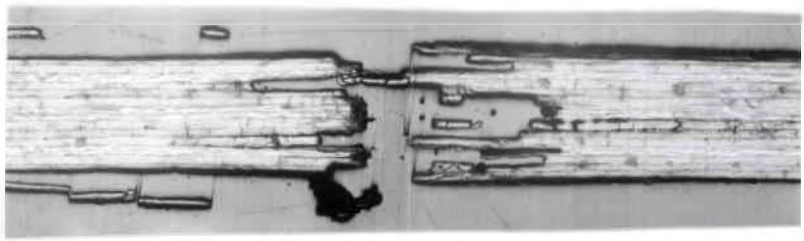

(a) 1-1-OHT specimen

(b) 1-2-OHT specimen

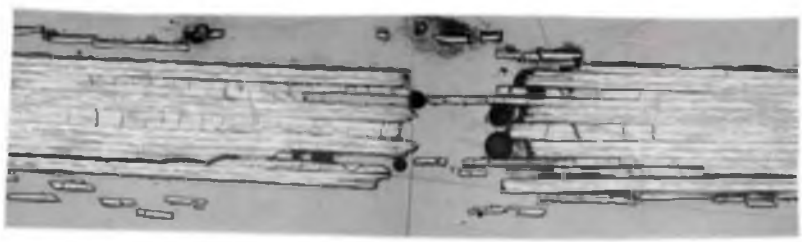

(c) 1-3-OHT specimen

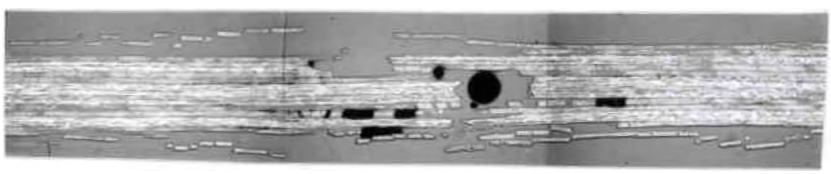

(d) 1-4-OHT specimen

Figure 33. Photomicrographs of tested, AS-4/3501-6, open hole tension specimens showing that stacking sequence and lay-up did not have a significant effect on the microscopic failure modes.

(a) 1-1-OHC specimen

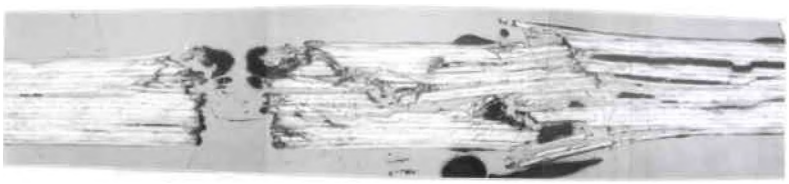

(b) 1-1-FHC specimen

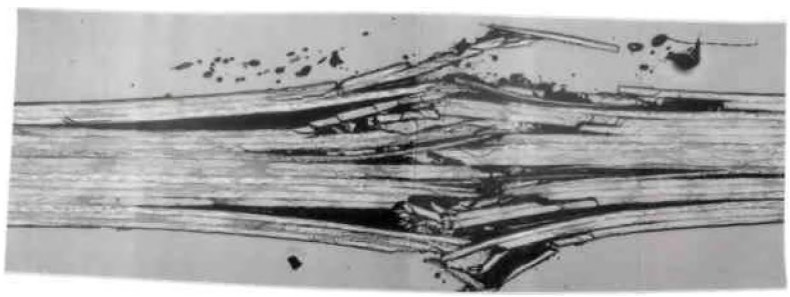

(c) 1-2-OHC specimen

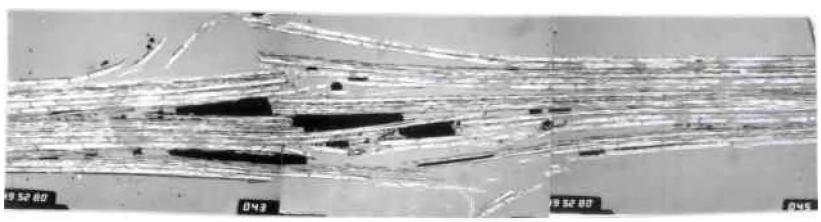

(d) 1-4-OHC specimen

Figure 34. Photomicrographs of tested, AS-4/3501-6, open and filled hole compression specimens showing that stacking sequence and lay-up had little effect on the microscopic failure modes.

analysis and experimental data for the graphite/epoxy, open hole compression specimens suggests that although failure may have initiated by delamination, the presence of these initial delaminations may not have had a significant effect on the final failure strength.

Similar observations were noted for the graphite/epoxy filled hole compression specimens. The graphite/epoxy filled hole compression specimens failed predominantly by ply buckling occurring at the washer edge. As with the open hole compression specimens, the only difference in failure mode noted for the various stacking sequences and lay-ups was the extent and location of the interior delaminations. In general, delaminations appeared to be more significant for the [45/90/-45/0]2s stacking sequence (lay-up 2) than for the $[45/-45/0/90]_{2s}$ stacking sequence (lay-up 1). This is consistent with what was observed for the open hole compression specimens. No significant difference in the amount of delaminations was observed for the two stacking sequences of the 0, 60 degree lay-up. Continuity of the delaminations through the kink zone suggests that delamination may have occurred as an initial failure mode. As with the open hole compression specimens, experimental data obtained for the filled hole compression specimens was found to be independent of stacking sequence. Once again, this apparent contradiction in the results obtained from the fractographic analysis and experimental data for the filled hole compression specimens suggests that the initial failure mode may not have a significant effect on the final failure strength.

By comparing the failure characteristics for the AS-4/3501-6 and IM-8/3501-6 materials for a given lay-up, information concerning the effect of fiber type on the failure mode was obtained. For the open and filled hole tension case, failures were found to be very similar for the two fibers, Figure 35. Both materials failed at the hole center in a tensile mode consisting of intralaminar and translaminar fractures. Slightly more delamination and intralaminar cracking were noted for the IM-8/3501-6 tensile specimens than for the AS-4/3501-6 specimens. This observation may be attributed to the lower transverse tensile strength of the IM-8/3501-6 material which makes this material less resistant to delaminations and intralaminar cracking. This observation may also indicate that the fiber, matrix interface had some effect on the mode of

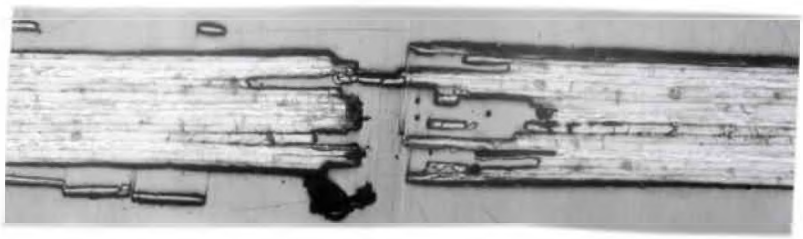

(a) 1-1-OHT specimen (AS-4 fiber)

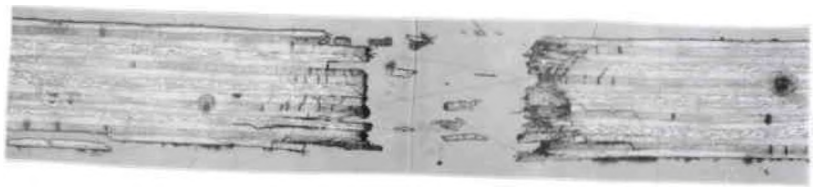

(b) 1-1-FHT specimen (AS-4 fiber)

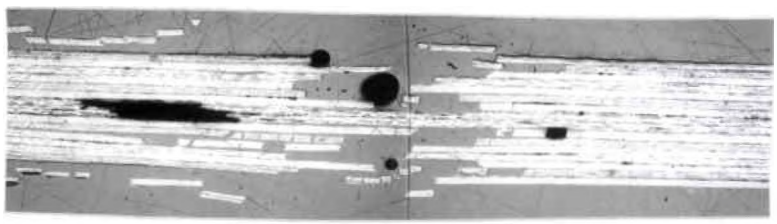

(c) 2-1-OHT specimen (IM-8 fiber)

(d) 2-1-FHT specimen (IM-8 fiber)

Figure 35. Photomicrographs of tested, AS-4/3501-6 (material 1) and IM-8/3501-6 (material 2), open and filled hole tension specimens showing slightly more delamination in the material containing the IM-8 fiber than in the material containing the AS-4 fiber.

failure for the open and filled hole tension specimens since the transverse tensile strength is somewhat dependent upon the interfacial properties. Another possible explanation for the observation that fiber type had an effect on the open and filled hole tensile failures, may be related to the difference in stiffness properties for the two fibers studied. As indicated previously, interlaminar stresses occur at free edges of angle ply laminates due to stiffness discontinuities occurring between the plies. Since the IM-8 and AS-4 fibers have significantly different stiffness, it is likely that the magnitude and nature of the interlaminar stresses generated around the hole edge for the two fibers is not the same. The probable difference in stress states may explain the observation regarding the effect of fiber type on the open and filled hole tensile failure modes. Similar observations were made for the two fibers in the PEEK matrix material.

Failures of the open hole compression specimens for the AS-4/3501-6 and IM-8/3501-6 materials were found to be somewhat similar, Figure 36. These specimens failed at the hole center in a shear dominated mode. The shear failure was accompanied by face ply and interior delaminations. As with the tensile case, more face ply delamination was found to occur in the IM-8/3501-6 open hole compression specimens than in the AS-4/3501-6 specimens. As indicated previously, the difference in failure modes for the IM-8/3501-6 and AS-4/3501-6 open hole compression specimens may be attributed to the material's transverse tensile strength which affects the material's ability to resist delaminations. Little difference in failure mode was noted for the AS-4/3501-6 and IM-8/3501-6 filled hole compression specimens. Longitudinal cross-sections of these specimens showed distinct areas of shear failure which terminated at large delaminations occurring at or near the mid-ply. The relative extent of the delaminations for the two materials appeared to comparable. It appeared as though the major delamination occurring at the mid-ply for the graphite/epoxy materials was continuous through the shear damage at the washer edge. As indicated previously, this observation suggests that delamination occurred prior to the shear failure. Transverse cross-sections of the AS-4/3501-6 and IM-8/3501-6 filled hole compression specimens showed a significant amount of delamination for both materials. Most of this damage occurred outside the washer edge. The catastrophic nature of the

(a) 1-1-OHC specimen (AS-4 fiber)

(b) 1-1-FHC specimen (AS-4 fiber)

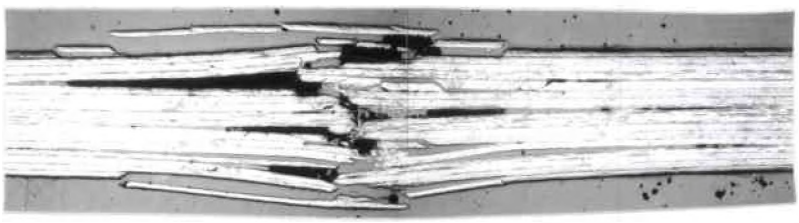

(c) 2-1-OHC specimen (IM-8 fiber)

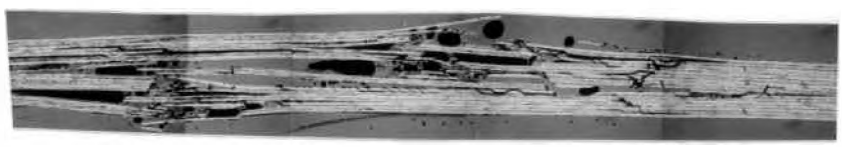

(d) 2-1-FHC specimen (IM-8 fiber)

Figure 36. Photomicrographs of tested, AS-4/3501-6 (material 1) and IM-8/3501-6 (material 2), open and filled hole compression specimens showing slightly more face ply delamination in the material containing the IM-8 fiber than in the material containing the AS-4 fiber.

damage areas made it difficult to compare relative extents of delamination for the two fiber types. A comparison of longitudinal cross-sections of the AS-4/APC-2 and IM-8/APC-2 filled hole compression specimens indicated that a greater degree of delamination occurred for the AS-4/PEEK specimen than for the IM-8/PEEK specimen. This observation is most likely attributed to the lower fiber, matrix interfacial strength of the AS-4 fiber in the PEEK matrix than that of the IM-8 fiber in the PEEK matrix which makes the AS-4/APC-2 material less resistant to delamination.

In order to study the effect of matrix material on the failure mode, fractographic data obtained from open hole tension specimens of IM-8/3501-6 and IM-8/ APC-2 materials and fractographic data obtained from filled hole tension specimens of the AS-4/3501-6 and AS-4/APC-2 were compared, Figure 37. Open and filled hole tension specimens of all four materials failed in a tensile failure mode dominated by intralaminar and translaminar fracture. Slightly more interlaminar delamination and intralaminar cracking was noted for the epoxy matrix specimens than for the PEEK matrix specimens which may be attributed to the inherently lower transverse tensile strength of the graphite/epoxy material.

Failure of the open hole compression specimens for both the graphite/epoxy and graphite/PEEK materials was dominated by shear fracture of the individual laminae, Figure 38. Although a slightly greater extent of delamination was found to occur for the graphite/epoxy material than for the graphite/PEEK material, the location of these delaminations were found to be similar for the two matrix types. The greater extent of delamination which occurred for the epoxy matrix specimens was expected, since the graphite/epoxy material has a significantly lower transverse tensile strength than that of the graphite/PEEK material. For both the graphite/epoxy and graphite/PEEK open hole compression specimens, the continuity of the delaminations through the shear failures of the individual laminae suggest that delamination may have occurred as an initial failure mode. The overall appearance of the failure mode for the graphite/PEEK, open hole compression specimens was found to be much more ductile than that of the graphite/epoxy specimens. It appeared as if the individual laminae of the graphite/PEEK specimens bent away from the mid-ply in response to the applied compressive load. Matrix

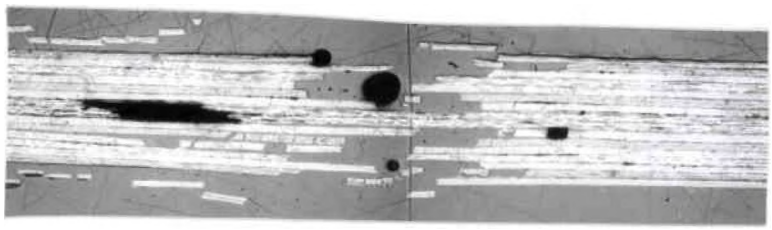

(a) 2-1-OHT specimen (epoxy matrix)

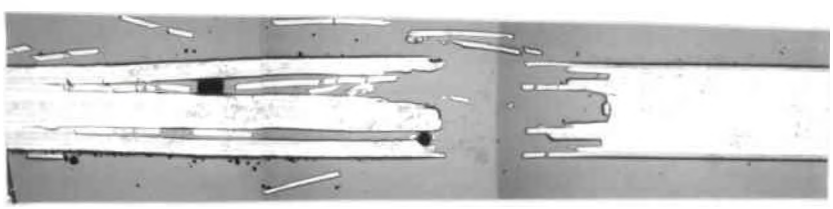

(b) 4-5-OHT specimen (PEEK matrix)

Figure 37. Photomicrographs of tested, IM-8/3501-6 (material 2) and IM-8/APC-2 (material 4), open hole tension specimens showing that matrix material had little effect on the microscopic failure mode for the case of tensile loading.

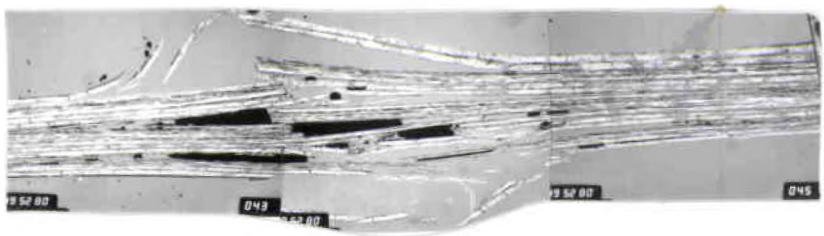

(a) 1-4-OHC specimen (epoxy matrix)

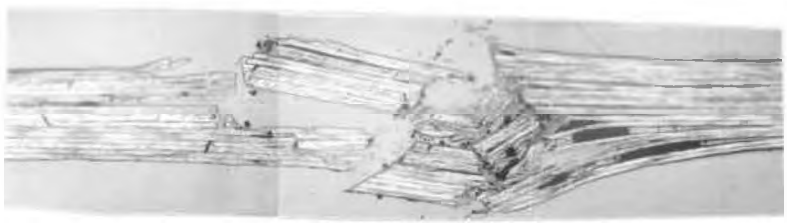

(b) 1-4-FHC specimen (epoxy matrix)

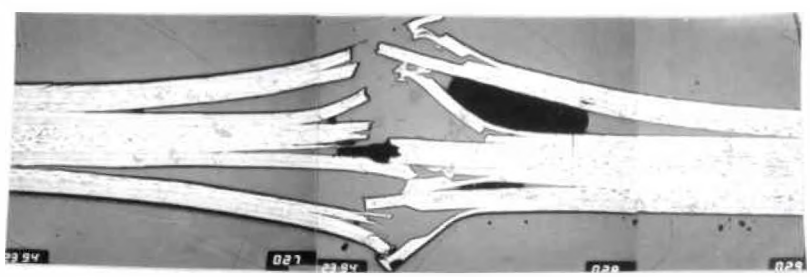

(c) 3-4-OHC specimen (PEEK matrix)

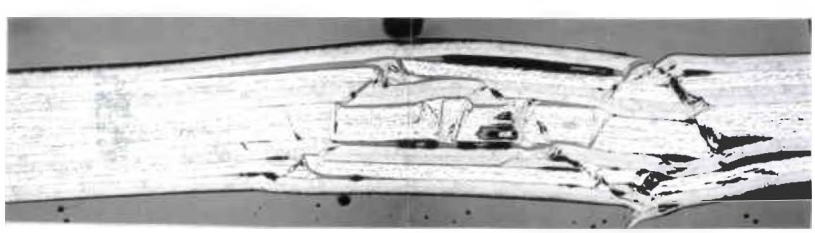

(d) 3-4-FHC specimen (PEEK matrix)

Figure 38. Photomicrographs of tested, AS-4/3501-6 (material 1) and AS-4/APC-2 (material 3), open and filled hole compression specimens showing that matrix material had little effect on the microscopic failure mode for the open hole case, but a rather significant effect on the microscopic failure modes for the filled hole case.

material appeared to have a significant effect on the failure mode of the filled hole compression specimens. Failure of the AS-4/3501-6, filled hole compression specimens was characterized by a definite kink band consisting of multiple plies. It was not obvious from the fractographs that delamination occurred prior to the kinking of the plies, therefore it is quite possible that shear failure preceded delamination for these specimens. The AS-4/APC-2 specimens appeared to fail by multiple kink band formation of the individual laminae. Delaminations were found to surround the area of damage, indicating that delamination may have occurred prior to the formation of the kink bands. The difference in failure modes for the AS-4/3501-6 and AS-4/APC-2 filled hole compression specimens may be attributed to the relative stiffness of the two matrix materials. The epoxy matrix material has a higher modulus than the PEEK matrix material. Previous investigations have shown that the matrix material provides lateral support to fibers when a composite structure is subjected to a compressive load. High stiffness matrix materials are capable of providing strong lateral support to the fibers in which case the compressive failure mode was found to be dominated by fiber shearing. Conversely, low stiffness matrix materials do not provide strong lateral support to the fibers in which case the compressive failure mode was found to be dominated by fiber buckling [23, 80]. As indicated previously, this difference in failure mode for the thermoplastic versus epoxy matrix materials was not observed for the open hole compression specimens. This observation may be related to the presence of the fasteners for the filled hole compression specimens. The presence of the tightened fasteners provides lateral support to the composite specimen thereby inhibiting large delaminations from occurring. In the open hole specimens these large delaminations are not inhibited, thereby allowing large displacement of the individual plies to occur and resulting in a failure mode dominated by shearing of the plies.

Analysis of Bearing Specimens

All of the bearing specimens failed in a bearing type mode, Figures 39 and 40. For all materials studied, the damage appeared to be slightly more significant for the 0.125 inch diameter hole specimens than for the 0.250 inch diameter hole specimens. The failures appeared to be

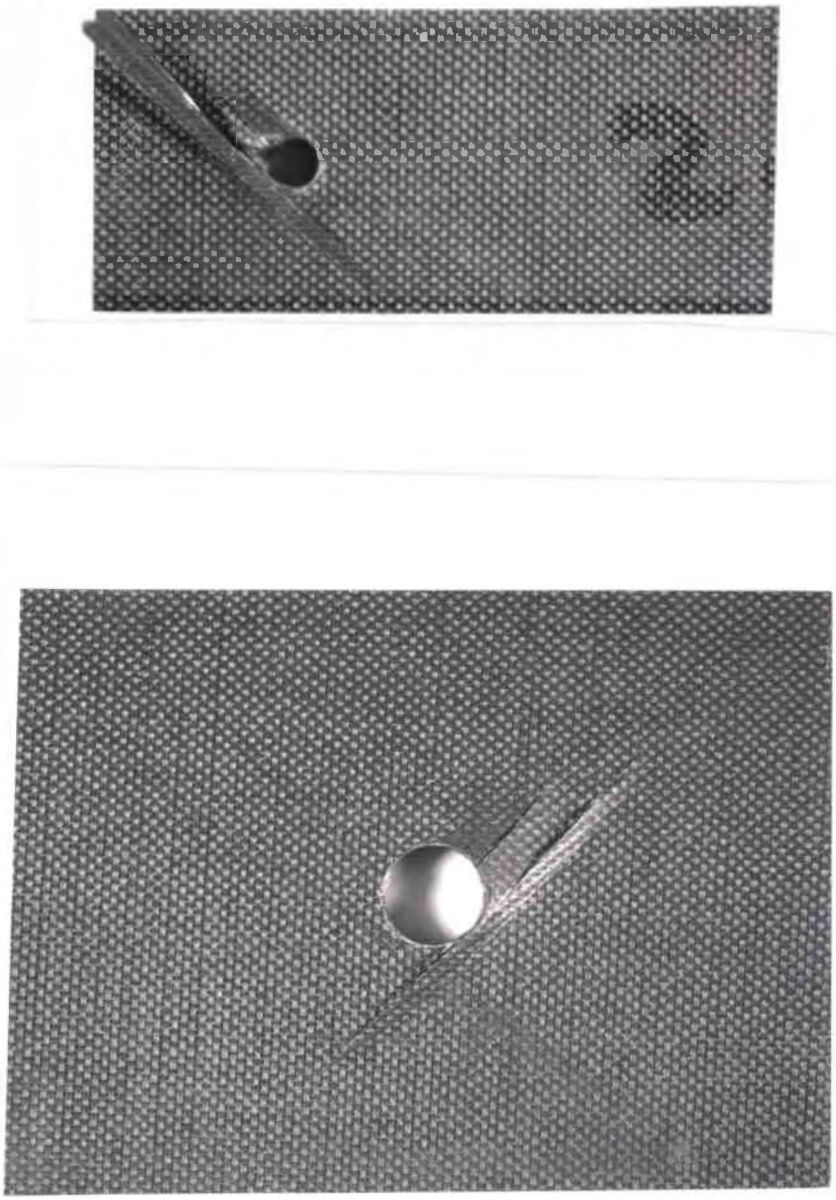

Figure 39. Macrophotographs of tested graphite/epoxy bearing specimens showing a bearing type failure mode and slightly more damage for the smaller hole diameter specimen (Ba) than the larger hole diameter specimen (Bb).

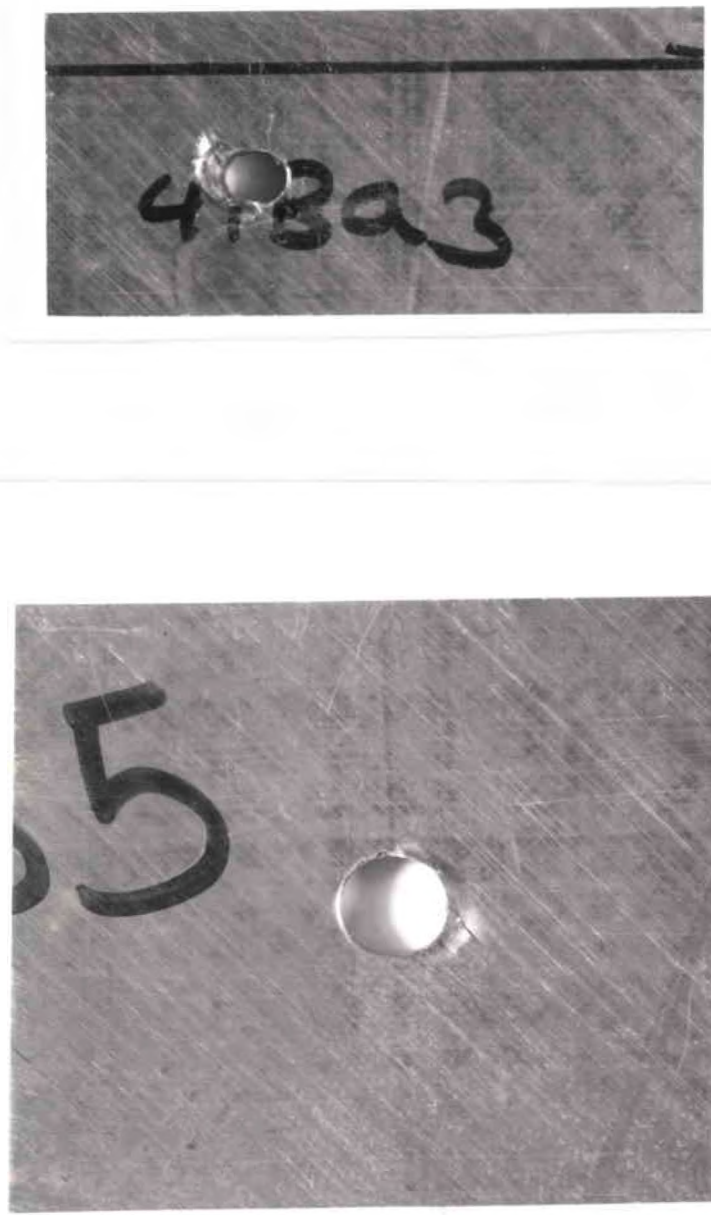

Figure 40. Macrophotographs of tested graphite/PEEK bearing specimens showing a bearing type failure mode and slightly more damage for the smaller hole diameter specimen (Ba) than the larger hole diameter specimen (Bb).

independent of lay-up or fiber type but somewhat dependent on matrix type. For the thermoset matrix specimens, the failure was characterized by limited local yielding with delaminations propagating from the hole edge. For the thermoplastic matrix specimens, a significant amount of local yielding was found to occur in the immediate vicinity of the hole. Very limited to no delamination was observed for the graphite/PEEK bearing specimens. The dependence of the failure mode on the matrix type for the bearing specimens may be related to the relative notch sensitivity of the materials studied. A notch insensitive material is one which allows some form of strain relief such as yielding to occur at the hole edge [19, 20, 21]. Generally, brittle matrix composite materials such as graphite/epoxy are considered to be more notch sensitive than ductile matrix composite materials such as graphite/PEEK. Strain relief in the form of local yielding was observed for the graphite/PEEK material but not for the graphite/epoxy material. This observation confirms the experimental data, where the graphite/epoxy materials were found to be more susceptible to the hole size effect than the graphite/PEEK materials.

Incremental Loading Study

Preliminary radiographs of untested specimens indicated the presence of drilling-induced damage in a majority of the graphite/epoxy test specimens. This initial damage was not evident from the preliminary ultrasonic inspection done on these specimen. The majority of the drilling-induced damage was in the form of delamination and transverse cracking and extended no more than 0.08 inches from the hole edge. For all of the cases examined, the drilling-induced delaminations did not appear to propagate with applied stress. However, the drilling-induced damage may have had some effect on subsequent damage initiation and propagation. Little to no drilling induced damage was observed in the graphite/PEEK specimens. The coordinate axis used to identify the location of failure around the circumference of the hole is shown in Figure 41.

Experimental Findings

Radiographs obtained from the incremental loading study of the AS-4/3501-6, open hole tension specimens indicated similar damage initiation and propagation for both stacking sequences of the 0, 45, 90 degree and 0, 60 degree lay-ups. The lay-up appeared to have some

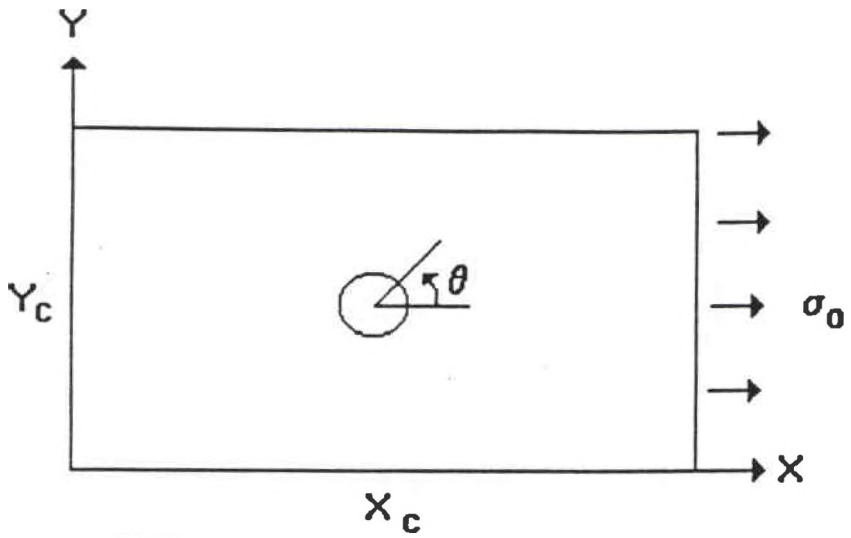

Figure 41. Identification of the coordinate axis used to locate damage around the circumference of the hole.

effect on the location of the initial damage and the direction with which this damage propagated, Figure 42. For both stacking sequences of the 0, 45, 90 degree lay-up damage was found to initiate between 35 % to 45 % of the failure stress in the form of transverse (90 degree) cracks occurring at the hole edge. These transverse cracks were found to occur at a location of 75 to 105 degrees and 225 to 285 degrees along the circumference of the hole. Longitudinal (0 degree) and angle cracks were observed at slightly higher stress levels (68% to 73% failure stress). Longitudinal, transverse and angle cracking continued to propagate with increasing stress level until ultimate failure occurred in the specimen at 48 ksi. Examination of the longitudinal cross-section obtained from a $[45/-45/0/90]_{2S}$, AS-4/3501-6, open hole tension specimen loaded to a stress level of 14 ksi showed damage to initiate by intralaminar fracture of the center, 90 degree plies. Drilling-induced damage in the form of delamination of the lower plies was also noted from this fractograph. Damage in the AS-4/3501-6, open hole tension specimens made up of 0 and 60 degree laminae was found to initiate at approximately 40 % to 45 % of the failure stress in the form of 60 degree cracks occurring at intervals of 60 degrees around

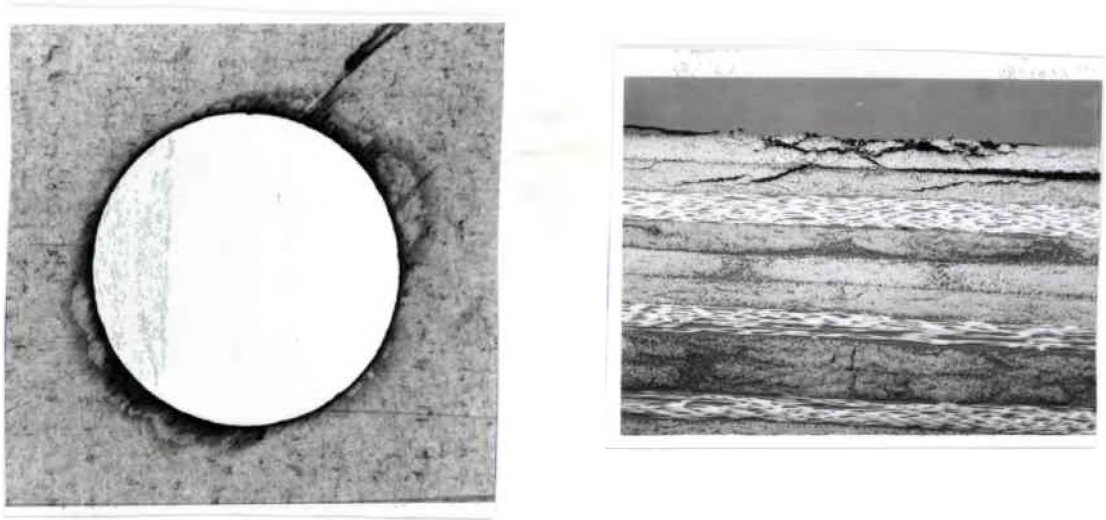

(a) 1-1-OHT specimen

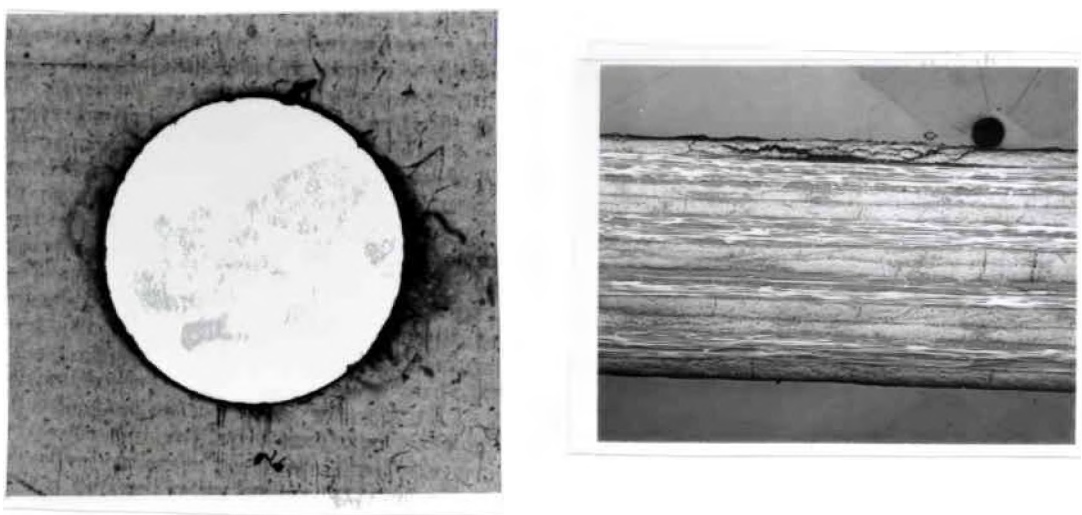

(b) 1-3-OHT

Figure 42. Radiographs and cross-sections obtained from tested graphite/epoxy, open hole tension specimens showing lay-up to have some effect on the location of damage initiation. Damage initiation occurred by transverse or angle ply cracks at approximately 40% of failure stress.

the circumference of the hole. Longitudinal cracks (0 degree) initiated at a location of 0 and 90 degrees between 50 % to 53 % of the failure stress. Propagation of the 60 degree and longitudinal cracks continued until final failure occurred at a stress level of 68 to 73 ksi. Longitudinal cross-sections of the $[\ 60/0_2/-60]_{2S}$, AS-4/3501-6, open hole tension specimen loaded to a stress level of 25 ksi showed damage to initiate by intralaminar cracking of the 60 degree plies. Drilling-induced damage in the form of delamination was also noted in this fractograph.

Data obtained from incremental loading of the $[\ 45/90/-45/0]_{2S}$, IM-8/3501-6 specimen indicated that fiber type had little influence on the initiation and propagation of damage for the open hole tension specimens, Figure 43. Damage was found to initiate at approximately 36 % to 42 % of the failure stress by transverse (90 degree) cracking occurring at 120 to 75 degrees and 255 to 290 degrees around the circumference of the hole. Subsequent damage in the form of longitudinal (0 degree) and angle cracking was found to occur at stress levels ranging between 48 % to 67 % of the failure stress. The density of the longitudinal, transverse and angle cracks continued to increase until final failure of the specimen occurred at a stress level of 77 ksi. Examination of the cross-section of the $[45/90/-45/0]_{2S}$, IM-8/3501-6 laminate loaded to approximately 75 % of the failure stress revealed that damage initiated by intralaminar cracking of the 45 and 90 degree plies.

Matrix material was found to have some effect on the damage initiation for the open hole tension specimens, Figure 44. Damage initiation in both AS-4/APC-2 and IM-8/APC-2, open hole tension specimens was found to occur at a significantly higher percentage of failure stress than their graphite/epoxy counterparts. Radiographs obtained for a $[45/90/-45/0]_{2S}$, AS-4/APC-2, open hole tension specimens indicated that damage initiation occurred between 89 % to 93 % of the failure stress in the form of transverse (90 degree) and angle cracking. The initial damage was found to occur between 75 and 105 degrees around the circumference of the hole. Subsequent transverse (90 degree) and angle cracking occurring between 255 and 285 degrees was noted at approximately 98 % of the failure stress. Final failure occurred in a tensile mode at

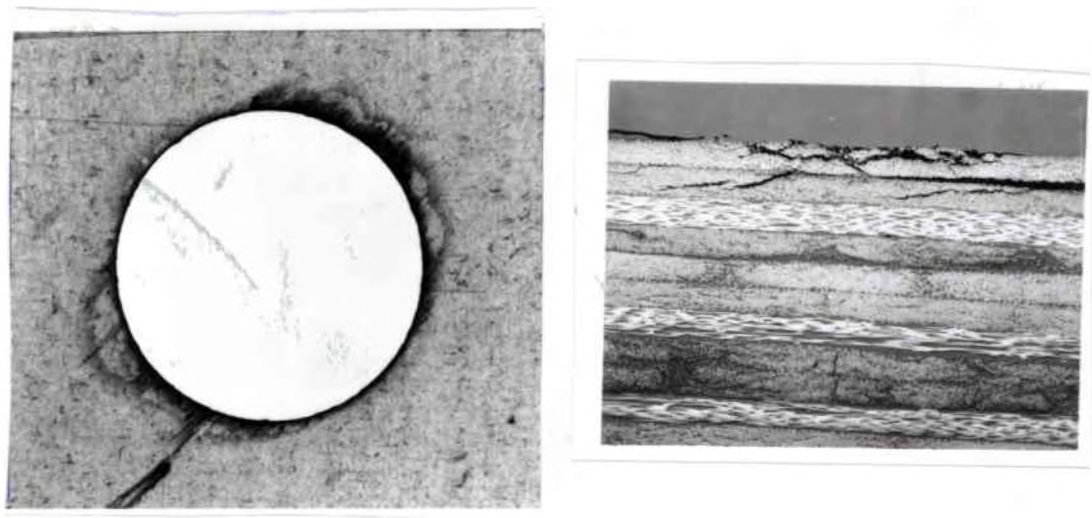

(a) 1-1-OHT specimen

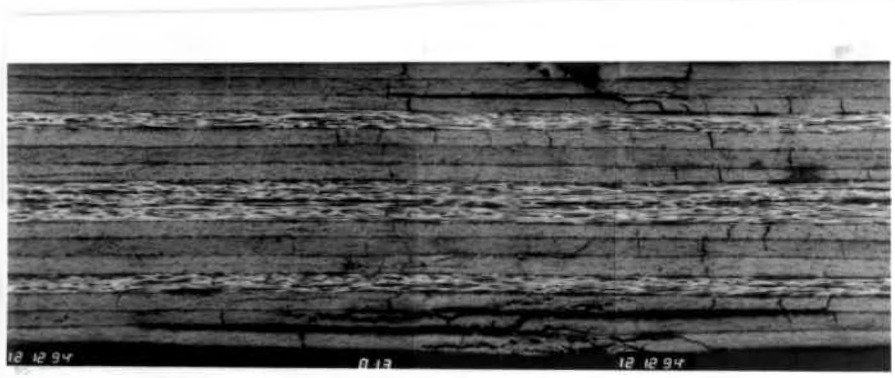

(b) 2-1-OHT

Figure 43. Radiographs and cross-sections obtained from tested graphite/epoxy, open hole tension specimens showing damage initiation to be essentially independent of fiber type and to occur at 35% to 45% of the failure load.

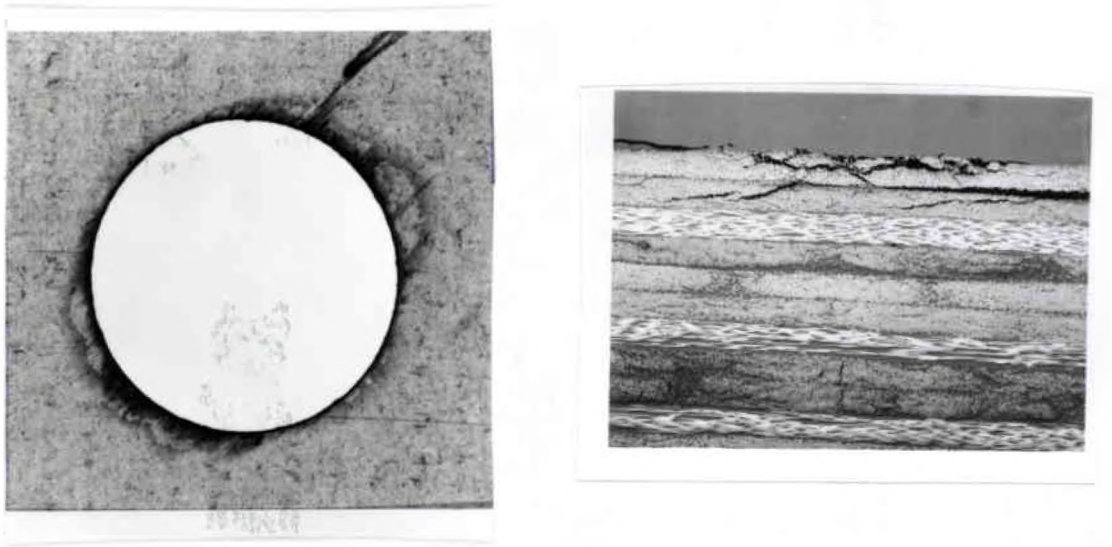

(a) 1-1-OHT specimen

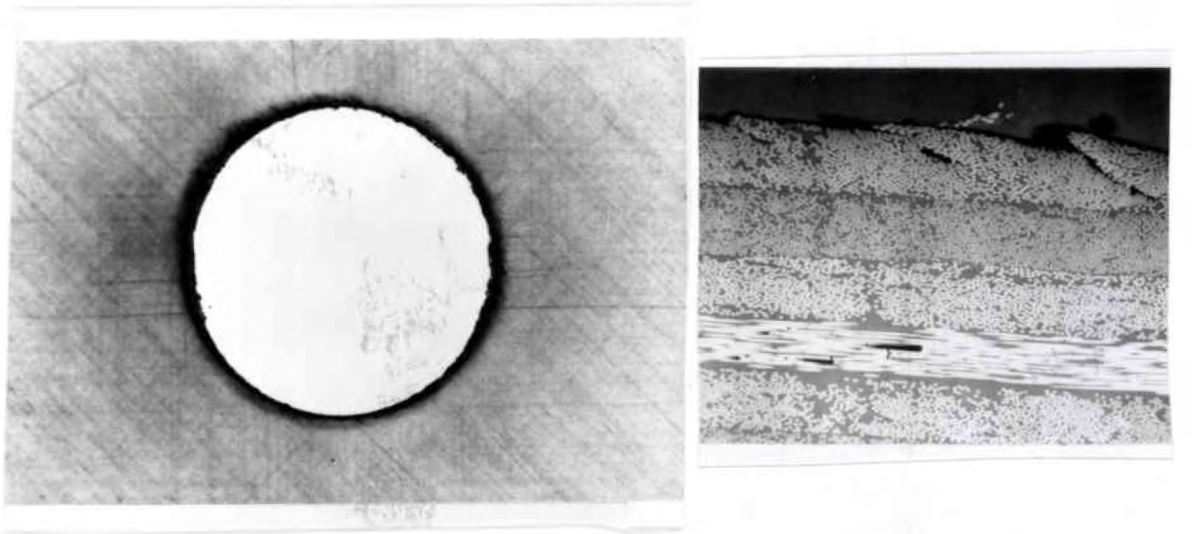

(b) 3-1-OHT specimen

Figure 44. Radiographs and cross-sections obtained from tested open hole tension specimens showing damage initiation in the graphite/epoxy (material 1) specimen to occur by intralaminar fracture of the angle plies while damage initiation in the graphite/PEEK (material 3) specimen to occur by translaminar fracture of the zero degree plies.

a stress level of 52 ksi. Examination of the cross-section for a $[45/90/-45/0]_{2S}$, AS-4/APC-2, open hole tension specimen loaded between 96 to 100 % of the failure stress indicated that damage initiation occurred by translaminar cracking of an outer 0 degree ply. This damage was observed on the accompanying radiograph as transverse cracking occurring between 75 to 105 degrees around the circumference of the hole. No apparent failure was observed in the radiographs obtained from the 0, 45, 90 lay-up of the IM-8/APC-2, open hole tension specimen loaded to 96.4 % of the failure stress. Final failure occurred in a tensile mode at a stress level of 70 ksi. The major difference noted in the mode of damage initiation of the graphite/epoxy versus graphite/PEEK material was that damage of the graphite/epoxy material occurred by intralaminar fracture of the angle plies where damage of the graphite/PEEK material occurred by translaminar or fracture of the zero degree plies. The first of these failure modes is a matrix dominated and the latter is a fiber dominated mode. Therefore, the above observation can be attributed to the higher transverse strength of the PEEK matrix material versus the epoxy matrix material which makes the graphite/PEEK material better able to resist the intralaminar fracture of the angle plies .

Radiographs obtained from the incremental loading study of the graphite/epoxy, filled hole tension specimens showed the mode of damage initiation and propagation to be similar to that of the open hole tension specimens. Failure initiation of filled hole specimens occurred at slightly greater percentages of the failure stress than the corresponding open hole specimens. However, final failure of the graphite/epoxy, filled hole tension specimens occurred at stress levels similar to that of the graphite/epoxy, open hole tension specimens. One possible explanation for the higher failure initiation loads obtained for the filled hole versus the open hole tension case may be associated with the technique used to examine the incrementally loaded specimens. In order for the radiographs to pick up damage in a specimen, the dye must be able to that penetrate to the damage area. In the case of filled hole tension specimens, if damage initiated at the washer edge instead of the hole edge than the dye would not have a path with which to reach that area of damage. Therefore, it is possible that damage initiated at lower stress levels at the washer edge. Failure initiation of the graphite/epoxy filled hole tension specimens

appeared to be independent of stacking sequence but the lay-up appeared to have some effect on the location of the initial damage and the direction with which this damage propagated. Additionally, fiber type appeared to have little effect on the damage initiation or propagation of the graphite/epoxy filled hole tension specimens. For both stacking sequences of the 0. 45 90 degree lay-up of the AS-4/3501-6 and IM-8/3501-6 materials damage was found to initiate between 48% to 57% of the failure stress in the form of transverse (90 degree), intralaminar cracks occurring in the 90 and 45 degree plies at a location similar to that of the open hole tension case. Longitudinal, transverse and angle cracking propagated until final failure occurred in the specimen at a stress range of 46 to 51 ksi. Damage in the AS-4/3501-6, open hole tension specimens made up of 0 and 60 degree laminae was found to initiate at approximately 40 % to 50 % of the failure stress in the form of intralaminar cracking of the 60 degree plies at intervals of 60 degrees around the circumference of the hole. Propagation of the 60 degree and longitudinal cracks continued until final failure occurred at a stress level of 69 to 74 ksi. Drilling-induced damage in the form of delamination was observed in the majority of the cross-sections examined for the graphite/epoxy filled hole tension specimens.

Some minor differences were observed in the mode of damage initiation and the associated stress levels for the graphite/PEEK filled versus open hole tension specimens. Radiographs obtained from the 0, 45, 90 lay-up of the graphite/PEEK filled hole tension specimens showed that the damage initiated by longitudinal (0 degree) and transverse (90 degree) cracking occurring at 90 and 270 degrees around the circumference of the hole. Examination of a representative cross-section showed the longitudinal (0 degree) cracking to be delaminations occurring at the outer +45, 90 interface. Additionally, damage initiation occurred between 80 % to 88 % of the failure stress which is somewhat lower than what was observed for the open hole tension case. Final failure of the incrementally loaded $[45/90/-45/0]_{2S}$, AS-4/APC-2 filled hole tension specimens occurred at approximately 56 ksi and final failure of the $[45/90/-45/0]_{2S}$, IM-8/APC-2, filled hole tension specimens occurred at approximately 70 ksi. These values are in the same range as what was obtained for the graphite/PEEK open hole tension

specimens. The occurrence of delamination as an initial failure mode for the filled hole tension specimens was a direct contradiction of what was expected. As discussed previously, the presence of the fastener should have inhibited delamination from occurring at the hole edge.

The incremental loading study of the open and filled hole compression specimens was limited to the 45, 90, 0 lay-ups of the AS-4/3501-6, IM-8/3501-6 and AS-4/APC-2 materials. Examination of the radiographs obtained for the incrementally loaded $[45/90/-45/0]_{2S}$, AS-4/3501-6, open hole compression specimen indicated damage initiation to occur at approximately 71 % of the failure stress. This damage occurred in the form of longitudinal (0 degree) cracks at 90 and 270 degrees around the circumference of the hole. Subsequent radiographs showed these initial longitudinal cracks to propagate to a region outside of the drilling induced damage area at a stress level of approximately 84.5 % of the failure stress. Examination of this radiograph showed no indication that the drilling induced delaminations propagated. Final failure of this specimen occurred at a stress level of 49.7 ksi in a shear or compressive type failure mode through the hole. A longitudinal cross-sections obtained from a similar test specimen loaded to approximately 89 % failure stress showed only a small amount of intralaminar cracking occurring in the surface 45 degree ply. No indication of any delamination or fiber buckling was observed in this photograph..

In a manner similar to that of the AS-4/3501-6, open hole compression specimen, damage in the $[45/90/-45/0]_{2S}$, IM-8/3501-6, open hole compression specimen initiated by longitudinal (0 degree) cracking occurring at a location of 270 degrees along the circumference of the hole. The damage initiation was found to occur at a stress level of approximately 90.6 % of the failure stress. This damage was found to propagate only slightly at a stress level of 94 % of the failure stress. Once again, there was no indication that the drilling-induced delaminations propagated. Final failure of this specimen occurred by a compressive or shear type mode through the hole at a stress level of 45.7 ksi. A longitudinal cross-section obtained from a $[45/90/-45/0]_{2S}$, IM-8/3501-6, open hole compression specimen loaded to a approximately 99 % of the failure stress showed significant delaminations and intralaminar cracking. The extent and nature

of the damage observed in the lower 45, 90 and 0 degree plies, suggests that this damage was the result of the drilling process. This may also be true for the damage observed in the upper 45 and 90 degree plies. However, the delaminations found to occur between the middle 45, 90 and 90, -45 interfaces do not appear to be the result of the drilling process. Likewise, the intralaminar cracks noted in the middle 45 and 90 degree plies did not appear to be drilling-induced. Therefore, it is likely that damage initiated in this specimen by delamination or intralaminar cracking in the middle 45 or 90 degree ply. No fiber kinking or buckling was observed in this cross-section. Comparison of the radiographs and cross-sections obtained for the AS-4/3501-6 and IM-8/3501-6 specimens indicated that fiber type had very little effect on the mode of damage initiation or propagation for the open hole compression case. This result is consistent with what was found through the experimental data and statistical analysis where fiber type was found to have little effect on the open hole compression strength.

Incremental loading of the [-45/0/45/90]2s, AS-4/APC-2 open hole compression specimen showed damage to initiate by longitudinal (0 degree) cracking occurring at 270 degrees, tangent to the hole edge. Longitudinal cracking initiated at a stress level of approximately 88 % of the failure stress. The initial longitudinal crack was found to propagate at a stress level of 93 % failure stress with no noticeable additional damage. Final failure of this specimen occurred at a stress of 48.3 ksi in a compress or shear type failure mode. The only damage observed in the cross-section obtained from a [45/90/-45/0]2s, AS-4/APC-2 open hole compression specimen loaded to approximately 94 % of the failure stress was a small intralaminar crack occurring in the upper 45 degree ply. This damage was not observed in the accompanying radiograph. Comparison of the radiographs indicated very little difference in the mode of damage initiation for the PEEK versus the epoxy matrix materials. However, as discussed in section 5.1.1 of this dissertation, some differences were noted in the final failure modes for these test specimens.

Radiographs obtained from the incrementally loaded $[45/90/-45/0]_{2S}$, AS-4/3501-6, filled hole compression specimen showed no damage occurring at the hole edge up to a stress level of 100 % of failure stress. Final failure of this specimen occurred in the grip region at a stress level

of 70 ksi. Additionally, no cross-section was available for a filled hole compression specimen of this material and this lay-up. Therefore, no conclusions can be made regarding the initiation and propagation of failure for the $[45/90/-45/0]_{2S}$, AS-4/3501-6, filled hole compression case.

Damage in the $[45/90/-45/0]_{2S}$, IM-8/3501-6, filled hole compression specimen was found to initiate by longitudinal (0 degree) cracking occurring tangent to the hole edge. Longitudinal cracks occurring at 90 and 270 degrees were found to propagate up to 97 % of failure stress. Final failure occurred in a compressive or shear type mode around the edge of the washer at a stress level of 69 ksi. No indication that any damage initiated at the washer edge was observed from the radiographs. However, as noted previously, damage occurring at the washer edge may not have shown up on the radiograph since the dye may not have been able to penetrate to this location. A longitudinal cross-section of a $[45/90/-45/0]_{2S}$, IM-8/3501-6, filled hole compression specimen loaded to 98 % of the failure stress showed significant delamination with little intralaminar cracking. Two of these delaminations were found to occur near the top and bottom surfaces of the test specimen and may be the result of the drilling procedure. A smaller delamination was observed between the middle +45, 90 interface. Intralaminar cracking appeared to propagate from that delamination into the 45 degree ply. This mode of failure initiation is similar to that observed for the $[45/90/-45/0]_{2S}$, IM-8/3501-6, open hole compression specimen, Figure 45. Therefore, it is possible that the presence of the fastener had little effect on the mode of damage initiation for the filled hole compression specimens. The presence of the washer did, however, have a noticeable effect on the mode of final failure for the filled hole compression specimens. Additionally, a statistically significant difference was noted in the experimental open versus filled hole compression data. This observation may suggest that the mode of damage initiation does not have a significant effect on the final failure mode and the associated strengths.

Failure of the incrementally loaded, AS-4/APC-2 filled hole compression specimen having the 0, 45, 90 lay-up occurred in the grip region at a stress of 72 ksi. Even though final failure occurred in the grip region, longitudinal (0 degree) cracks were observed tangent to the hole edge

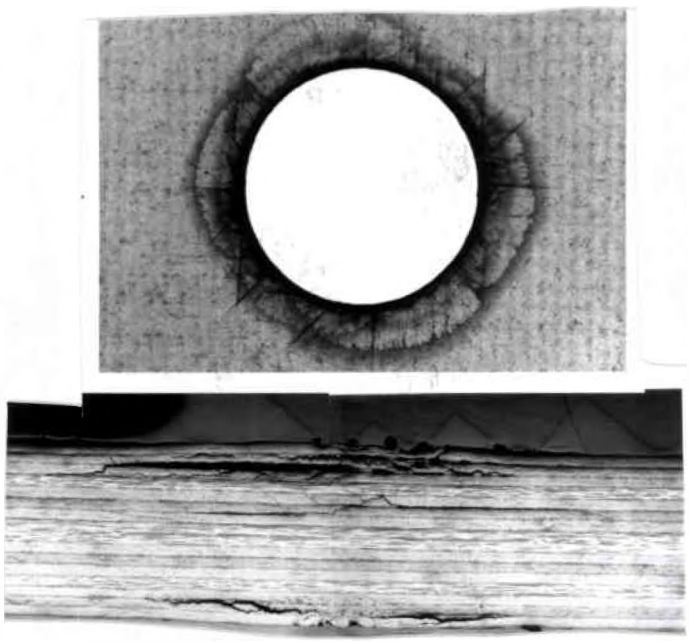

(a) 2-1-OHC specimen

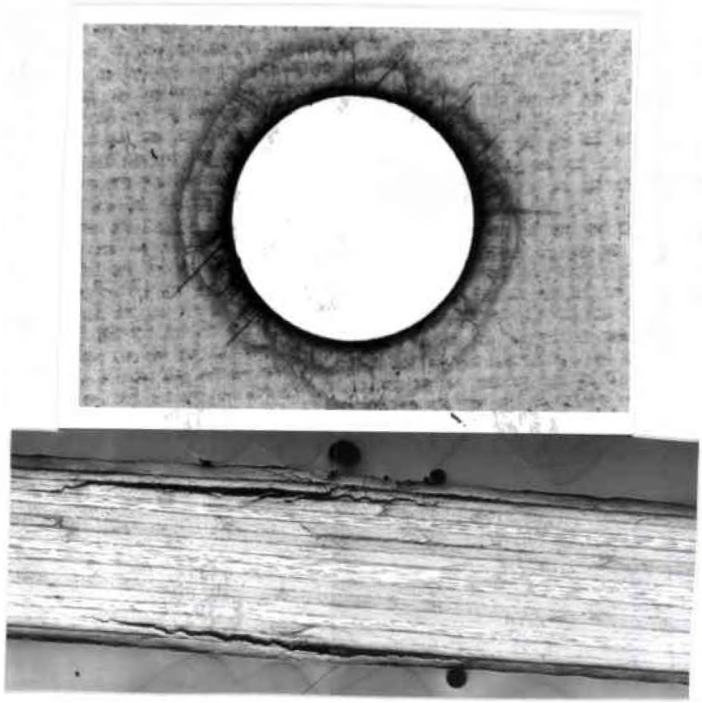

(b) 2-1-FHC specimen

Figure 45 Radiographs and cross-sections obtained from tested graphite/epoxy, open and filled hole compression specimens showing that the presence of the fastener had little effect on the mode of damage initiation for the filled hole compression specimens.

at a stress level of 98 % of failure stress. A longitudinal cross-section of a $[-45/90/45/0]_{2S}$, AS-4/APC-2 filled hole compression specimen loaded to 97 % failure stress showed the initiation of fiber buckling to occur in the 0 degree plies at the washer edge, Figure 46. With the exception of one ply, no delamination was detected in the areas surrounding these regions of fiber buckling. This result suggests that fiber buckling occurred prior to delamination for these specimens. As indicated previously, investigations have shown that the matrix material provides lateral support to fibers when a composite structure is subjected to a compressive load. For the case of low stiffness matrix materials, such as PEEK, fiber buckling can occur due to the lack of strong lateral support provided to these fibers by the matrix material [23, 80]. Conversely, failure of similar graphite/epoxy specimens was found to initiate by delamination and intralaminar fracture. This difference in mode of failure initiation for the thermoplastic versus epoxy matrix materials was not observed in the open hole compression specimens.

Correlation with Three-Dimensional Stress Analysis

An attempt was made to correlate the results of the fractographic analysis with data obtained from the three-dimensional stress analysis described in reference [73]. In this stress analysis, the three-dimensional stresses occurring around the circumference of the hole were determined on a ply-by ply basis using a spline approximation technique. The resulting stresses were then compared with the material properties and a form of the maximum stress failure criteria was applied to predict the mode, location and ply with which failure was likely to occur. A short summary of the failure criteria used in this analysis is included in Appendix D.

The data provided by the three-dimensional stress analysis and failure criteria provided in reference [73] and the observations made through the incremental loading study is compared in Table 19. From this table it can be seen that the failure analysis consistently predicted failures to initiate at slightly lower stress levels than what was observed thorough the incremental loading study. In most cases, however, the location and ply in which failure was predicted to initiate corresponded rather well with the fractographic observations. For the 0, 45, 90 degree lay-ups, the theoretical analysis predicted failure to initiate by interlaminar shear. For the 0, 60 degree

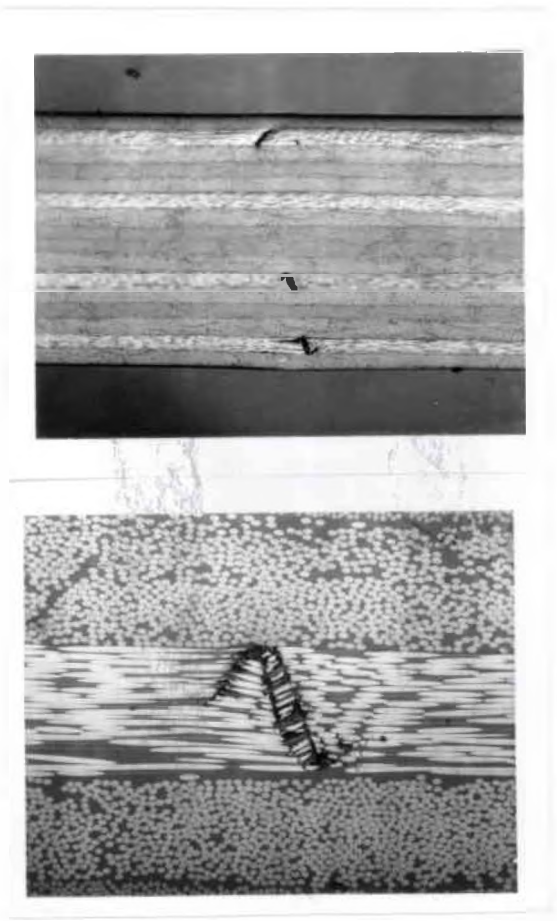

Figure 46. Radiographs and cross-sections obtained from a tested graphite/PEEK, filled hole compression specimen (3-5-FHC) showing damage initiation to occur by fiber buckling of the zero degree plies at approximately 97% of the failure stress.

lay-ups, however, the theoretical analysis predicted failure to initiate by transverse tension. The observed initial failure mode for all lay-ups was intralaminar cracking which is a possible failure mode for either stress state.

Comparison of the data provided in Figure 14 with the values of failure initiation stress provided in Table 19 indicates there to be little correlation between the experimentally determined final failure stress and the observed and predicted failure initiation stress. For example, the stress analysis predicted failure to initiate in the IM-8/3501-6 open hole tension specimen prior to the AS-4/3501-6, open hole tension specimen. The radiographs indicated that failure initiation occurred at essentially the same percentage of failure stress for these two materials. However, experimental data showed the IM-8/3501-6, open hole compression specimens to fail at significantly higher stresses than the AS-4/3501-6, open hole compression specimens. This observation suggests that the mode and load at which failure initiation occur may not have a significant effect upon the resulting failure strength.

TABLE 19

COMPARISON OF OBSERVED AND PREDICTED FAILURE INITIATION MODES AND LOCATIONS

	Predicted				Observed			
Specimen	Form	Location [Deg]	Location [ply]	Stress [%]	Form	Location [Deg]	Location [ply]	Stress [%]
1-1-OHT	13	107	[0]1	29	INTRA	105	[90]2	29
1-1-OHC	13	69	[-45]1	29	INTRA	90	[45]1	85
1-2-OHT	22,13	107	[90]1	28	INTRA	105	[90]2	29
1-3-OHT	22	78	[60]2	30	INTRA	60	[60]	34
1-4-OHT	22	77	[60]2	22	INTRA	60	[60]	36
2-1-OHT	13	107, 113	[0]2	22	INTRA	75-120	[45], [90]	36
2-1-OHC	13	71, 68	[0]2, [-45]1	26	INTRA, DEL	90	[45]2, [90]2	36

Where: INTRA corresponds to intralaminar cracking; DEL corresponds to delamination, 13 and 22 correspond to the stress component, σ_{ij}, likely to cause failure; location in degrees correspond to the location around the hole as identified in Figure 41 and location in plies identifies the ply in which failure is predicted to initiate.

There are several possible sources of error which may be responsible for any lack of correlation between the predicted and observed failure mode and location. One such source arose from the fact that the three-dimensional stress analysis does not account for drilling

induced-damage occurring at the hole edge. Additionally, the stress analysis is not capable of predicting the stresses at the hole edge subsequent to failure initiation. Finally, a comparison of cross-sections obtained from specimens which showed no damage in the accompanying radiograph indicated that the sensitivity of the radiographs is limited. Therefore, the stresses at which initial failure was found to occur may be somewhat higher than the actual failure initiation load.

CHAPTER 6

SUMMARY AND CONCLUSIONS

Summary

One of the major problems facing the composite design community stems from the nearly inevitable need to join composite parts via mechanical fasteners in the assembly of an aerospace structure. The use of mechanical fasteners requires that a hole be drilled in the composite part resulting in a material discontinuity. These material discontinuities produce areas of high stress concentrations which not only reduce the load carrying capability of the composite structure, but can also initiate undesirable interlaminar failures at the edge of the hole. In order to minimize the problems associated with the use of mechanical fasteners in composite structures, a fundamental understanding of the material and design parameters which affect bolted joint strength and the mode of failure initiation and propagation must be obtained.

The objective of this investigation was to experimentally and fractographically study the effects of various material and design parameters on the bolted joint performance of composite materials. To accomplish this, an in-depth parametric study was conducted which evaluated the effects of fiber stiffness, matrix properties, lay-up, stacking sequence and test type on the bearing, open and filled, drilled hole tension and compression performance of commonly used aerospace composite materials. Tested specimens were examined fractographically, and the modes of final failure compared. Additionally, representative specimens were subjected to an incremental loading study in which the initiation and propagation of damage was tracked. Information gained from the fractographic and incremental loading studies was correlated with the experimental data and with existing failure analysis data obtained from a three-dimensional stress analysis. A two-dimensional analysis which evaluated the stress distribution occurring at the hole edge for the open hole tension specimens was also conducted to provide information concerning

the effect of fiber type and matrix type on the ability of the material to dissipate stress concentrations associated with the presence of the drilled hole.

The data generated from this investigation supplies the composite community with an in-depth, fundamental understanding of the effect of composite constituent properties, test type, lay-up and stacking sequence on the bolted joint performance of composite materials. Additionally, the results obtained from the fractographic analysis provide invaluable information concerning the effect of these parameters on the initiation and propagation of damage in a bolted composite joint. Correlation of the fractographic and experimental data was useful in assessing the applicability of two- versus three-dimensional stress analysis. The conclusions drawn from this investigation will be critical to the development of appropriate failure criteria and models capable of predicting the strength of bolted composite joints. Furthermore, fractographic and experimental procedures were developed which will be useful to researchers in the future.

Conclusions

A more fundamental understanding of the parameters affecting the bearing, open and filled hole tension and compression performance of composite materials has been achieved. Fiber type was found to have a statistically significant effect on the open and filled hole tensile strength for the composite material systems studied. For both the epoxy (3501-6) and PEEK (APC-2) matrices, the IM-8 fiber was found to provide superior strengths. This result is attributed to the inherently higher constituent strength and modulus of the IM-8 fiber which provided better resistance to the fiber dominated tensile failure mode observed for the open and filled hole tensile specimens and enhanced the materials' ability to dissipate the stress concentrations occurring at the hole edge. No significant differences were observed in the mode of failure initiation or propagation for the two different fibers studied. Failure was found to initiate by intralaminar cracking of the off-axis plies and propagate transverse to the direction of the applied stress. Final failure occurred at the hole center in a tensile dominated mode and consisted of interlaminar, intralaminar and translaminar cracking. Slightly more delamination and intralaminar cracking was noted for the IM-8 specimens than for the AS-4 specimens. This observation may be attributed to

the lower transverse tensile strength of the IM-8 materials, suggesting that the fiber, matrix interface may have some effect on the mode of failure for the open and filled hole tension specimens. The effect of fiber type on the open and filled hole tensile failure modes may also be due to a difference in the interlaminar stress state generated for the materials studied which is a function of the fiber stiffness properties. For the graphite/epoxy, open hole tensile specimens, failure initiation was predicted to occur as a result of interlaminar shear stresses occurring at the hole edge. The mode of damage initiation appeared to have little effect on the ultimate strengths or modes of failure.

Fiber type was found to have little effect on the open and filled hole compression strengths for both the epoxy and PEEK matrix material systems. No significant difference in mode of failure initiation or propagation was noted for specimens containing the AS-4 versus IM-8 fibers. For the graphite/epoxy open and filled hole compression specimens, failure was found to initiate by intralaminar cracking and delamination at the hole edge. Slightly more delamination was noted for the IM-8/3501-6 specimens than for the AS-4/3501-6 specimens. For both the AS-4/3501-6 and IM-8/3501-6, open hole compression specimens, failure initiation was predicted to occur as a result of interlaminar shear stresses occurring at the hole edge. Failure of the open and filled hole compression specimens for all the materials studied was found to propagate parallel to the direction of the applied stress. Final failure of the open hole compression specimens occurred in a shear or compressive type mode through the hole. Final failure of the filled hole compression specimens occurred in a compressive or shear type failure mode occurring around the washer edge. The lack of dependence of fiber type on the open and filled hole compressive strength is attributed to the fact that the failure is dominated by fiber buckling and kinking or shear which is more dependent upon the fiber, matrix interfacial strength and matrix stiffness than fiber strength and modulus.

Bearing strength and mode of failure was found to be essentially independent of fiber type. All of the specimens failed in a bearing type failure mode. The lack of dependence of

bearing strength on fiber type is attributed to the fact that the bearing type failure mode is more dependent upon matrix properties than upon fiber properties.

Although the statistical analysis indicated that the matrix type did not have a significant effect on the open and filled hole tensile strength, the graphite/PEEK specimens were found to provide consistently higher strengths than the graphite/epoxy specimens. The higher open and filled hole tensile strength obtained for the graphite/PEEK specimens is attributed to the inherently higher strength of the PEEK matrix material over the epoxy matrix material and the ability of the PEEK matrix material to provide greater stress relief at the hole edge than the epoxy matrix material. As indicated previously, the ability of the matrix material to relieve stresses at the hole edge is important for notched specimens loaded in tension. The matrix material was found to have some effect on the mode and stress level at which failure initiated. For the epoxy matrix materials, failure was found to initiate by intralaminar fracture of the off-axis plies whereas failure initiation in the graphite/PEEK materials occurred by translaminar fracture of the 0 degree plies. The difference in failure initiation modes was attributed to the difference in transverse tensile strengths for the graphite/PEEK versus the graphite/epoxy materials. The inherently lower transverse tensile strength associated with the graphite/epoxy material resulted in failure initiation by intralaminar fracture at relatively low percentages of failure stress. In both cases, failure propagated 90 degrees to the direction of the applied stress. Final failure for both materials occurred by tensile failure through the hole.

As with the open and filled hole tension specimens, the statistical analysis indicated that the matrix type did not have a significant effect on the open and filled hole compression strength. However, the graphite/epoxy specimens were found to provide consistently higher open and filled hole compression strengths than the graphite/PEEK specimens. This difference in open and filled hole compression strength for the two matrix materials was attributed to the fact that the PEEK matrix material is not as stiff as the epoxy matrix material making the PEEK matrix material less able to provide adequate lateral constraint to its fibers. This explanation was verified through the fractographic analysis in that failure initiation of the graphite/PEEK specimens was found to occur

by buckling of the zero degree plies, whereas failure initiation of the graphite/epoxy specimens occurred by intralaminar fracture of the off-axis plies. For both matrix materials, failure was found to propagate by longitudinal cracking. Final failure of the graphite/epoxy specimens was characterized by kink bands consisting of multiple plies, whereas final failure of the graphite/epoxy specimens occurred by kinking of the individual plies.

The graphite/PEEK specimens were found to provide consistently higher bearing strengths than the graphite/epoxy specimens. However, the effect of matrix type was not found to be statistically significant for the bearing case. The greater strengths obtained for the graphite/PEEK specimens is attributed to the greater notch sensitivity of the epoxy matrix material over the PEEK matrix material. This conclusion was confirmed by the fact that a significant amount of local yielding was observed in the graphite/PEEK bearing specimens, whereas virtually no local yielding was observed for the graphite/epoxy bearing specimens.

The bearing, open and filled hole tensile and compressive strengths were found to be independent of stacking sequence for all the materials studied. Similarly, no difference in mode of failure initiation was observed for a given material and loading condition. The result that stacking sequence did not significantly affect the bearing, open and filled hole tensile and compressive strength may imply that the occurrence of interlaminar stresses is not an important consideration in the design of bolted, composite joints. This conclusion is supported by the observation that although interlaminar stresses may initiate failure, the mode and stress at which failure initiation occur have little effect on the final failure mode or ultimate strength. Additionally, data obtained from the three-dimensional stress analysis suggested the failure initiation of the graphite/epoxy test specimens to be essentially independent of stacking sequence. Therefore, the need for a three-dimensional stress analysis of bolted composite joints is questioned.

Lay-up was found to have a statistically significant effect on the open and filled hole tensile and compressive strength for all materials studied. In general, the lay-ups consisting of 0 and 60 degree layers were found to provide slightly higher tensile and compressive strengths than those containing 0, 45 and 90 degree plies. Some difference in the initiation and

propagation of damage in the open and filled hole tensile specimens was noted for the various lay-ups. In the 0, 45, 90 degree lay-ups of the graphite/epoxy specimens, failure initiated by intralaminar fracture of the off-axis plies. Failure propagated 90 degrees to the direction of the applied load. For the 0, 60 degree lay-ups of the graphite/epoxy material failure was found to initiate by intralaminar failure of the 60 degree plies. Propagation of failure occurred 60 degrees to and parallel to the direction of the applied stress. Lay-up was not found to have a statistically significant effect on the bearing strengths or failure modes for any of the materials studied.

The presence of the fastener in the filled hole specimens was found to have little effect on the tensile strength of the materials studied. The mode of damage initiation and propagation was found to be essentially independent of test type (open versus filled hole testing). The mode of damage initiation and propagation for the open and filled hole tension specimens was found to be similar. Both initiated by intralaminar fracture of the angle plies and propagated transversely from the hole edge. Damage initiation for the filled hole specimens occurred at slightly higher percentages of failure stress than for the open hole specimens, but this had little effect on the ultimate failure strengths. The only effect that the presence of the fasteners was found to have on the ultimate failure mode of the graphite/epoxy and graphite/PEEK tensile specimens was to suppress the delaminations to a region outside of the washer area and to encourage a greater degree of intralaminar fractures of the angle plies.

The presence of the fastener was found to have a significant effect on both the strength and failure mode of the specimens loaded in compression. The stress levels at which damage initiation and ultimate failure occurred were significantly higher for the filled hole compression specimens than the open hole compression specimens. Failure initiation for both test types occurred at high percentages of failure stress indicating a catastrophic type failure. Damage initiation of the open hole compression specimens occurred by intralaminar cracking of the angle plies. Damage initiation of the graphite/epoxy filled hole compression specimens also occurred by intralaminar cracking. Failure in the graphite/PEEK filled hole compression specimens initiated by buckling of the 0 degree plies. Ultimate failure of the open hole compression specimens

occurred by a shear type failure at the washer edge. In the filled hole compression specimens, two distinct regions of failure were noted. These regions corresponded to the washer and hole edge with the majority of the damage occurring outside the washer area. Therefore, the lateral constraint provided by the torqued fastener appeared to be effective in suppressing a majority of the damage to a region outside the washer area.

Hole size was found to have a significant effect on the bearing strengths. This result was attributed to the more concentrated distribution of the normal stresses at the hole edge for the smaller hole size. which translated to higher bearing strengths. For all the materials studied, the damage appeared to be slightly more significant for the smaller hole size specimens than the larger hole sized specimens.

The three-dimensional stress analysis and failure criteria described in [73] provided useful information concerning the location and mode of initial damage. However, the relative applicability of a three-dimensional versus two-dimensional technique such as this is questioned, since there appeared to be little correlation between the damage initiation mode and strengths with the ultimate failure mode and strengths. Additionally, a three-dimensional stress analysis is not independent of stacking sequence whereas a three dimensional stress analysis is independent of stacking sequence. Since the experimental data suggests that stacking sequence, hence the occurrence of interlaminar stresses had little effect on the failure modes or strengths than a two-dimensional stress analysis may be sufficient to model bolted composite joints for the materials and lay-ups studied.

The technique used for the incremental loading study which consisted of loading the specimen to a percentage of failure stress then subjecting it to radiography was found to be very useful in identifying the failure initiation stress and location for the open hole test specimens. Some questions concerning the applicability of this methodology to the filled hole test specimens arose, since the dye may not have been able to penetrate to initial damage areas occurring at interior regions of the test specimen such as the washer edge. Longitudinal cross-sectioning of tested specimens provided very useful information concerning the mode and location of initial and

ultimate failure. The noise associated with the acoustic emissions output made it very difficult to extract any useful information, especially in the case of filled hole compression tests. Drilling induced damage was noted in many of the graphite/epoxy test specimens. This damage was most likely the result of dull drill bits. Although the drilling induced damage did not appear to propagate with applied static stress, this type of damage is undesirable in an experimental investigation such as this one. Therefore, it is critical that special precautions such as frequent replacement of the drill bits, be taken to limit the occurrence of drilling induced damage. The two-dimensional approximation technique used to determine normal stress distribution at the hole edge was found to have very little correlation with the experimental data. The difference of mean technique was found to be very useful in assessing the relative effects of the parameters studied.

CHAPTER 7

RECOMMENDATIONS

The results obtained from this investigation helped to provide many directions for future research in the area of bolted composite joints. Many of the graphite/epoxy test specimens examined in this investigation contained a substantial amount of drilling induced damage. Although this damage did not appear to propagate with applied static stress, it is possible that the presence of this damage had some effect on the mode of damage initiation and on the ultimate failure stress. Additionally, the presence of this damage may have a large effect on the strength and failure mode of specimens subjected to fatigue loading. This may be especially true in the case of tension-compression or compression-compression fatigue where drilling induced delaminations may propagate or cause premature kink band formation in these specimens. Therefore, it is recommended that a study be conducted which assesses the effect of different levels of drilling induced damage on the performance of open and filled hole specimens loaded both staticly and in fatigue. Additionally, the three-dimensional stress analysis developed in [73] may need to be modified to account for the presence of drilling induced damage. If the data obtained from these investigations suggests that drilling induced damage has a large effect on the performance of bolted composite joints, then research in the area of perfecting the drilling procedure so that drilling induced damage is minimized will need to be conducted.

Data obtained from the incremental loading study conducted on the filled hole tension and compression specimens resulted in some questions concerning the applicability of radiography in identifying failure initiation of these specimens. It is possible that damage may have initiated in the filled hole specimens at the washer edge instead of at the hole edge at lower percentages of failure stress than what the radiographs indicated. The reason for this is that the dye may not have been able to penetrate to the interior region of the specimen corresponding to

the washer edge. Therefore, it is recommended that a study be conducted to assess the applicability of radiography in identifying failure initiation and mode for filled hole specimens. To accomplish this an incremental loading study needs to be conducted which incorporates both radiography and the serial sectioning technique. The serial sectioning technique consists of preparing a cross-section then repeatedly photographing the cross-section at different sanding depths.

Additionally, a more in-depth fractographic study may need to be conducted on a more select group of specimen to further identify the mode of damage initiation, propagation and ultimate failure. One such group of specimens which may provide some interesting information concerning the formation of kink band formation and buckling of composites might include open hole compression tests on composite materials having low modulus matrices, such as graphite/PEEK. A more in-depth fractographic analysis on bearing specimens may also be an interesting area for future research.

It is recommended that a small research project aimed at perfecting the acoustic emissions technique be conducted so that this technique can be used with confidence in identifying major failure events occurring within a composite test specimen. This research must focus on reducing the noise associated with the acoustic emissions output and on correlating peaks in the hits or counts versus load curve with actual failure events.

A parametric study which assesses the effects of elevated temperature and moisture absorption on the open and filled hole tension and compression performance of composite materials is also needed. This study should provide information concerning the effect of these variables on the failure initiation and ultimate failure strengths as well as the mode of damage initiation, propagation and final failure.

An investigation which examines the effects of various parameters including material constituent properties and lay-up on the performance of open and filled hole specimens loaded in fatigue is also needed. This is needed since most applications involving mechanically fastened joints are loaded in fatigue rather than subjected to static loading conditions. In the case of fatigue

loading, the occurrence of premature delaminations resulting from out-of-plane stresses occurring at the hole may have a deleterious effect on the performance of open and filled hole test specimens. If this is the case, then a failure model which incorporates three-dimensional stress analysis may be required.

It may also be desirable to incorporate the Moiré interferometrey technique to determine the in-plane stress distribution occurring in the vicinity of the hole for both open and filled hole test specimens. A study of this sort would require some further development of the Moiré technique such that it could be accurately applied to specimens having torqued fasteners. Data obtained from such an analysis might be useful in developing a more accurate model for determining the stress distribution around an open hole and a hole containing a tightened fastener. Additionally, the results of such an investigation would provide useful information concerning the effect of the fastener on the performance of a bolted composite joint.

An analytical study aimed at developing a progressive damage failure model capable of accurately predicting the effect of the various parameters on the ultimate strength and failure mode of bolted composite joints is greatly needed by the aerospace community. It is likely that a two-dimensional analysis would be sufficient for this model.

APPENDIX A

INTERLAMINAR STRESS APPROXIMATION

A three-dimensional state of stress exists at the free edge of laminates in a boundary region approximately equal to one laminate thickness, Figure 47. Interlaminar normal stresses can initiate premature delamination type failures in this boundary region. To approximate the relative magnitude of the maximum interlaminar normal stresses occurring at the mid-plane of a symmetric, 16 ply laminate subjected to uniaxial tension, the moment about the z axis due to the stresses occurring in the y direction were considered, Figure 48 [26, 40-43, 45, 49].

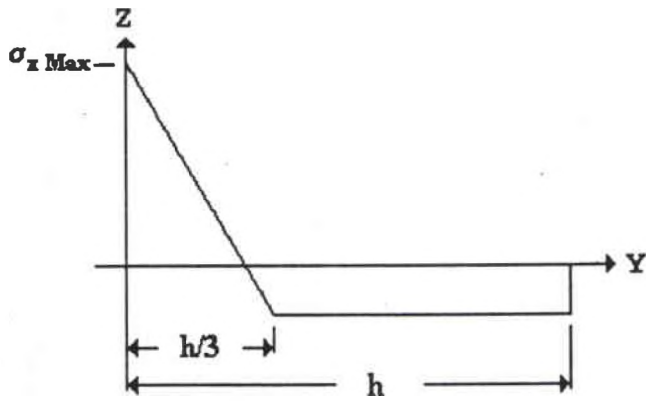

Figure 47. Approximate distribution of interlaminar normal stress vs. y.

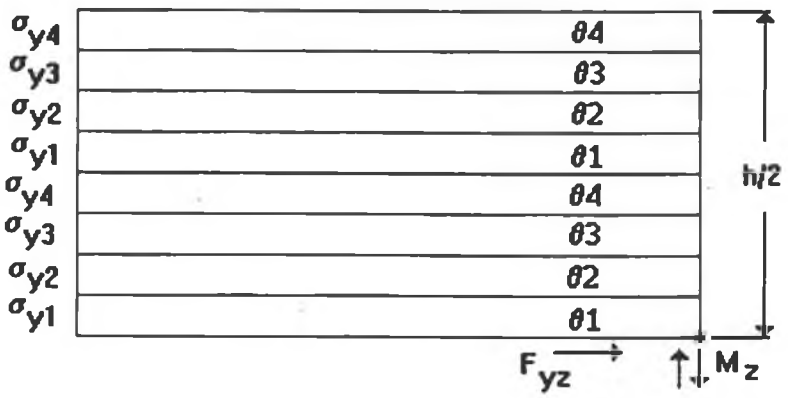

Figure 48. Moments about the z-axis for a 16 ply symmetric laminate.

$$\sigma_{zmax} = (90\ M_z) / (7\ h^2) \quad (1)$$

For a laminate subjected to uniaxial tension:

$$N_x/h = \sigma_0 = \text{constant} \quad (2)$$
$$N_y = N_{xy} = 0$$

Where: N_x, N_y, N_{xy} = components of stress resultant
h = laminate thickness
σ_0 = applied stress
σ_{zmax} = maximum interlaminar normal stress

For plane stress, $Q_{26} = 0$:

$$\sigma_y^k = Q_{12}^k \varepsilon_1 + Q_{22}^k \varepsilon_2 \quad (3)$$

Where: σ_y^k = component of stress acting on the kth ply
Q_{ij} = components of reduced stiffness
$\varepsilon_1, \varepsilon_2$ = components of strain

For the case of uniaxial tension with no thermal loads:

$$N_x = A_{11}\ \varepsilon_1^0 + A_{12}\ \varepsilon_2^0 + A_{16}\ \varepsilon_6^0 = \sigma^0 h \quad (4)$$

$$N_y = A_{12}\ \varepsilon_1^0 + A_{22}\ \varepsilon_2^0 + A_{26}\ \varepsilon_6^0 = 0 \quad (5)$$

$$N_{xy} = A_{16}\ \varepsilon_1^0 + A_{26}\ \varepsilon_2^0 + A_{66}\ \varepsilon_6^0 = 0 \quad (6)$$

For an orthotropic laminate, $A_{16} = A_{26} = 0$:

$$\sigma^0 h = A_{11}\ \varepsilon_1^0 + A_{12}\ \varepsilon_2^0 \quad (7)$$

$$0 = A_{12}\ \varepsilon_1^0 + A_{22}\ \varepsilon_2^0 \quad (8)$$

$$0 = A_{66}\ \varepsilon_6 \quad (9)$$

For a laminate of the form $[\theta_1 / \theta_2 / \theta_3 / \theta_4]_{2s}$:

$$A_{ij} = (h/4) * (Q_{ij}^{(1)} + Q_{ij}^{(2)} + Q_{ij}^{(3)} + Q_{ij}^{(4)}) \quad (10)$$

At the mid-plane:

$$\varepsilon_1 = \varepsilon_1^0$$

$$\varepsilon_2 = \varepsilon_2^0$$

$$\varepsilon_6 = \varepsilon_6^0$$

Solving equation (7) through (10) in terms of A_{ij}:

$$\varepsilon_1 = (-A_{22}\,\sigma^0\,h)/(A_{11}\,A_{22} + A_{12}^2) \quad (11)$$

$$\varepsilon_2 = (A_{12}\,\sigma^0\,h)/(A_{11}\,A_{22} + A_{12}^2) \quad (12)$$

Calculating reduced stiffness in terms of laminate coordinates, Figure 49:

$$Q_{11}' = E_{11} / (1-\nu_{12}^2\,(E_{22}/E_{11})) \quad (13)$$

$$Q_{22}' = E_{22} / (1-\nu_{12}^2\,(E_{22}/E_{11})) \quad (14)$$

$$Q_{12}' = (\nu_{12}\,E_{22}) / (1-\nu_{12}^2\,(E_{22}/E_{11})) \quad (15)$$

$$Q_{66}' = G_{12} \quad (16)$$

Where: E_{11}, E_{22}, G_{12} = Longitudinal, Transverse and Shear moduli
ν_{12} = Poisson's Ratio

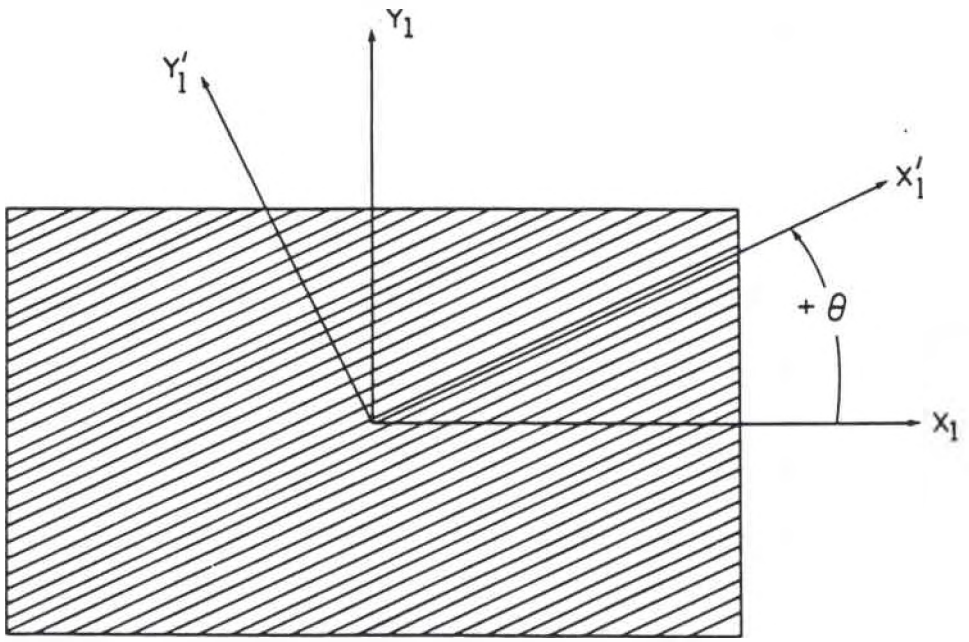

Figure 49. Definition of laminate versus material coordinate systems.

Transforming Q's to material coordinates:

$$Q_{11}^k = m^4 Q_{11}' + 2 m^2 n^2 (Q_{12}' + 2 Q_{66}') + Q_{22}' n^4 \quad (17)$$

$$Q_{12}^k = m^2 n^2 (Q_{12}' + Q_{22}' - 4 Q_{66}') + Q_{12}' (m^4 + n^4) \quad (18)$$

$$Q_{11}^k = n^4 Q_{11}' + 2 m^2 n^2 (Q_{12}' + 2 Q_{66}') + Q_{22}' m^4 \quad (19)$$

Where:

$$m = \cos \theta^k \quad (20)$$

$$n = \sin \theta^k \quad (21)$$

Solving equations (3), (11) and (12) for the σ_y in each ply:

$$\sigma_y^k = [(\sigma_o h) / (A_{11} A_{22} + A_{12}^2)] * [A_{12} Q_{22}^k - A_{22} Q_{12}^k] \quad (22)$$

Summing the moments about the z axis:

$$\begin{aligned} M_z = {} & [\sigma_o h^3] / [256 (A_{11} A_{22} + A_{12}^2)] \\ & * [5 (A_{12} Q^1_{22} - A_{22} Q^1_{12}) \\ & + 7 (A_{12} Q^2_{22} - A_{22} Q^2_{12}) \\ & + 9 (A_{12} Q^3_{22} - A_{22} Q^3_{12}) \\ & + 11 (A_{12} Q^4_{22} - A_{22} Q^4_{12})] \end{aligned} \quad (23)$$

Combining equation (1) and (23):

$$\begin{aligned} \sigma_{z\,max} = {} & [45 \sigma_o h] / [896 (A_{11} A_{22} + A_{12}^2)] \\ & * [5 (A_{12} Q^1_{22} - A_{22} Q^1_{12}) \\ & + 7 (A_{12} Q^2_{22} - A_{22} Q^2_{12}) \\ & + 9 (A_{12} Q^3_{22} - A_{22} Q^3_{12}) \\ & + 11 (A_{12} Q^4_{22} - A_{22} Q^4_{12})] \end{aligned} \quad (24)$$

An EXCEL spreadsheet was used to make the necessary calculations. Data obtained from this analysis is summarized in Table 20

TABLE 20

APPROXIMATION OF INTERLAMINAR NORMAL STRESSES AT MIDPLY

	σ3/σ0			
Material	$[45/90/-45/0]_{2s}$	$[45/-45/0/90]_{2s}$	$[60/02/-60]_{2s}$	$[60/-60/02]_{2s}$
AS-4/3501-6	1.04E-02	6.25E-03	8.89E-18	1.47E-02
IM-8/3501-6	8.90E-03	5.87E-03	0.00E+00	1.80E-03
Material	$[-45/0/45/90]_{2s}$	$[-45/45/90/0]_{2s}$	$[30/902/-30]_{2s}$	$[60/-60/02]_{2s}$
AS-4/APC-2	1.80E-03	1.75E-02	2.60E-17	1.84E-02
IM-8/APC-2	7.72E-04			

APPENDIX B

STATISTICAL ANALYSIS

Difference of Means Technique

Definition of Variables

Calculation of the main and interaction effects in this investigation consisted of breaking the data up into several data sets and analyzing each of these data sets individually. The data was broken up as indicated below. The variables of interest are defined for each data set.

1. Graphite/Epoxy Material:

Notched tension, notched compression and bearing data was analyzed individually for these materials.

VARIABLE	LEVEL 1 (-)	LEVEL 2 (+)	TOTAL
Stacking Sequence	low (2,4)	high (1,3)	2
Lay-up	low (3,4)	high (1,2)	2
Fiber	IM-8	AS-4	2
Test	FH, b	OH, a	2

Where: OH = Open Hole (tension and compression tests)
FH = Filled Hole (tension and compression tests)
a = 0.125 inch diameter hole (bearing tests)
b = 0.250 inch diameter hole (bearing tests)
The numbers in parentheses for the stacking sequence and lay-up correspond to the lay-ups as defined below:

(1) $[45/90/-45/0]_{2s}$
(2) $[45/-45/0/90]_{2s}$
(3) $[60/0_2/-60]_{2s}$
(4) $[60/-60/0_2]_{2s}$

2. Graphite/PEEK Material:

Notched tension, notched compression and bearing data was analyzed individually for these materials.

VARIABLE	LEVEL 1 (-)	LEVEL 2 (+)	TOTAL
Stacking Sequence	low (2)	high (1)	2
Fiber	IM-8	AS-4	2
Test	FH, b	OH, a	2

Where: The numbers in parentheses for the stacking sequence and lay-up correspond to the lay-ups as defined below:

(1) $[-45/0/45/90]_{2s}$

(2) $[-45/45/90/0]_{2s}$

3. Matrix Comparison:

Notched tension, notched compression and bearing data was analyzed individually for these materials.

VARIABLE	LEVEL 1 (-)	LEVEL 2 (+)	TOTAL
Matrix	3501-6	APC-2	2
Test	FH, b	OH, a	2

4. Notched versus Unnotched (Graphite/Epoxy material):

Notched tension, notched compression and bearing data was analyzed individually for these materials.

VARIABLE	LEVEL 1 (-)	LEVEL 2 (+)	TOTAL
Notched	No	Yes	2
Filled	No	Yes	2
Fiber	IM-8	AS-4	2
Lay-up	Low (4)	High (1)	2

The data set for the graphite/epoxy material (data set 1) will be used as an example to show the calculations carried out in this analysis.

Design Matrix

Trial	Stacking Seq.	Lay-up	Fiber	Test	mean
1	-	-	-	-	y_1
2	-	-	-	+	y_2
3	-	-	+	-	y_3
4	-	-	+	+	y_4
5	-	+	-	-	y_5
6	-	+	-	+	y_6
7	-	+	+	-	y_7
8	-	+	+	+	y_8
9	+	-	-	-	y_9
10	+	-	-	+	y_{10}
11	+	-	+	-	y_{11}

12	+	-	+	+	y_{12}
13	+	+	-	-	y_{13}
14	+	+	-	+	y_{14}
15	+	+	+	-	y_{15}
16	+	+	+	+	y_{16}

Calculation of Main and Interaction Effects

Effects of a variable were calculated by taking the average of the differences of data obtained from tests conducted at the two levels for that particular variable. Therefore, for this example:

$$\text{Main Effect of Stack. Seq.} = [(y_9-y_1)+(y_{10}-y_2)+(y_{11}-y_3)+(y_{12}-y_4) (y_{13}-y_5)+(y_{14}-y_{16})+(y_{15}-y_7)+(y_{16}-y_8)]/8 \quad (1)$$

Effects of other variables including lay-up, fiber type and test type were calculated in a similar manner. The two factor interactions possible for this example include the following:

(1) Stacking Sequence X Lay-up;
(2) Stacking Sequence X Fiber;
(3) Stacking Sequence X Test Type;
(4) Lay-up X Fiber;
(5) Lay-up X Test Type;
(6) Fiber X Test Type.

The interaction effects were calculated by taking half of the difference between the average effect of a variable at level 1 and the average effect at level 2. For this example the stacking sequence X lay-up interaction were calculated as follows:

$$\text{Stack. Seq. X Lay-up Interaction Effect} = (e_+ - e_-)/2 \quad (2)$$

Where: $e_+ = (y_{13}-y_9+y_{14}-y_{10}+y_{15}-y_{11}+y_{16}-y_{12})/8$
$e_- = (y_5-y_1+y_6-y_2+y_7-y_3+y_8-y_4)/8$

The remaining interactions were calculated in a similar manner.

Miscellaneous Statistical Calculations

Mean for Each Trial:

$$y_i = \Sigma y_j / n_i \quad (3)$$

Degrees of Freedom for Each Trial:

$$v_i = n_i - 1 \quad (4)$$

Total Number of Observations:

$$N = \Sigma n_i$$

Variance for Each Trial:

$$s_i^2 = \Sigma [(y_j - y_i)2/v] \quad (6)$$

Pooled Estimate of Run Variance:

$$s^2 = (\Sigma v_i s_i^2) / (\Sigma v_i) \quad (7)$$

Standard Error:

$$SE\ mean = [(s^2 * 4.0)/ N]^{0.5} / 2 \quad (8)$$

$$SE\ effect = [(s^2 * 4.0)/ N]^{0.5} \quad (9)$$

Probability of Each Effect (for a design matrix having 16 trials):

$$P = 100 * (Rank\ of\ Effect - 0.5)/15 \quad (10)$$

Where:

	y_i	=	trial mean (i = 1,16)
	y_j	=	individual repeated measure (j = 1,5)
	n_i	=	number of observations for trial (i = 1,16
	N	=	total number of observations

Analysis of Residuals

Normal plotting of the main and interaction effects suggested that certain effects for each of the data sets analyzed could not be explained by random noise in the data. As a check to this conclusion, the residuals were calculated and plotted on normal probability paper. If all of the points from the residual plot lie close to the line, the conjecture that the aforementioned effects could not be explained by random noise was confirmed. The residuals were calculated by first establishing a table separating the effects believed to be significant. As an example, consider the case of the tension data generated from the graphite/epoxy material.

TRIAL	FIBER x_2	LAYUP x_3	FIBER X LAYUP x_{23}	yi	Y	yi-Y	rank
1	-1	-1	+1	103.81	106.83	-3.02	3
2	-1	-1	+1	110.83	106.83	4.00	16
3	+1	-1	-1	72.64	72.77	0.83	10
4	+1	-1	-1	75.71	72.77	2.94	14
5	-1	+1	-1	69.12	68.13	0.99	11
6	-1	+1	-1	66.03	68.13	-2.10	4
7	+1	+1	+1	46.98	49.07	-2.09	5
8	+1	+1	+1	45.40	49.07	-3.67	1
9	-1	-1	+1	107.12	106.83	0.29	9
10	-1	-1	+1	105.56	106.83	-1.27	7
11	+1	-1	-1	69.73	72.77	-3.04	2
12	+1	-1	-1	72.06	72.77	-0.71	8
13	-1	+1	-1	70.94	68.13	2.81	13
14	-1	+1	-1	69.44	68.13	-1.69	6
15	+1	+1	+1	52.49	49.07	3.42	15
16	+1	+1	+1	51.44	49.07	2.37	12

Y is calculated by taking into consideration the effects calculated for the mean, fiber, lay-up and the fiber X lay-up interaction:

Effects

Fiber (-26.56)
Lay-up (-31.20)
Fiber X Lay-up (7.50)
Mean (74.20)

$$\mathbf{Y} = 74.20 + (-26.56/2)^* x_2 + (-31.20/2) * x_3 + (7.50/2)\, x_{23} \qquad (11)$$

The residuals for the remaining data sets were analyzed in a similar manner and plotted on normal probability paper.

APPENDIX C

EXTENDED ISOTROPIC ANALYSIS

Calculation of Reduced Stiffness Terms

$$Q_{11}' = E_{11}/(1-\nu_{12}^2 * E_{22}/E_{11}) \quad (1)$$

$$Q_{12}' = (E_{11}*\nu_{12})/(1-\nu_{12}^2 * E_{22}/E_{11}) \quad (2)$$

$$Q_{22}' = E_{22}/(1-\nu_{12}^2 * E_{22}/E_{11}) \quad (3)$$

$$Q_{66}' = G_{12} \quad (4)$$

Where: Q_{ij}' = reduced stiffness in terms of material coordinates
E_{ij}, G_{12} = Young's and shear moduli
n_{12} = Poisson's ratio

Transformation of Reduced Stiffness Terms

$$Q_{11} = m^4 Q_{11}' + 2 m^2 n^2 (Q_{12}' + 2 Q_{66}') + n^4 Q_{22}' \quad (5)$$

$$Q_{22} = n^4 Q_{11}' + 2 m^2 n^2 (Q_{12}' + 2 Q_{66}') + m^4 Q_{22}' \quad (6)$$

$$Q_{12} = m^2 n^2 (Q_{11}' + Q_{22}' - 4 Q_{66}') + (m^4 + n^4) Q_{12}' \quad (7)$$

$$Q_{66} = m^2 n^2 (Q_{11}' + Q_{22}' - 2 Q_{12}') + (m^2 - n^2)^2 Q_{66}' \quad (8)$$

Where: Q_{ij}' = reduced stiffness in terms of laminate coordinates
m = $\cos\theta$
n = $\sin\theta$
θ = angle between material and laminate coordinate axis

Calculation of A_{ij}

For a 16 ply laminate of the form $[q_1/q_2/q_3/q_4]_{2s}$:

$$A_{ij} = (h/4) * (Q_{ij}^{(1)} + Q_{ij}^{(2)} + Q_{ij}^{(3)} + Q_{ij}^{(4)}) \quad (9)$$

Where: h = laminate thickness
$Q_{ij}^{(k)}$ = reduced stiffness term for kth ply

Calculation of K_T

$$KT = 1+\{(2/A_{22})*[(A_{11}A_{22})^{0.5}-A_{12}+(A_{11}A_{22}-A_{12}^2)/(2A_{66})]\}^{0.5} \quad (10)$$

Calculation of $\sigma_y\ (x,0)/\sigma_0$

$$\sigma_y\ (x,0)/\sigma_0 = [1+0.5\ x^{-2}+1.5\ x^{-4}-((K_T-3)/2)*(5\ x^{-6}-7\ x^{-8})] \quad (11)$$

Where:

σ_y	=	tensile stress occurring at the hole
σ_0	=	remote applied tensile stress
x	=	x/r
x	=	Distance from hole center
r	=	radius of hole

APPENDIX D

FAILURE CRITERIA USED WITH THREE-DIMENSIONAL STRESS ANALYSIS

The three-dimensional stress analysis described in reference [73] is capable of determining the distribution of stresses around a hole on a ply-by-ply basis. A spline variational approach was used in this stress analysis. The maximum tensile and compressive values of normal stress components and the maximum absolute values of shear stress components generated from this stress analysis were used in a failure onset analysis for the graphite/epoxy open hole tension and compression specimens. A maximum stress type failure criterion which predicts failure to occur when any one of the stress components is equal to the corresponding intrinsic strength was used for the failure analysis. In this analysis either the tensile or compressive failure stress in the direction of the fibers, σ_{11}, was considered as a reference.

$$\underline{\sigma_0} = \min [\, X_C / |\min (\sigma_{11} / \sigma_0), (\sigma_{11} < 0)|,\ X_t / |\max (\sigma_{11} / \sigma_0), (\sigma_{11} > 0)|\,] \qquad (1)$$

Where:
- $\underline{\sigma_0}$ = reference stress
- X_c, X_t = compressive and tensile strength, respectively
- σ_{11} = in plane stress in fiber direction
- σ_o = applied unidirectional stress

Using equation (1) and the values of the stress components obtained from the three-dimensional stress analysis a dimensionless coefficient was calculated.

$$X_{kl}^{t\,(c)} = [S_{kl}^{t\,(c)} / \max (| \sigma_{kl}^{t\,(c)} | / \sigma_o)] [1 / \underline{\sigma_0}] \qquad (2)$$

Where:
- $X_{kl}^{t\,(c)}$ = dimensionless coefficient for tension (compression)
- $S_{kl}^{t\,(c)}$ = components of the tensile (compressive) strengths
- $\sigma_{kl}^{t\,(c)}$ = components of tensile (compressive) normal and shear stress

The components of tensile and compressive strength correspond to the material properties in the following manner:

$$S_{11}{}^{t\,(c)} = S_L{}^{t(c)} \text{ (longitudinal strength)} \quad (3)$$

$$S_{33}{}^{t(c)} = S_{22}{}^{t(c)} = S_T{}^{t\,(c)} \text{ (transverse strength)} \quad (4)$$

$$S_{13} = S_{12} = S_{32} = S \text{ (shear strength)} \quad (5)$$

The dimensionless coefficients obtained from equation (2) represent the value for which the applied stress reaches a ultimate value for the corresponding stress component. If this coefficient is less than one then the corresponding stress component will reach its ultimate value sooner than the reference component. Therefore, small values of $X_{kl}{}^{t\,(c)}$ prescribe the location and mode of initial damage.

REFERENCES

[1] Cole, R.T., et al, *Photoelastic Investigation of Bolted Joints in Composites,* Composites, July 1982, pp. 253-256.

[2] Lin, H. J., *Strength of Composite Laminates with Continuous Fiber around a Circular Hole,* Composite Structures, Vol. 21, pp. 155-162.

[3] Nejhad, M.N.G., Chou, T.W., *Compression Behavior of Woven Carbon Fiber-Reinforced Epoxy Composites with Moulded-In and Drilled Holes* Composites, Vol. 21, No. 1, Jan. 1990, p. 33.

[4] Rowlands, R.E., et al, *Single- and Multiple-Bolted Joints in Orthotropic Materials,* Composites, July, 1982, pp. 273-279.

[5] Zimmerman, K.B., *Mechanical Fastening of Composite Materials,* Experimental Techniques, July/August 1992, p. 36-40.

[6] Hart-Smith,L.J., Bolted Joints in Graphite-Epoxy Composites, NASA CR-144899, 1977.

[7] Packman, P.F., Hietala, H.J., Schulz, K.C., *An Experimental and Statistical Analysis of Some Fastener Anomalies on the Bolted Joint Strength of Graphite/Epoxy Laminates,* Advanced Materials Performance Through Technology Insertion: Proceedings of the 38th International SAMPE Symposium and Exhibition, V. Bailey, G. Janicki and T. Haulik, eds., Anaheim, CA, May 10-13, 1993, pp. 65-79.

[8] Xue, Y.,Zhang, S., Xu, G., *Effect of Laminate Configuration on Failure of Bolted Composite Joint,* Proceedings of International Symposium on Composite Materials and Structures, T.T. Loo and C. T. Sun, eds., Technomic Publishing, June 10-13, 1986, p. 422.

[9] Arnold, W.S., Marshall, I.H., Wood, J., *Optimum Design Considerations for Mechanically Fastened Composite Joints,* Composite Structures, Vol. 16, 1990, p. 85.

[10] Collings, T.A., *The Strength of Bolted Joints in Multi-Directional CFRP Laminates,* Composites, January 1977, p. 43.

[11] Gunderson, S.L., Hall, R.B., *Preformed Holes for Improved Mechanical Properties of Laminated Composites with Unidirectional Plies,* Advanced Materials Performance Through Technology Insertion: proceedings of the 38th International SAMPE Symposium and Exhibition, V. Bailey, G. Janicki and T. Haulik, eds., Anaheim, CA, May 10-13, 1993, pp. 81-91.

[12] Gunderson, S.L., Lute, J.A., *The Use of Preformed Holes for Increased Strength and Damage Tolerance of Advanced Composites,* Fatigue/Fracture/Damage I., pp. 460-470.

[13] Katz, Y., Haftka, R.T., Altus, E., *Optimization of Fiber Directions for Increasing the Failure Load of a Plate with a Hole,* Proceedings of The American Society For Composites: Fourth Technical Conference, Technomic Publishing, October 3-5, 1989, p. 62.

[14] Eriksson, I., *On the Bearing Strength of Bolted Graphite/Epoxy Laminates,* Journal of Composite Materials. Vol. 24, Dec. 1990, pp. 1246-1269.

[15] Lee, J.H., Mall, S., *Strength of Composite Laminate with Reinforced Hole,* Journal of Composite Materials, Vol. 23, April 1989, p. 337.

[16] Fracchia, C.A., Bohlmann, R.E., *The Effects of Assembly Induced Delaminations atFastener Holes on the Mechanical Behavior of Advanced Composite Materials,* Proceedings of the 39th International SAMPE Symposium. April 11-14, 1994, pp. 2665-2678.

[17] Shalev, D., Reifsnider, K.L., *Study of the Onset of Delamination at Holes in Composite Laminates,* Journal of Composite Materials, Vol. 24, Jan 1990, p. 42.

[18] Soutis, C., Fleck, N.A., Smith, P.A., *Failure Prediction Technique for Compression Loaded Carbon Fiber-Epoxy Laminate with Open Holes,* Journal of Composite Materials, Vol. 25, November 1991, p.1476-1498.

[19] Starnes, J.H., Williams, J.G., *Failure Characteristics of Graphite-Epoxy Structural Components Loaded in Compression,* Mechanics of Composite Materials: Recent Advances , Z. Hashin and C. T. Herakovich, eds., Pergamon Press, New York, August 1982, p. 253.

[20] Soutis, C., Fleck, N.A., *Compression Failure of Carbon Fiber Composite Plate with a Single Hole,* Journal of Composite Materials, Vol. 22, Nov. 1990, p. 211.

[21] Soutis, C., Fleck, N.A., *Static Compression Failure of Carbon Fiber T800/924C Composite Plate with a Single Hole,* Journal of Composite Materials, Vol. 24, May 1990, p. 536-558.

[22] Naik, N.K., Sai Ram, K.S., *Effect of Fiber and Resin Properties on Stress Gradients Around Openings in FRP Orthotropic Plates,* Proceedings of International Symposium of Composite Materials and Structures. T.T. Loo, C.T. Sun, Eds., Technomic, June 10-13, 1986, pp. 100-105.

[23] Guynn, E.G., Bradley, W.L., *Measurement of the Stress Supported by the Crush Zone in Open Hole Composite Laminates Loaded in Compression,* Journal of Reinforced Plastics and Composites. Vol. 8, March 1989, p. 133.

[24] Walsh, R., Vedula, M., Koczak, M. J., *A Comparative Assessment of Bolted joints in a Graphite Reinforced Thermoset vs. Thermoplastic,* SAMPE Quarterly, July 1989, p. 15-19.

[25] Beaumont, P.W.R., Schultz, J.M., Friedrich, K., Delaware Composites Design Encyclopedia: Failure Analysis of Composite Materials, Volume 4, L.A. Carlsson and J.W. Gillespie, eds., Technomic Publishing Co., Lancaster, 1990.

[26] Smith, P.A., Pascoe, K.J., *The Effect of Stacking Sequence on the Bearing Strengths of Quasi-isotropic Composite Laminates,* Composite Structures, Vol. 6, 1986, pp. 1-20.

[27] Whitney, J.M., Kim, R.Y., *Effect of Stacking Sequence on the Notched Strength of Laminated Composites,* Composite Materials: Testing and Design (Fourth Conference), ASTM STP 617, American Society for Testing and Materials,1977, pp. 229-242.

[28] Aronsson, C.G, *Stacking Sequence Effects on Fracture of Notched Carbon Fibre/Epoxy Composites,* Composites Science and Technology: 24,1985. pp. 179-198.

[29] Chang, F.K., Scott, R.A., Springer, G.S., *Strength of Mechanically Fastened Joints,* Journal of Composites, Vol. 16, Nov 1982, p. 471.

[30] Jen, M.H.R., Kau, Y.S., Hsu, J.M., *Initiation and Propagation of Delamination in a Centrally Notched Composite Laminate,* Journal of Composite Materials , Vol. 27, No 3, 1993, p. 272.

[31] Lessard, L.B., Shokrieh, M.M., Esbensen, J.H., *Analysis of Stress Singularities in Laminated Composite Pinned/Bolted Joints,* Advanced Materials Performance Through Technology Insertion: Proceedings of the 38th International SAMPE Symposium and Exhibition, V. Bailey, G. Janicki and T. Haulik, eds., Anaheim, CA, May 10-13, 1993, pp. 53-60.

[32] Lessard, L.B., Chang, F.K., *Damage Tolerance of Laminated Composites Containing an Open Hole and Subjected to Compressive Loadings: Part II-Experiment,* Journal of Composite Materials, Vol. 25, Jan. 1991, p.44.

[33] Chang, F.K.,Lessard, L.L, *Damage Tolerance of Laminated Composites Containing an Open Hole and Subjected to Compressive Loadings: Part I-Analysis* Journal of Composite Materials, Vol. 25, Jan 1991, pp. 2-43.

[34] Levin, K., Chang, F.K., Static Compression Test Methods for CFRP Laminates, M. Sc. Thesis, Chalmers Institute of Technology, Gothenburg, Nov. 1983.

[35] Boeman, R.G., Interlaminar Deformations on the Cylindrical Surface of a Hole in Laminated Composites: an Experimental Study ,CCMS-91-07, Virginia Polytechnic Institute and State University Center for Composite Materials and Technology, Blacksburg, Virginia , March 1991.

[36] Ko, C.C., Chien-Chang Lin, *Method for Calculating the Interlaminar Stresses in Symmetric Laminates Containing a Circular Hole,* AIAA Journal , Vol. 30, No.1, January 1992, p. 197.

[37] Ko, C.C., Chien-Chang Lin, Hsiang Chin, *Prediction for Delamination Initiation Around Holes in Symmetric Laminates,* Composite Structures:22, 1992, p. 187-191.

[38] Ditcher, A. K., Webber, J. P. H., *Edge Effects in Uniaxial Compression Testing of Cross-Ply Carbon-Fiber Laminates,* Journal of Composite Materials, Vol. 16, May 1982, pp. 228-242.

[39] Lagace, P.A., *Notch Sensitivity and Stacking Sequence of Laminated Composites,* Composite Materials: Testing and Design, ASTM STP 893, J.M. Whitney, Ed., American Society for Testing and Materials, Philadelphia, 1986, pp. 161-176.

[40] Pagano, N.J., Pipes, R.B., *Interlaminar Stresses in Composite Laminates Under Uniform Axial Extension,* Journal of Composite Materials, Vol. 4,1970, pp. 538-548.

[41] Pagano, N.J., Pipes, R.B., *The Influence of Stacking Sequence on Laminate Strength,* Journal of Composite Materials, Vol. 5, Jan. 1971, pp. 50-57.

[42] Pagano, N.J., Pipes, R.B., *Some Observations on the Interlaminar Strength of Composite Materials,* International Journal of Mechanical Sciences, Vol. 15,1973, pp. 678-688.

[43] Pagano, N.J., *On the Calculation of Interlaminar Normal Stress in Composite Laminates,* Journal of Composite Materials, Vol. 8,1974, p. 65-82.

[44] Whitney, J.M., Nuismer, R.J., *Stress Fracture Criteria for Laminated Composites Containing Stress Concentrations,* Journal of Composite Materials, Vol. 8, July 1974, p. 253.

[45] Whitney, J.M., Daniel, I.M., Pipes, R.B., Experimental Mechanics of Fiber Reinforced Composite Materials, Society of Experimental Mechanics and Prentice Hall, 1984.

[46] Rybicki, E.F., Schmueser, D.W., *Effect of Stacking Sequence and Lay-Up Angle on a Free Edge Stresses Around a Hole in a Laminated Plate Under Tension,* Journal of Composite Materials, Vol. 12, July 1978, p. 300.

[47] Ratwani, M.M., Kan, H.P., *Effect of Stacking Sequence on Damage Propagation and Failure Modes in Composite Laminates,* Damage In Composite Materials, ASTM STP 775, 1982, pp. 211-228.

[48] Zhang, K.D., Ueng, C.E., *A Simplified Approach for Interlaminar Stresses Around a Hole in [0/90]s Laminates* Journal of Composite Materials , Vol. 22, Feb.,1988, p. 192.

[49] Whitney, J.M., Structural Analysis of Laminated Anisotropic Plates, Technomic Publishing Co., Inc., Lancaster, 1987.

[50] Chang, F.K.,Chang, K.Y., *Damage in and Residual Strength of Bolted Composite Joints in Tension or Shear-Out Mode Failure,* Sixth International Conference on Composite Materials, ICCM&ECCM, Vol. 5,F.L. Matthews, et al, eds., Elsevier Applied Science, New York, 1987, pp. 173-182.

[51] Chang, K.Y., Liu, S., Chang F.K., *Damage Tolerance of Laminated Composites Containing an Open Hole and Subjected to Tensile Loading,* Journal of Composite Materials, Vol. 25, March 1991, pp. 274-301.

[52] Quinn, W.J., Matthews, F.L., *The Effect of Stacking Sequence on the Pin-Bearing Strength on Glass Fibre Reinforced Plastic,* Journal of Composite Materials, Vol. 11, April 1977, pp. 139-145.

[53] Boeman, R.G., *Interlaminar Strains at the Free Edge of a Hole in Laminated Composites: An Experimental Study,* Proceedings of the American Society of Composites Eighth Technical Conference, Technomic Publishing Co., Lancaster, 1993, pp. 298-307.

[54] Chang, F.K.,Lessard, L.L, Tang, J.M., *Compression Response of Laminated Composites Containing an Open Hole* , SAMPE Quarterly, Vol. 19, No. 4, July 1988, pp. 46-51.

[55] Chamis, C.C., *Simplified Procedures for Designing Composite Bolted Joints,* Journal of Reinforced Plastics and Composites, Vol 9, November 1990, pp. 614-626.

[56] Matthews, C.M., et al, *Stress Distribution Around a Single Bolt in Fibre-Reinforced Plastic,* Composites, July 1982, pp. 316-322.

[57] Lessard, L.B., Chang, F.K., *Effect of Load Distribution on the Fiber Buckling Strength of Unidirectional Composites,* Journal of Composite Materials, Vol. 25, Jan. 1991, p.65.

[58] Collings, T.A., *On the Bearing Strength of CFRP Laminates,* Composites. July 1982, p. 241-252.

[59] Cole, R.T., et al, *Fasteners for Composite Structures,* Composites, July 1982, pp. 233-240.

[60] Andrews, S. D., Ochoa, O.O., Owens, S. D., *The Effect of Fastener Hole Defects,* Journal of Composites, Vol. 27, No. 1, 1993, p. 2.

[61] Grove, R., Smith, B., Compendium of Post Failure Analysis Techniques for Composite Materials, AFWAL-TR-86-4137, 1986.

[62] Godwin, E.L., et al, *Strength of Multi-Bolt Joints in GRP,* Composites, July 1982, pp. 268-272.

[63] Lin, C.C., Ko, C.C., *Stress and Strength Analysis of Finite Composite Laminates with Elliptical Holes,* Journal of Composite Materials, Vol 22, April 1988, pp. 373-385.

[64] Rubin, A. M., *Common Failure Modes For Composite Aircraft Due to Secondary Loads,* Composites Engineering, Vol. 2, Nos 5-7, 1992, pp. 313-320.

[65] Kim, R.Y., Whitney, J.M., *Effect of Temperature and Moisture on pin Bearing Strength of Composite Laminates,* Journal of Composites, Vol. 10, April 1976, p. 149-155.

[66] Ireman, T., Nyman, T., Helborn, K, *On Design Methods for Bolted Joints in Composite Aircraft Structures,* Composite Structures, 25, 1993, pp. 567-578.

[67] Snell, M.B., Burkitt, G.P., *Test Specimens for Bearing and By-Pass Stress Interaction in Carbon Fibre Reinforced Plastic Laminates,* HMSO, London, 1987, pp. 1-21.

[68] Jones, R. M., Mechanics of Composite Materials, McGraw-Hill Book Company, New York, 1975.

[69] Rowlands, R.E., *Strength (Failure) Theories and their Experimental Correlation,* Handbook of Composites, Vol. 3-Failure Mechanics of Composites, G.C. Sih and A.M. Skudra, eds., Elsevier Science Publishers B.V., 1985.

[70] El-Zein, M.S. and Reifsnider, K.L., *The Strength Prediction of Composite Laminates Containing a circular Hole,* Journal of Composites Technology & Research, Vol. 12, No. 1., Spring 1990, pp. 24-30.

[71] Garbo, S.P., Ogonowski, J.M., *Strength Predictions of Composite Laminates with Unloaded Fastener Holes,* AIAA Journal, Vol. 18, NO. 5, May 1980, pp. 585-589.

[72] Konish, H.J., Whitney, J.M., *Approximate Stresses in an Orthotropic Plate Containing a Circular Hole,* Journal of Composites, Vol. 9, April 1975, p. 157.

[73] AdTech Systems Research, Inc., Failed Stress Modeling for Molded and Drilled Hole Composites, Final Technical Report, Subcontract No RI-89640X, Prime Contract No. F33615-91-C-5618, Period ending 31 December 1994.

[74] Iarve, E.V., et. al., *Stress Analysis of Laminated Composites with Preformed Holes,* Proceedings of the American Society of Composites Technical Conference, Technomic Publishing, Lancaster, October 1993, pp. 975-981.

[75] Ramkumar, R.L., *Bolted Joint Design,* Test Methods and Design Allowables for Fibrous Composites, ASTM STP 734, C.C. Chamis, ed. American Society for Testing Materials, 1981, p. 376-395.

[76] Greenhalgh, E.S., Cox, P.C., *A Method to Determine Propagation Direction of Compressive Fracture in Carbon-Fibre Composites,* Composite Structures: 21, 1992, pp. 1-7.

[77] Guynn, E.G., Bradley, W.L., *A Detailed Investigation of the Micromechanisms of Compressive Failure in Open Hole Composite Laminates,* Journal of Composite Materials, Vol. 23, May 1989, p. 479-504.

[78] Khamseh, A.R., Waas, A.M., *Failure Mechanisms of Uni-Ply Composite Plates With a Cirular Hole Under Static Compressive Loading,* Transactions of the ASME, Vol. 114, July, 992, pp. 304-310.

[79] Lessard, L.B., Chang, F.K., *Effect of Load Distribution on the Fiber Buckling Strength of Unidirectional Composites,* Journal of Composite Materials, Vol. 25, Jan. 1991, p.65.

[80] Poon, C., et al, *Damage Progression Under Compressive Loading in Composite Laminates Containing an Open Hole,* AGARD, San Diego, CA, 1992.

[81] Tan, S.C., *Finite-Width Correction Factors for Anistropic Plate Containing A Central Opening,* Journal of Composite Materials, Vol. 22, Nov. 1988, pp. 1080-1097.

[82] Tan, S.C., Kim, R.Y., *Damage Accumulation and Fracture of Notched Composite Laminates Under Tensile And Compressive Loading,* Composite Materials: Testing and Design (Tenth Volume), ASTM STP 1120, Glenn C. Grimes, Ed., American Society for Testing Materials, Philadelphia, 1992, pp. 414-427.

[83] Fiberite Product Data Sheet

[84] Hercules Product Data Sheet

[85] Lessard, L.B..,Compression Failure in Laminated Composites Containing an Open Hole, Ph D Dissertation, Stanford University, March 1989.

[86] ASTM Standards and Literature References For Composite Materials, ASTM, Philadelphia, 1987.

[87] Zabora, R. F., *Edge Stabilized Compression Testing of Composite Laminates,* Proceedings of the 38th International SAMPE Symposium and Exhibition, Vol. 38., Vince Bailey, et.al., eds., Anaheim, California, May 10-13, 1993.

[88] Wilson, D. W., et.al., *On the Use of Laminate Test Methods to Characterize Lamina Compression Strength,* Proceedings of the 37th SAMPE Symposium, March 9-12, 1992.

[89] Fastening Systems Installation Instructions, hi-shear Corporation, Ca.

[90] SACMA Recommended Test Method for Bearing Strength Properties of Oriented Fiber Resin Composites, SRM 9-89.

[91] Box, G. E. P., Statistics for Experimenters, John Wiley & Sons, New York, 1978.

[92] Caulcutt, R., Statistics in Research and Development, Chapman & Hall, London & New York, 1983.

[93] Fisher, R., Statistical Methods for Research Workers, Hafner Publishing Company, 1973.

[94] Mann, H.B., Analysis and Design of Experiments, Dover Publications, Inc., New York, 1949.

[95] Scheffe, H., The Analysis of Variance, John Wiley & sons, Inc., New York, 1959.

[96] Sanedecor, G. W., Calculation and Interpretations of Analysis of Variance and Covariance, Collegiate Press, Inc., Ames, Iowa, 1934.